

A METHODOLOGY FOR CONDITION ASSESSMENT OF T-BEAM BRIDGES WITHOUT
STRUCTURAL PLANS

A Thesis

Presented to

the faculty of the School of Engineering and Applied Science at
University of Virginia

in partial fulfillment

of the requirements for the degree

Master of Science

by

Abdou K. Ndong

May

2018

APPROVAL SHEET

The thesis
is submitted in partial fulfillment of the requirements
for the degree of
Master of Science

Abdou K. Ndong

The thesis has been read and approved by the examining committee:

Osman E. Ozbulut

Co-Advisor

Devin K. Harris

Co-Advisor

Jose Gomez

Chair

Accepted for the School of Engineering and Applied Science:

Craig H. Benson, Dean, School of Engineering and Applied Science

May

2018

A METHODOLOGY FOR CONDITION ASSESSMENT OF T-BEAM BRIDGES WITHOUT STRUCTURAL PLANS

ABSTRACT

This study presents a nondestructive method for load rating of reinforced concrete T-beam bridges with limited or missing structural information. To compute load rating factor of a bridge, the capacity of the bridge as well as the dead load and live load effects need to be determined. In the proposed approach, a large number of T-beam bridges with different structural dimensions such as skew angle, span, width, and thickness was first analyzed using finite element method to obtain their natural frequencies. Then, a non-dimensional frequency parameter that plays an important role in identifying the flexural rigidity of T-beam bridges was computed using the natural frequencies obtained from numerical analyses. This population of generated data was then used to create an artificial neural network model that can predict non-dimensional frequency parameters for any T-beam bridges with different geometrical characteristics. Next, the flexural rigidity of a bridge was determined based on the measured natural frequencies derived from vibration testing. The cross-sectional area of the internal reinforcing steel was estimated through a quasi-static load test coupled with an optimization approach. Finally, these structural and material properties that were initially unknown but were estimated through the proposed methodology were used to determine load effects and ultimately the bridge's capacity and rating factor. Experimental tests on two in-service RC T-beam bridges were conducted and the proposed methodology was used to obtain the rating factors of the bridges. Results indicate that the nondestructive methodology described in this work can satisfactorily estimate the rating factors of T-beam bridges without structural plans.

Keywords: Bridge load rating; unknown structural information; nondestructive method; structural capacity; load effect.

DEDICATION

*Dedicated
to my inspiring parents
and siblings,
for being the
pillows, role models, catapults,
cheerleading squad and sounding boards
I have needed*

ACKNOWLEDGMENTS

I would like to thank those around me who helped me through the process of pursuing a Master's degree as, without their support and guidance, it would have not been possible.

Dr. Osman E. Ozbulut: Thank you for all of guidance and patience and for always keeping a positive attitude. I tend to approach problems and decisions by trying to consider all possible outcomes, and I appreciate your patience while I work my way through them. I have learned so much from you and I look forward to learning more. Thank you for being a remarkable teacher and I am very grateful to have you as a teacher. And thank you for giving me a chance to work in this project.

Dr. Devin K. Harris: Thank you for giving me the opportunity to work in this VTRC funded research and for serving as the chair of my committee and for being my secondary advisor. Your guidance and assistance in the topic of bridge testing was vital in my work. Your leadership and management during my research project was a key element in the successful achievement of my set targets.

Dr. Jose Gomez: Thank you for your inspiration and support, for the patient guidance, encouragement and advice you have provided throughout my time as a master's student. I am also grateful that you served in my thesis committee.

Mohamad Alipour: Thank you for your continual advice and insight into experimental bridge testing. I appreciate the opportunity to gain valuable experience with field testing. Your constant support and guidance in my research was definitely the key element of success in my work. You are always such a help, and I appreciate your support in every way.

Muhammad M. Sherif: Your excellent teaching skills and courteous personality has helped me tremendously through my journey at UVA. Thank you for your advice and acting as a mentor to me. Without your helpfulness and directness, school would have been more challenging. I appreciate you being stern and letting me know what I am doing wrong along with giving my ways I can correct my mistakes. It is comforting to know that whenever I have a question you answer right away, which you know is all the time.

Dr. Abdollah Bagheri: Thank you for assisting me in my research work. You were a great resource to learn more about structural dynamics.

Keegan: Thank for the tremendous support and help during a busy or difficult time, above-and-beyond assistance with a project at work.

Uncle Jesse: Thank you for the inspiration and daily motivation that you have given me.

Current, Ex Graduate Students, friends and friends from Overseas including **Sherif Daghash, Benjamin Goffin, Erin Robartes, Ugur Kilic, Mehrdad Dizaji, Farzad Dizaji, Zhangfan Jiang, Syed Ahmed Kazmi, Emily White, Ruoxi Xie, Lucas Duvall Elliott, Arun Kumar Subramiam, Baikuntha Silwal, amedebrhan asfaw, Tony Zhang, Mesut Kaplan, Thierno Barry, Duale Nasri, Heze Chen, Eve, Prof Mehmet Caputcu, Prof Darcin Akin, Prof Carmen Amaddeo, Prof Nida Noorani** I greatly appreciate all your help and company and good thoughts on me during my time as a graduate student. Your presence in the graduate office made for a great learning environment.

My family for your love, support and warmth during times of joy and times of need. You have been the leading proponents for my education and career. Thank you for everything. The most special thanks goes to my best friend, my mom. Amy Sene, you gave me your unconditional support and love through all this long process. Je vous aime.

NOMENCLATURE

ABBREVIATION	DESCRIPTION
AASHTO	American Association of State Highway and Transportation Officials
ANN	Artificial Neural Network
A_s	Amount of longitudinal reinforcement area
BDI	Bridge Diagnostics Inc.
b_e	Effective width of the beam of the cross section.
D	Flexural Rigidity
DAQ	Data acquisition
DC	Dead load of structural components.
DW	Dead load of future wearing surface
EFDD	Enhanced Frequency Domain Decomposition
e	Cantilever
E_c	Elastic modulus
FDD	Frequency Domain Decomposition
FFT	Fast Fourier Transform
f_c'	compressive strength of the concrete
g_{m1}	Distribution factor for one lane loaded
g_{m2}	Distribution factor for two or more lanes loaded
h_{eq}	Equivalent thickness
h	Slab thickness
h_s	Stem height

A Methodology for Condition Assessment of T-Beam Bridges without Structural Plans

I	Moment of inertia of the flanged section including one rib and the top slab of width S
IM	Impact or dynamic load allowance
LL	Vehicular live load.
LRFD	Load and Resistance Factor Design
MAC	Modal Assurance Criteria
PSD	Power Spectral Density
IM	Impact or dynamic load allowance
S	center-to-center distance between the ribs
SDOF	Single Degree of Freedom
SVD	Singular Value Decomposition
VSM	Vibration-based Simplified Method
λ_i	Non-dimensional frequency parameter
θ	skew angle
w	Stem width
ω_n	Modal frequency n
$\varepsilon^{Ana.}$	Analytical Strain
$\varepsilon^{Exp.}$	Experimental Strain
M_u	Bending Capacity
β	Coefficient for considering the effect of reinforcing steel in calculating the elastic modulus of the concrete material
t	Age of bridge in days

TABLE OF CONTENTS

ABSTRACT	I
DEDICATION	II
ACKNOWLEDGMENTS	III
LIST OF TABLES	X
LIST OF FIGURES	XI
1 INTRODUCTION	1
1.1 Background and Motivation.....	1
1.2 Research Objectives	2
1.3 Thesis Organization.....	4
2 LITERATURE REVIEW	5
2.1 Overview	5
2.2 Load Rating through Dynamic Testing.....	5
2.3 Load Rating through Static Testing	8
2.4 Condition Assessment using Video Imaging	11
2.5 Summary	12
3 VIBRATION-BASED SIMPLIFIED METHOD FOR BRIDGE LOAD RATING.....	13
3.1 Overview	13
3.2 Description of Methodology	13
3.2.1 Step 1: Determine Geometric Characteristics of Bridge.....	13
3.2.2 Step 2: Conduct Live Load Testing	13
3.2.3 Step 3: Conduct Vibration Testing	14
3.2.4 Step 4: Identify Modal Properties of Bridge.....	15
3.2.5 Step 5: Identify Flexural Rigidity of Bridge	17
3.2.6 Step 6: Determine Elastic Modulus and Compressive Strength of Concrete	24

A Methodology for Condition Assessment of T-Beam Bridges without Structural Plans

3.2.7	Step 7: Estimate Yield Strength and Area of Reinforcing Steel.....	26
3.2.8	Step 8: Determine Capacity	30
3.2.9	Step 9: Determine Load Effects.....	30
3.2.10	Step 10: Compute Load Rating.....	33
3.3	Summary	33
4	EXPERIMENTAL TESTING.....	34
4.1	Overview	34
4.2	Equipment	34
4.3	Bridge Descriptions and Instrumentation Plan.....	36
4.3.1	Flat Creek Bridge.....	36
4.3.2	Bratton Creek Bridge	41
4.4	Bridge Testing	45
4.4.1	Live Load Testing.....	45
4.4.2	Vibration Testing	46
4.5	Summary	47
5	EXPERIMENTAL RESULTS	48
5.1	Overview	48
5.2	Modal Identification Method	48
5.3	Load Rating of Flat Creek Bridge through VSM.....	49
5.3.1	Time Domain Data.....	49
5.3.2	Frequency and Damping Ratio Extraction.....	52
5.3.3	Flexural Rigidity Estimation.....	55
5.3.4	Elastic Modulus and Compressive Strength of Concrete	56
5.3.5	Live Load Test results.....	57
5.3.6	Yield Strength and Area of Steel Estimation.....	57

A Methodology for Condition Assessment of T-Beam Bridges without Structural Plans

5.3.7	Bending Capacity Estimation	60
5.3.8	Load Effects Computation	61
5.3.9	Load Rating Computation.....	67
5.4	Load Rating of Bratton’s Creek Bridge through VSM	68
5.4.1	Time Domain Data.....	68
5.4.2	Frequency and Damping Ratio Extraction.....	69
5.4.3	Flexural Rigidity Estimation.....	72
5.4.4	Elastic Modulus and Compressive Strength of Concrete	73
5.4.5	Live Load Test results.....	74
5.4.6	Yield Strength and Area of Steel Estimation.....	74
5.4.7	Bending Capacity Estimation	77
5.4.8	Load Effects Computation	78
5.4.9	Load Rating Computation.....	84
5.5	Summary	85
6	CONCLUSION AND RECOMMENDATIONS	87
	REFERENCES	89

LIST OF TABLES

Table 3-1 Yield strengths of unknown reinforcing steel (adapted from [1]).....	26
Table 5-1 Modal Parameters.....	54
Table 5-2 MAC Values.....	55
Table 5-3 Estimated reinforcement area and bending moment	59
Table 5-4 Estimated reinforcement area and bending moment	59
Table 5-5 Design Bending Moment of each load for Interior Beam	63
Table 5-6 Design Bending Moment of each load.....	66
Table 5-7 Modal Parameters.....	71
Table 5-8 MAC Values.....	72
Table 5-9 Estimated reinforcement area and bending moment	76
Table 5-10 Estimated reinforcement area and bending moment	76
Table 5-11 Design Bending Moment of each load for interior beam.....	81
Table 5-12 Design Bending Moment of each load.....	84
Table 5-13 Estimated Parameters and Load Ratings based on VSM-LR Approach	85
Table 5-14 Inventory Load Rating Results from Different Analyses.....	86

LIST OF FIGURES

Figure 1-1 Flowchart of the proposed method for load rating of T-beam bridges	3
Figure 2-1 Hypothetical Probability Density Functions for the Load Effect Resistance (Azizinamini et al. 2000)	9
Figure 3-1 Geometric Characteristics of the T-beam bridges.....	13
Figure 3-2 Enhanced Frequency Decomposition steps.....	16
Figure 3-3 Flowchart of the finite element database generation.....	19
Figure 3-4 Flowchart of the computation required to determine λ_i	20
Figure 3-5 Schematic of the evolution of the mean squared errors (averaged over three runs) with increase in the number of epochs.....	22
Figure 3-6 Histogram of errors	22
Figure 3-7 Curve fitting	23
Figure 3-8 The rib pattern for each type of reinforcing steel.....	26
Figure 3-9 Plot of the objective functions defined in: (a) Eq. (11), and (b) Eq. (3-27) (Bagheri et al.2017)	28
Figure 4-1 (a) BDI Accelerometer, (b) PCB Signal Conditioner, (c) BDI STS-Wi-Fi Node, (d) PCB Impact Hammer, (e) ST350 Strain Transducer	35
Figure 4-2 A side view of the Flat Creek bridge	36
Figure 4-3 Plan view of Flat Creek bridge.....	37
Figure 4-4 Elevation view of Flat Creek bridge	37
Figure 4-5 3D view of Flat Creek bridge.....	37
Figure 4-6 Dimensions of the tested Spans (Plan View)	38
Figure 4-7 Dimensions of the bridge (elevation view)	38
Figure 4-8 Instrumentation layout and strain sensors location	39
Figure 4-9 – Instrumentation Configuration for Flat Creek Bridge: Vibration Testing	40
Figure 4-10 Side View of Bratton’s Creek Bridge	41
Figure 4-11 Plan View of Bratton’s Creek	42
Figure 4-12 Elevation View of Bratton	42
Figure 4-13 3D View of Bratton’s Creek (Showing the tested span in green).....	42
Figure 4-14 Dimensions of the Bridge.....	43

A Methodology for Condition Assessment of T-Beam Bridges without Structural Plans

Figure 4-15 Live Load Testing: Strain Sensors Location.....	44
Figure 4-16 Instrumentation Configuration for Bratton’s Creek Bridge: Vibration Testing.....	45
Figure 4-17 Live Load Testing	46
Figure 4-18 Impact Excitation Location: (a) Flat Creek, (b) Bratton’s Creek.....	47
Figure 5-1 Time histories of acceleration data from all sensors of test setup 1 during ambient vibration testing of Flat Creek bridge	50
Figure 5-2 Time histories of acceleration data from all sensors of test setup 2 during ambient vibration testing of Flat Creek bridge	50
Figure 5-3 Time histories of acceleration data from all sensors of test setup 1 during impact hammer testing of Flat Creek bridge	51
Figure 5-4 Time histories of acceleration data from all sensors of test setup 2 during impact hammer testing of Flat Creek bridge	51
Figure 5-5 Singular values for EFDD method (Ambient Data).....	53
Figure 5-6 Singular values for FDD method (Impact Hammer data).....	53
Figure 5-7 Mode shapes of Modes 1-3, 3D representation.....	54
Figure 5-8 Modal Assurance Criterion	55
Figure 5-9 Maximum Strain at each Girder.....	57
Figure 5-10 Schematics showing loaded lanes on bridge cross section for special analysis: Position of HL-93 trucks for two design lanes loaded case.....	65
Figure 5-11 Time histories of acceleration data from all sensors during ambient vibration testing of Bratton’s Creek bridge.....	68
Figure 5-12 Time histories of acceleration data from all sensors during impact hammer testing of Bratton’s Creek bridge	69
Figure 5-13 Singular values for EFDD method (Ambient Data).....	70
Figure 5-14 Singular values for EFDD method (Impact Hammer Data).....	70
Figure 5-15 Mode shapes of Modes 1-3, 3D representation.....	71
Figure 5-16 Modal Assurance Criterion	72
Figure 5-17 Maximum Strain at each Girder.....	74
Figure 5-18 Schematics showing loaded lanes on bridge cross section for special analysis: Position of HL-93 trucks for two design lanes loaded case.....	79

1 INTRODUCTION

1.1 Background and Motivation

Bridges represent the weakest links of a healthy transportation system, and hence should be highly maintained to allow safe movement of their users. Bridge structures are commonly rated using analytical procedures based on structural plans and visual inspection and are seldom tested with loading. According to 2016 bridge inventory statistics, about 56,007 bridges out of 614,387 nationwide in the United States are structurally deficient. Managing the aging infrastructure is an enormous problem and of national significance. Therefore, effective strategies and techniques need to be implemented to maintain these bridges in a way that will ensure public safety and minimize the risks associated with them within the limited resources.

Conventional load rating procedures require design plans or as-built drawings of a bridge and the latest inspection report for rating the bridge. However, there are cases where the structural information is missing due to different factors such as lack of documentation at the time of construction and improper storage. When this structural information is missing, the condition assessment and load rating of the bridge becomes a challenge for the bridge engineers. This is due to the fact that the nominal capacity of the bridge, which is used in the load rating calculations, is normally determined from structural drawings and information. The Manual for Bridge Evaluation (MBE) is developed to assist the engineers and bridge owners by establishing procedures that meet the National Bridge Inspection Standards (NBIS). However, the MBE provides very limited guidance to the engineers for load rating of the bridges without structural plans. In most cases, the rating is estimated by a qualified or experienced engineer. Based on the previous inspection report and some other factors such as the age of the bridge and current condition of the bridge, this engineer can arrive at a judgement based load rating.

The judgment-based ratings can be subjective and may pose a risk, as this approach may not accurately describe a bridge's behavior. Therefore, bridge engineers often tend to be overly conservative about determining the rating factor of a bridge without plans. On the other hand, overly conservative ratings may lead to restriction of large trucks to travel on the bridge, which might have a negative impact on the commerce. As a result, there is a need to develop better tools that can be used in the management and decision-making for this inventory. In this study, an

approach for estimating the load bearing capacity of T-beams bridges without structural plans is studied.

1.2 Research Objectives

The objective of this work is to develop a methodology for load rating reinforced concrete (RC) T-beam bridge structures that are difficult to rate as a result of either limited or missing as-built information. The method described in this thesis is a nondestructive method and mainly relies on vibration measurements for estimating the load carrying capacity of RC T-beam bridges without structural plans. To estimate load rating factor of a bridge, the capacity, dead load and live load effects need to be determined. In the proposed approach, a series of finite element analyses are first conducted to describe the modal properties of a large population of T-beam bridges with different geometric characteristics. Results and geometric inputs are then used to estimate the flexural rigidity of a bridge based on the measured modal frequencies derived from vibration testing. Due to the uncertainty in internal geometry of concrete, nondestructive approaches are presented to obtain the cross-section dimensions of bridge as well as the elastic modulus and compressive strength of concrete. Next, the cross-sectional area of the internal reinforcing steel is estimated through a quasi-static load test coupled with an optimization approach. These structural and material properties are then used to determine load effects and ultimately the bridge's capacity. The flowchart of the methodology, named as Vibration-based Simplified Method (VSM), is illustrated in Figure 1-1.

A Methodology for Condition Assessment of T-Beam Bridges without Structural Plans

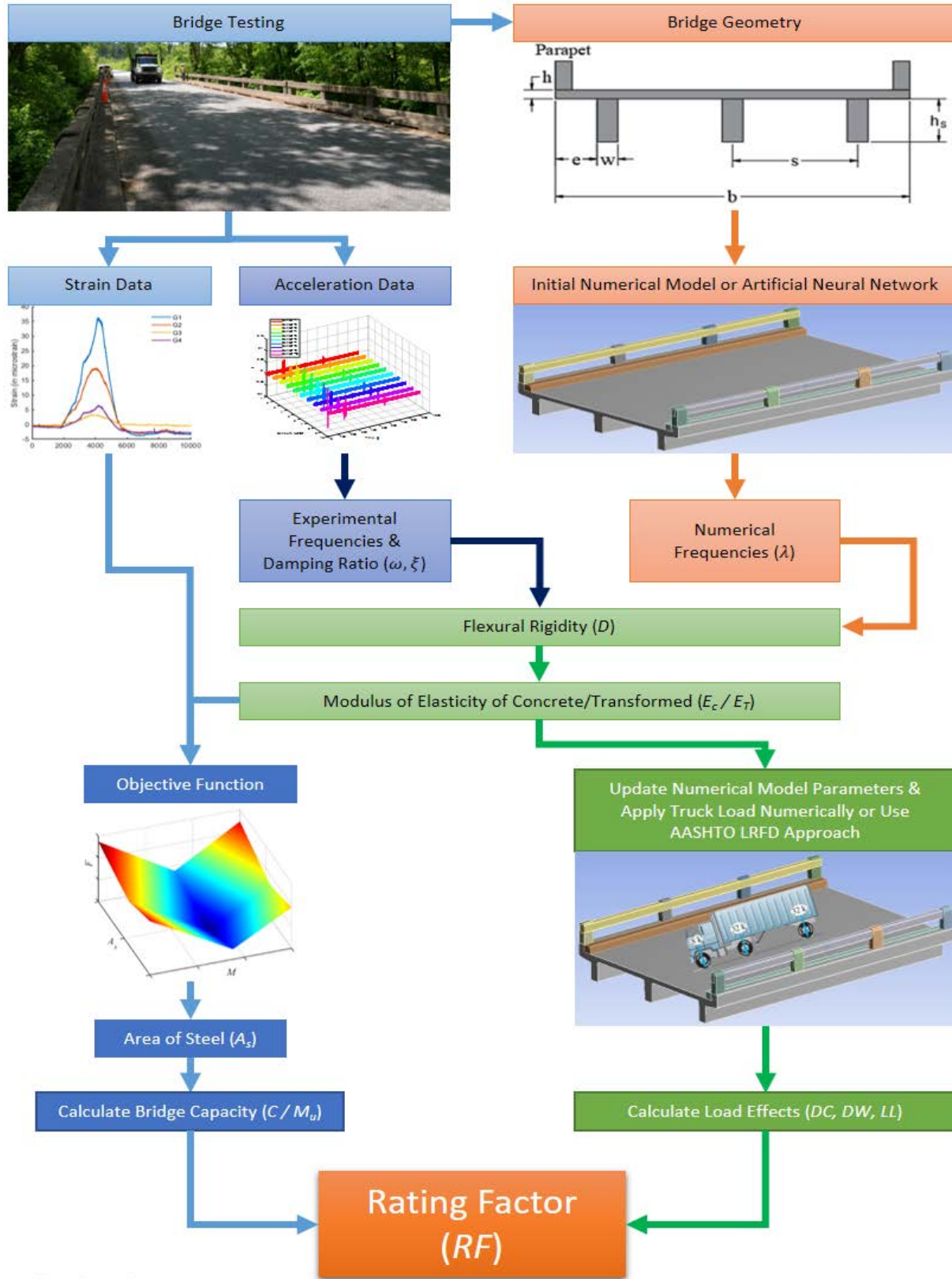


Figure 1-1 Flowchart of the proposed method for load rating of T-beam bridges

1.3 Thesis Organization

A chapter-by-chapter overview of this thesis is provided as follows:

Chapter 1 introduces the motivation for this work, describes the research objectives as well as the organization of the thesis.

Chapter 2 provides a literature review on the load rating of bridges with and without structural plans using static and dynamic field testing.

Chapter 3 includes an overview of the methodology which is discussed step-by-step. While describing each step of the methodology, background information related to this step is provided first and then a detailed explanation is given.

Chapter 4 illustrates the application of the proposed methodology in load rating of two in-service T-beam bridges. The instrumentation and testing of the bridges are described first. Then, the proposed load rating methodology is implemented to obtain load rating factor of both bridges.

Chapter 5 discusses the main conclusions and makes recommendations for further research.

2 LITERATURE REVIEW

2.1 Overview

During their service life, bridges deteriorate due to various reasons such as cracking in concrete, fatigue cracks in steel, and corrosion of steel reinforcement. As a result, the load bearing capacity of bridges decreases over time and needs to be evaluated periodically. In this section, previous studies on bridge load rating methods that employ static field testing and dynamic measurements are reviewed. Most of these studies used the results from static or dynamic testing of the bridge to calibrate a finite element model, which, in turn, is used for load rating.

2.2 Load Rating through Dynamic Testing

Several researchers have concentrated on the dynamic response of the structures to estimate their stiffness and load bearing capacity. Islam et al. (2014) developed a method for load rating of prestressed box beam (PSBB) based on the dynamic response collected via wireless sensors networks (WSNs). Two single-span bridges were selected for this study: one of which was 85 ft, long and 36 ft wide and used to collect the data used in the development of the proposed load rating method; and the other one which was 90 ft. long and 44 ft. wide and was used for validation. Two WSNs were set out on the PSBB to collect data at a sampling rate of 100 Hz at 2g scale, and three trucks were run (12 runs) with three variable loads and at four different speeds for collecting real time dynamic response of the bridge at current condition. Each set of WSN included four small programmable object technology wireless accelerometer sensors and one base station connected via serial bus cable to a laptop. Finite element (FE) simulations of 3D bridge models under vehicular loads were performed to get the dynamic response of the bridge at its initial state and then the model get validated by field testing and numerical analysis. Fast Fourier Transform and pick-picking algorithms were used to get the maximum peak amplitudes and their corresponding frequencies. Using the SDOF method and the load displacement relationship, the bending stiffness of the bridge was calculated to estimate its load-bearing capacity and which is the same as the actual rating of the structure. The results obtained from the FE is used for software application that can instantaneously determine the load rating of the bridge from the collected dynamic response.

Siswobusuno et al. (2004) proposed a load rating technique`e based on modal testing and ambient traffic measurements on a single span bridge that has a concrete deck with steel girders. The instrumentation composed of a sledge hammer of 20lb applied to the deck at specific spatial points

and a single piezoelectric accelerometer fixed underneath the middle of the outermost steel girder to extract the mode shapes and vibration frequencies. A grid of 42 nodes was specified on the first bridge and 54 for the second bridge. Each node was excited with sledge hammer five times and data was collected at a sampling rate between 500 to 1000 Hz. The signals were collected using a 12-channel data acquisition system (DAQ) along with a 4-channel ICP Sensor Signal Conditioner to enhance the signals. The bending frequencies were determined from the response functions computed from the collected time domain signals. The bridge first bending frequency is used to back calculate the stiffness and load capacity of the bridge. The bridge design capacity which was obtained by subtracting the change in load capacity from the maximum load was then validated using a static load test. The static test consisted of a 2-axle truck placed in 9 different positions and with different weight increment applied to the bridge top and 9 dial gages below the deck to measure the deflection. The results were satisfactory, showing that the dynamic test results being very close to the static test results and may employed for bridge load rating.

Samali et al. (2007) suggested a novel dynamic based method is presented by which the in-service stiffness of the bridge is estimated first.. This method involves the attachment of few uniaxial accelerometers underneath the bridge girders. The vibration measurement of the bridge superstructure were collected considering two phases. These phases are when the bridge is unloaded and when loaded with one more loads applied at mid-span. Two sets of bending frequencies were measured for the bridge: 'as is' and when loaded by extra weight. Upon the application of additional loading to the bridge, the bending frequency of the bridge decreased. From the resulting frequency shift due to added weight, the flexural stiffness of the bridge was calculated. From the obtained flexural stiffness, load carrying capacity of the bridge is computed through a user friendly software by adopting a statistically based approach. The reliability and simplicity of the proposed methodology has been demonstrated by testing over 200 bridge spans covering a wide range of single and multi-span timber bridges. The results pertaining to two spans of one of these bridges are reported in this paper, along with the underlying principles and methodology adopted.

Samali et al. (2003) dynamic two-span bridge assessment method. The procedure involves the attachment of few uniaxial accelerometers underneath the bridge girders. The vibration measurement of the bridge superstructure is collected in two stages. The first one is done when the

bridge is unloaded and the second one with a relatively small mass applied at the mid-span. The bridge was excited by a calibrated 12 lb sledge hammer which was used to impact the unloaded bridge and then impact again with a relatively small mass added at the mid-span. After getting the recorded vibration data collected in two set-ups test and the data was named as “No mass test” and “Added mass test” data and the natural frequencies and mode shapes were extracted for each set of data. The difference in modal response was used to calculate the load carrying capacity of the bridge.

Application of finite element tools for condition assessment of arch bridges was studied by Boothby and Atamturktur (2007) with detailed instructions in relation with geometric and solid models as well as meshing and implying boundary conditions. The physical parameters of FE models are adjusted during the calibration process with reasonable assumptions for accuracy of the 3D finite element models of stone arch bridges by Fanning and Boothby (2001). Similarly, Caglayan et al. (2009) investigated a three-span arch bridge located in a region prone to earthquake. The researchers generated a finite model of the bridge using a commercial software. Accelerations data test that were conducted on the bridge were used to refine the model by changing the structural parameters of the bridge. The obtained final model was used for condition assessment.

Studies have shown that about one third of the bridges in the United States are structurally deficient or functionally obsolete. Wang et al. (2005) proposed a condition assessment methodology. The process consists of generating a finite element (FE) model, calibrating that model to match experimental data, and using the results from calibration to rate the condition of the bridge or investigate unique loadings or retrofit schemes. During the calibration process, different parameters are adjusted using two condition of loadings that are static and dynamic. These selection of the parameters is made by referring the work of Turer (2000). Taking the response of the two conditions of loadings is used to achieve convergence between the analytical and experimental results by using some objective functions. The final calibrated which can mimic the real structure can be used for load rating.

2.3 Load Rating through Static Testing

The combination of field test and theoretical analysis can be used to assess the load carrying capacity of bridges without plans. Researchers at the University of Delaware previously developed a method called the steel area method (SAM) to rate concrete bridges without plans (Thomson, 1999). They used strain or displacement measurements from field testing in synchrony with basic mechanics principles, beam theory to estimate the unknown area of steel of a reinforced concrete bridge. In another study, Huang and Shenton (2010) extended and improved the SAM method and derived equations to accommodate more general load configuration, such as that used in a typical diagnostic load test of a bridge. A novel procedure on the basis of SAM without incorporating the results of the diagnostic load tests is developed. The proposed procedures was validated by testing a concrete bridge with original structural drawings.

Analytical and experimental studies to investigate the behavior of concrete slab bridges at service and ultimate load levels was conducted by Azizinamini et al. (1994a, 1994b). In these studies, the focus was placed on the failure probability of concrete slab bridges and attempt was made to develop a more accurate approach for rating those bridges. A five-span concrete slab bridge was subjected to numerous tests including ultimate load tests. Only three span continuous portion of the bridge was considered. The bending moment's frequency distributions were obtained using Monte Carlo simulation technique. This simulation was used developed the probability density functions (PDF) for both load effect and resistance. Figure 2-1 shows possible PDF for Q and R. The PDF of load effect, $f(Q)$, is shaped by contributions from PDFs of the local traffic variables such as vehicle type and weight. The probability of failure is equivalent to the cross hatched area. Obviously, the probability of failure is zero when $L_R \leq V_Q$ meaning that the bridge is deemed to be safe for the specified distribution Q and R. The outcome of this work shows that the concrete slab bridges have a large reserve capacities and might carry the modern trucks on the highway.

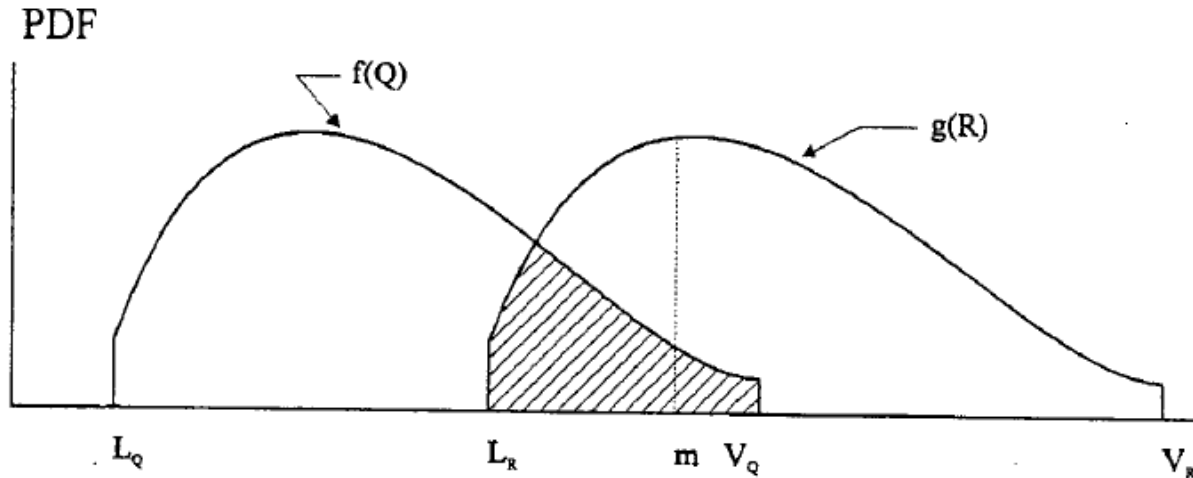


Figure 2-1 Hypothetical Probability Density Functions for the Load Effect Resistance
(Azizinamini et al. 2000)

Highway bridge rating practice in the United States currently follows the procedures outlined in the American Association of State Highway Transportation Officials (AASHTO). Field tests results of old bridges show that there is a considerable reserve capacity in term of strength in most of the bridges that is not justified by the rating procedure within the standards of AASHTO which classify them as structural deficient. Azizinamini et al. (1994) outlined the experimental part of the aged reinforced concrete bridges both at service and ultimate levels in order to be rated more realistically. To accomplish these objectives, six concrete slab bridges were tested under the selected weights of truck loads so that the bridge responses would be confined to the elastic regime (service load tests). Also, a five span reinforced concrete built in 1938 was tested destructively and that was performed by applying loads that simulated two trucks side by side on the structure. Experimental test results show that the reinforced slab bridges have much higher strengths than the indicated by AASHTO rating procedures.

Dauids et al. (2012) explored the potential improvement of the equivalent strip width method described in the AASHTO. Prior studies that involved the FE analysis of slab bridges have relied on FE software packages (Jauregui et al. 2007, 2010; Masbout et al. 2004; Saraf 1998). However, Dauids et al. (2012) developed a software in MATLAB called SlabRate which was designed to analyze the flat slab concrete bridges. The developed FE analysis program assumes linearly elastic, isotropic materials and small deformations and relies on eight-noded, quadratic, shear deformable element that follows the Mindlin plate theory. The results obtained from this software was verified

with available analytical solution with simply supported, rectangular plates under uniform and point loads. The comparison between the FE-predicted and measured response of the existing structure indicates that the FE analyses of the type reported in this study are conservative tools for load rating flat slab bridges. Despite this conservatism, the FE analyses predict significantly higher rating factors than AASHTO approximate analysis.

Chajes et al. (1997) conducted an experimental load rating of a posted, three-span, slab and steel-girder-and-slab bridge. Each span of the bridge consisted of a cross section of nine non-composite steel girders, with the outer girders spaced 1.37 m apart and the interior girders spaced 1.52 m on center. They conducted a load diagnostic test and found that the girders act compositely with the concrete deck and a high restraint observed at the supports. Along the diagnostic test, a predetermined load was placed at several different locations along the bridge and the bridge response was measured. The measured response was then used to develop a numerical model of the bridge. This numerical model was employed to determine the maximum allowable load by applying the load incrementally until a target load was attained or a predetermined limited state was exceeded. The results indicate that the bridge's load carrying capacity may be substantially higher than the current load levels indicate and suggest that the posting levels on the bridge may be unnecessary.

Cai and Shahawy (2004) conducted a load test on six prestressed concrete bridges with different geometric characteristics to evaluate analytical methodologies for load rating, which was shown to be unreliable (Cai et al. 1999). The main objective was to compare the results from the measurements obtained from their study with AASHTO codes specifications and with those ratings predicted using finite element analysis. The comparison showed a notable difference between the analytical and experimental due to the effects of several factors. However, to examine these effects, the authors included some field factors in their finite element models which in turn had a large effect on the maximum strain than on the load distribution factor. Parametric studies on the effects of the components of the bridges were also carried out in this studies to assess how the distribution and maximum strain were affected.

Turer and Shahrooz (2011) presented an investigation of the use of 2D grid models for field-calibrated model based load rating of concrete deck on steel stringer bridges. The authors began with a review of the concept and the calculation of load rating and then discussed three different

levels of analytical modeling for bridge load rating; namely the 1D line-based, the 2D grid-based and the 3D finite element models. The main hypothesis in this work was that 2D grid models are an efficient tool for modeling concrete deck on steel stringer bridges which will be then used for model calibration against bridge tests and the calibrated models can be finally used for load rating. The 2D grid model used in this paper employed linear elastic beam elements configured as a grid simulating the entire superstructure and the deck. As to their model calibration, the researchers used a code written in Matlab based on an automatic updating algorithm which performs structural analysis and objective function optimization. As to the response variable used for updating, they used both modal data (frequencies, modal assurance criteria (MAC) and order of modes) and static deformations (BGCI-Bridge Girder Condition Index). Therefore, their objective (or error) function was a sum of normalized strain error, frequency error, MAC error and mode order errors. The optimization was performed in a step-by-step and staged manner in which similar parameters were grouped and treated as one parameter so as to find an initial approximate solution and then group was divided to subgroups of parameters and the process was repeated until convergence. The proposed method was then applied on an actual three-span four-lane concrete deck on a steel stringer bridge built in 1968. Load ratings were calculated using the allowable stress rating (ASR) and the load factor rating (LFR). The authors concluded that the updating scheme had been efficient and successful, 2D grid models provided results close to 3D models and that transverse members were the critical and controlling members in the system's load rating.

2.4 Condition Assessment using Video Imaging

As discussed above, static or dynamic load tests have been mainly conducted to assess the condition of a structure. However, load testing on bridges might require a closure of at least one lane of the bridge impeding the traffic from moving fast. Although good information can be extracted to be used for rating purpose, this requires time and effort for execution of testing. To overcome these issues, some researchers explored the use of computer vision and sensing in bridge testing. Video image-based structural health monitoring (SHM) have received attention of various researchers (Wahbeh et al. 2003; Catbas et al. 2004; Fraser and Elgamal 2006; Chen and Feng 2006; Zaurin and Catbas 2007; Fraser et al. 2010). Catbas et al. (2011) described a new methodology that uses image and sensor data to obtain an experimental load rating of bridges. They instrumented a movable bridge located in Fort Lauderdale, Florida called Sunrise Bridge built in 1989. The bridge had double bascule leaves, each approximately 22.4-m (73 ft 10 in.) long and

26.15-m (53 ft 4 in.) wide, carrying three traffic lanes. Data from a video stream were processed to detect, classify, and track vehicles, with unknown load configuration, as they cross the bridge while traditional sensors measure the responses. Images and responses were correlated and used to obtain the unit influence lines (UILs). A finite element model (FEM) of the bridge was also developed along with the data collection to validate with the real-life traffic operation and to support the applicability of UILs. The UILs were used for load rating by multiplying the UIL vector of the critical section with load vector from the HL-93. The results were compared with the FEM results and showed a good agreement.

2.5 Summary

A number of researchers have explored an acceptable method for predicting the load bearing capacity of a bridge structure from its measured static or dynamic response in the field. Most of these studies calibrated an initial finite element model of structure based on measured response and used this calibrated model to carry out the load rating, while there has been limited efforts that examined a method to obtain load rating without a calibrated finite element model. Next section describes a simplified load rating procedure for T-beam bridges based on limited field response measurements.

3 VIBRATION-BASED SIMPLIFIED METHOD FOR BRIDGE LOAD RATING

3.1 Overview

This section describes a load rating methodology for RC T-beam bridges without structural plans. The method was originally proposed by Bagheri et al. (2017) for RC slab bridges and is extended to T-beam bridges in this work. It relies on dynamic measurements to identify flexural rigidity of the bridge and employ the strain measurements to estimate the area of reinforcing steel. A detailed description of the methodology is provided below.

3.2 Description of Methodology

3.2.1 Step 1: Determine Geometric Characteristics of Bridge

Since the structural plans are missing, geometric characteristics of the bridge such as span length, width, girder dimensions need to be measured. The measurements are taken in the field by using some digital measuring devices or other devices such as a tape measure to obtain the dimensions of exterior geometry of bridge structure as shown in Figure 3-1.

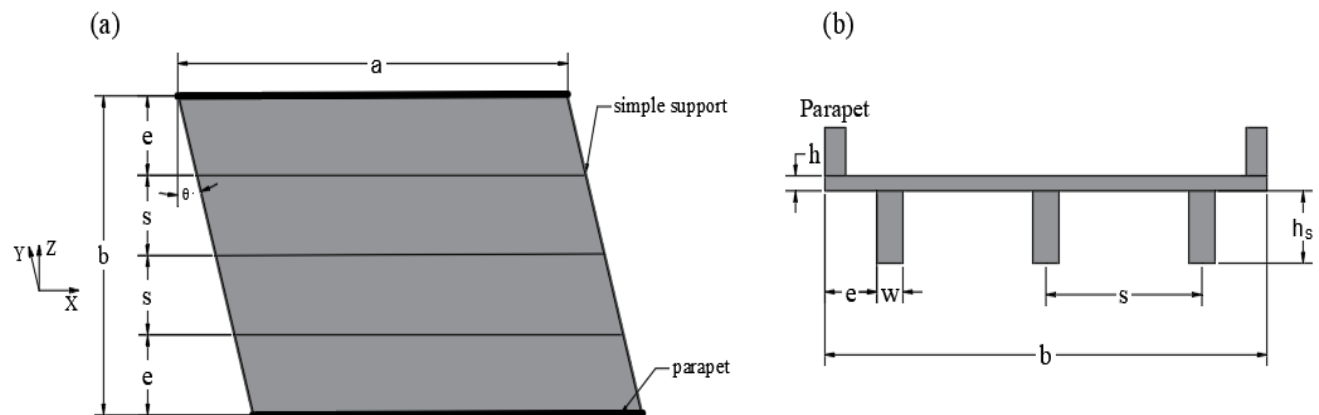


Figure 3-1 Geometric Characteristics of the T-beam bridges

3.2.2 Step 2: Conduct Live Load Testing

Live load testing is defined by AASHTO as an “effective means of evaluating the structural response of a bridge”. In the proposed method, a live load testing is conducted to obtain strain response of the bridge at certain locations. This measured response will be used later to estimate the area of reinforcing steel in the concrete member.

For live load testing, one span of the bridge can be instrumented with strain transducers underneath the beams for T-beam bridges. Strain sensors can be installed at mid-point of span in longitudinal direction. For T-beam bridges, the number of required sensors depends on the number of girders of the bridge. The sensors can be positioned at the midpoint of each girder, where the maximum deflection is most likely to occur.

The steps discussed below can be followed when conducting a live load testing on a bridge structure:

1. Load trucks to approximate AASHTO HS20 and legal VDOT truck configuration and utilize truck weigh stations to determine actual axle weights.
2. Based upon actual axle weight, mark a point on each truck in such a way that when this point is aligned with midspan locations of deck panels, the truck load causes the maximum moment in deck panels. Measure transversely for wheel paths.
3. While the trucks are being loaded prior to testing, the survey crew sets up and determines girder midspan locations (T-beam bridges). These locations are marked for future alignment of truck marks and midspan locations in Step 5.
4. Measure surface elevations of points to establish a baseline for testing scenario 1.
5. Move Truck at crawl speed ~5 mph across the bridge.
6. Record the time the truck is in position and ensure that the truck stays in position long enough to allow the sensors to register their readings (sensors collect data at 5-second increments during the 10-minute time period, and these readings were averaged).
7. Move the truck off the bridge.
8. Repeat Steps 4 to 7 for the remaining testing scenarios.

Note that in the live load testing, a 1 *min* of strain signal can be recorded with a sampling frequency of 100 *Hz*.

3.2.3 Step 3: Conduct Vibration Testing

The proposed methodology requires the determination of natural frequencies of the analyzed bridge. Therefore, a vibration testing on the bridge needs to be conducted. For the vibration testing, the selected T-beam bridge needs to be instrumented with accelerometers attached underneath the girders. Installation of a few accelerometers is sufficient for identifying modal frequencies of the bridge. In particular, three accelerometers are suggested to be installed to measure acceleration response of bridge in vertical direction. Accelerometers can be installed at mid-span to maximize

the sensitivity to the amplitude of vibration response of the bridge. The vibration response of the bridge can be collected under ambient loading conditions including wind loading and normal traffic. An impact hammer can also be used to excite the structure but that will require partial closure of the bridge. In ambient vibration testing, bridge vibration should be recorded for 15 minutes with a sampling frequency of 500 Hz.

3.2.4 Step 4: Identify Modal Properties of Bridge

Operational modal analysis enables the derivation of the modal parameters from the dynamic response of a structure under operational loads. A number of methods have been developed for output-only system identification of structures. In this study, the frequency domain decomposition (FDD) or Enhanced Frequency Domain Decomposition (EFDD) algorithm was used for identifying the modal properties of the bridge from the collected acceleration response. In the FDD method, unknown inputs and acquired outputs are related through their power spectral densities and frequency response functions (Brincker et al. 2001). By processing the outputs from the experimental data, the power spectral density matrix is estimated. The output power spectral density at discrete frequencies is then decomposed by taking the singular value decomposition of the matrix. The corresponding singular value is the power spectral density function of the single degree of freedom system. This power spectral density function is identified by isolating the peak and comparing the mode shape estimate with the singular vectors obtained for frequency lines around the peak. Enhanced frequency domain decomposition method is an extension to frequency domain decomposition (FDD) method, which is a basic method that is extremely easy to use. In the method, modes are simply picked locating the peaks in singular value decomposition plots (SVD) calculated from the spectral density spectra of the responses. As FDD method is based on using a single frequency line from the Fast Fourier Transform (FFT), the accuracy of the estimated natural frequency depends on the FFT resolution and no modal damping is calculated. However, EFDD method gives an improved estimation of both the natural frequencies, the mode shapes and includes the damping ratios. The EFDD technique allows us to extract the resonance frequency and the damping of a particular mode by computing the auto and cross-correlation functions. The Single Degree of Freedom (SDOF) power spectral density function, identified around a peak of resonance, is taken back to the time domain using the Inverse Discrete Fourier Transform. The

A Methodology for Condition Assessment of T-Beam Bridges without Structural Plans

resonance frequency is obtained by determining the zero crossing times and the damping by the logarithmic decrement of the corresponding SDOF normalized auto correlation function.

In this study, the results for the modal identification techniques were obtained from the ARTeMIS Modal Pro software (ARTeMIS Modal Pro 2016) ; however, other tools are available for performing similar analyses. The steps of EFDD can be summarized as in Figure 3-2.

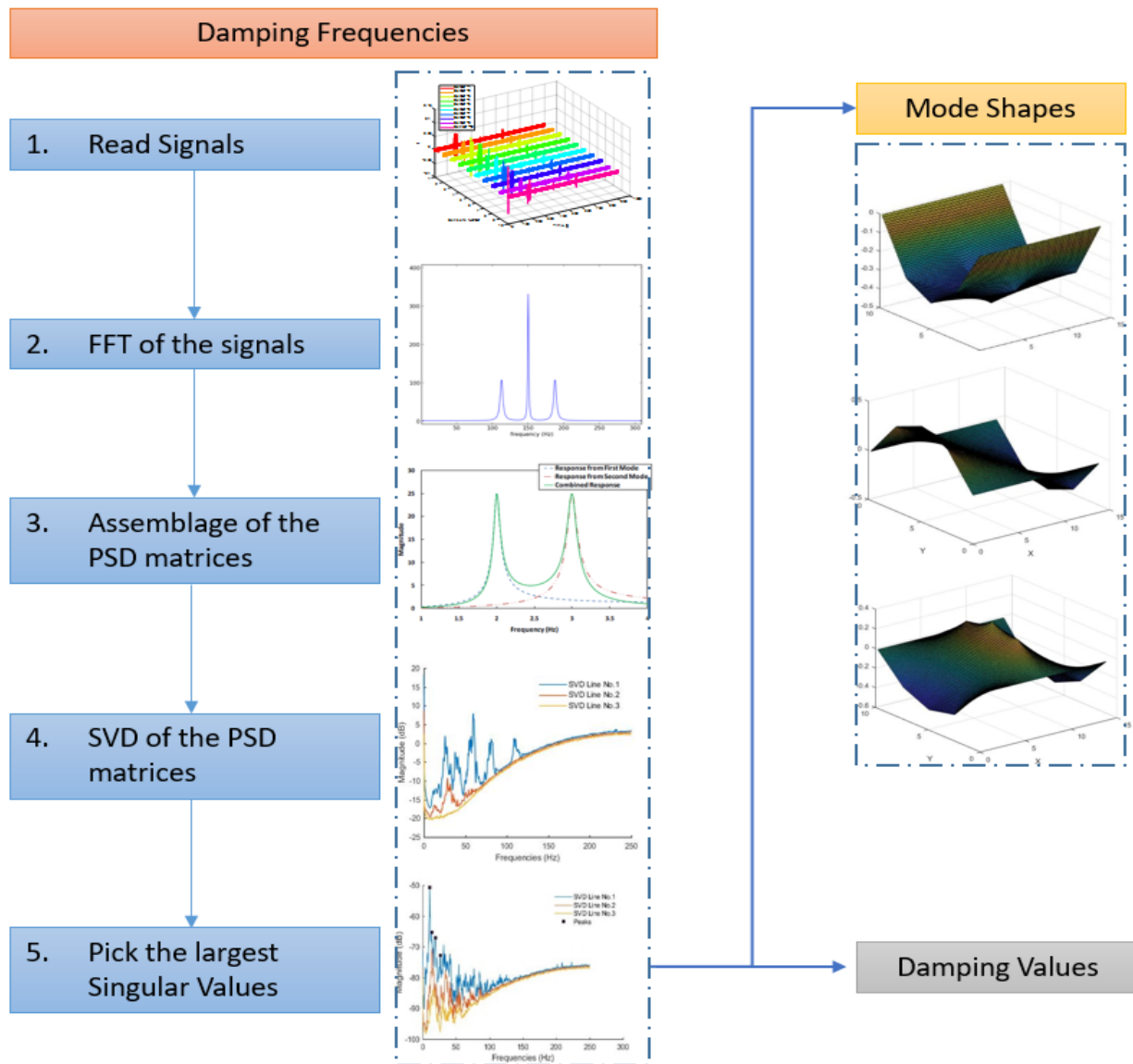


Figure 3-2 Enhanced Frequency Decomposition steps

3.2.5 Step 5: Identify Flexural Rigidity of Bridge

The RC T-beam bridges evaluated in this report are simplified to a plate-like structure with an equivalent thickness, which provides a basis for describing the vibration response of the bridge. From structural dynamics, the relationship between the i -th angular natural frequency ω_i of a continuous plate-like structure and the flexural rigidity D can be established as follows (Leissa 1969):

$$\omega_i^2 = \lambda_i^2 \frac{D}{m}, \quad i=1, 2, \dots \quad (3-1)$$

where λ_i is a non-dimensional frequency parameter associated to the i -th vibration mode; the parameter m is the mass per unit area of the plate and given as ρh , where ρ and h are the density of material and the thickness of plate, respectively; and D is the flexural rigidity of the plate.

If the natural frequency of a plate-like structure is known, which can be determined experimentally through vibration testing as discussed above, the flexural rigidity D can be solved for in Eq. (3-2). However, since the experimentally obtained natural frequencies will inherently include the effects of structural and material damping, the natural frequency ω_i needs to be replaced by $\omega_{d,i}/(1-\zeta_i^2)^{1/2}$, where $\omega_{d,i}$ and ζ_i are the measured damped natural frequency and the damping ratio of the system, respectively. Thus, the flexural rigidity D identified from the i -th modal data is expressed as:

$$D = \frac{\omega_{d,i}^2 \rho h}{(1-\zeta_i^2) \lambda_i^2}, \quad i=1, 2, \dots \quad (3-3)$$

This generalized approach can be used to identify the flexural rigidity of a typical T-beam bridge as long as the value of non-dimensional frequency parameter λ_i is known.

Many T-Beam bridges in the U.S. are constructed as simple spans with supports at two ends of the span and rigid parapets along the two free edges of the structure. Due to their longitudinal rigidity, these parapets may provide a significant contribution to the bridge's overall stiffness. Note that the analytical equations describing the non-dimensional frequency parameter λ_i for plate structures with simple boundary conditions are readily available in the literature; however, this parameter is not suitable for skewed structures with edge stiffening, such as that described by a skewed slab bridge with rigid concrete parapets. Here, a soft computing approach based on the results of a

parametric finite element analysis is described in detail below and was used to compute the parameter λ_i .

The approach described above for plate like-structure was used to determine the flexural rigidity of the T-beam bridges. To this end, the cross-section of T-beam bridge was converted to a uniform cross-section of a plate. A generalized approach of an equivalent thickness was used for this purpose. This is an approximate method that is recommended by the *Concrete Reinforcing Steel Institute Handbook* for use in estimating the vertical deflection of waffle slab panels (Abdul-Wahab and Khalil 2000). The equivalent thickness is defined as the thickness of a uniform plate that has the same bending stiffness as the waffle slab. For a slab under transverse load, the equivalent thickness is obtained by averaging the gross moment of inertia; thus

$$h_{eq} = \left(\frac{12I}{S} \right)^{1/3} \quad (3-4)$$

where S = center-to-center distance between the ribs; and I = moment of inertia of the flanged section including one rib and the top slab of width S . (See Figure 3-1)

To obtain the parameter λ_i for simply-supported T-beam bridges with various geometric properties, a parametric study was conducted using finite element analyses. First, typical ranges of geometric parameters of T-beam bridges such as bridge's span length a , width b , skew angle θ , stem width w , stem height h_s , cantilever e , spacing between girders s , slab thickness h , and number of beams were selected. In numerical models of bridges, an elastic modulus of $2 \times 10^{10} \text{ N/m}^2$, a Poisson's ratio of 0.2, and a density of 2400 kg/m^3 were assumed for the material properties of concrete for the T-beams. With these assumptions, the non-dimensional frequency parameter λ_i becomes a function of the bridges geometric parameters. For a given set of parameters, the natural frequencies of simply supported T-beam bridges were obtained through finite element analysis, and the non-dimensional frequency λ_i was calculated by solving Eq. (3-1) for λ_i . A parametric finite element analysis investigation was performed with variations in the key geometric parameter bridge's span length a , width b , skew angle θ , stem width w , stem height h_s , cantilever e , spacing between girders s , slab thickness h , and number of beams, with a goal of quantifying the parameter λ_i for these variations. Based on the selected ranges for each parameter, the required number of finite element models was 165888. To minimize the modelling and computational efforts, a *MATLAB-ANSYS*

interface was created to run the finite element simulations as shown in Figure 3-3. The geometric parameter of the bridge was written in *MATLAB* and fed into ANSYS to automatically analyze and obtain the natural frequencies of the bridges with different geometric parameters.

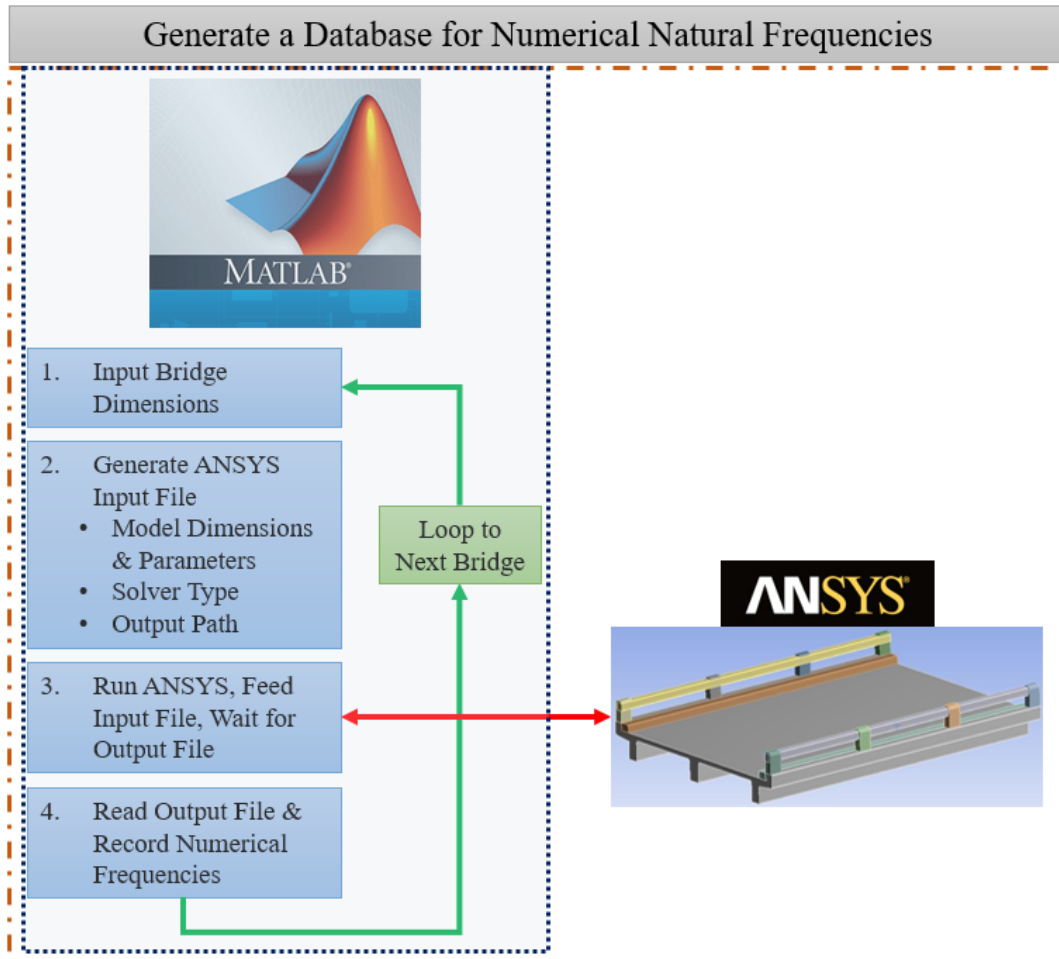


Figure 3-3 Flowchart of the finite element database generation

As mentioned earlier, the obtained frequencies of each bridge were incorporated in Eq. (3-1) and then the non-dimensional frequency parameter for each structure was calculated. In the analysis, the first three modal frequencies of each model were derived for computational efficiency. The results from this parametric study highlighted the complex relationship between the non-dimensional frequency parameters and the bridge parameters. Therefore, an artificial intelligent approach was employed to develop a link between the parameter λ_i and bridge geometric characteristics. To obtain the non-dimensional frequency parameter λ_i , bridge's span length a ,

A Methodology for Condition Assessment of T-Beam Bridges without Structural Plans

width b , skew angle θ , stem width w , stem height h_s , cantilever e , spacing between girders s , slab thickness h , and number of beams (see Figure 3-1 Geometric Characteristics of the T-beam bridgesFigure 3-1) were inputted to neural network model developed for T-beam bridges and the model provides the value of λ_i . Once the λ_i is determined, Eq. (3-2) is used to obtain flexural rigidity D .

The computational framework required for the determination of λ_i from the geometric characteristics is presented in Figure 3-4.

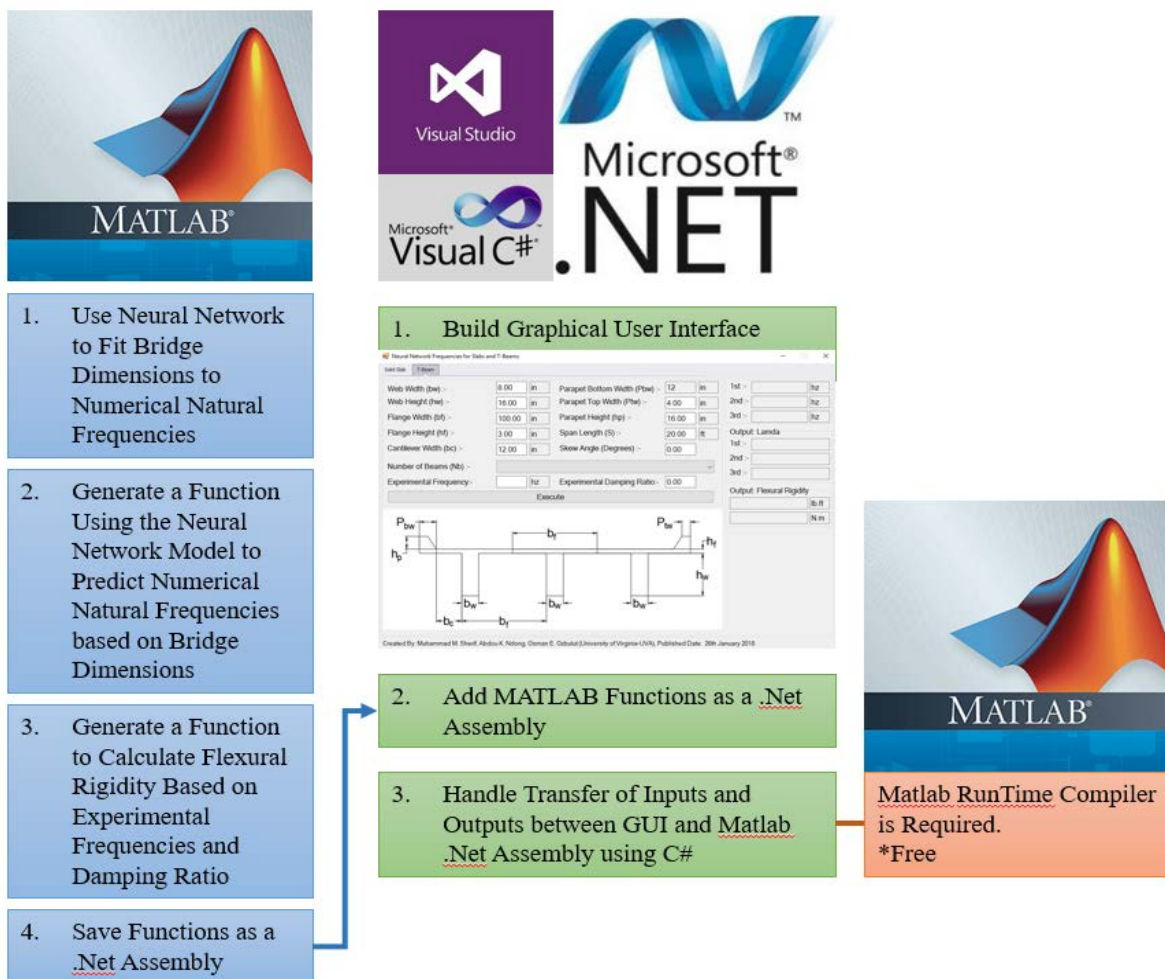


Figure 3-4 Flowchart of the computation required to determine λ_i

An Artificial Neural Network (ANN) was created to estimate the non-dimensional frequency parameter λ_i . The data obtained from finite element simulations of T-beam bridges with various geometric characteristics were used in the development of ANN. The total data consisted of 165,888 data points was divided into three parts: 60% training, 10% validation and 30% testing. The training was made using the Levenberg-Marquardt Algorithm. The Levenberg-Marquardt algorithm is an iterative technique that locates the minimum of a function that is expressed as the sum of the squares of nonlinear functions (Levenberg 1944, Marquardt 1963). Least squares problems results in the context of fitting a parameterized function to a set of measured data points by minimizing the sum of the squares of the errors between the data points and the function. The Levenberg-Marquardt curve-fitting is a combination of the gradient descent method and Gauss-Newton method. The sum of the squares errors was decreased by updating the parameters in the steepest descent direction in the gradient descent method, and reduced by assuming the least squares function to be quadratic in the Gauss Newton method.

For the hidden layer, 40 neurons were selected by means of a trial and error method, and the hyperbolic tangent sigmoid transfer function was employed. For the input and output layers, a linear transfer function was used. The output layer was defined to have two nodes that provide the values of λ_1 , λ_2 and λ_3 . The performance level was tested using the means squared error, with the maximum number of iterations set to 10000 iterations and a mean squared error goal with 10^{-20} . Note that the neural network stops the error even before reaching the goal, if the mean squared error stops decreasing (see Figure 3-5). The best performance was at 513 iterations and the mean squared error was 0.29098. The histogram plot (see Figure 3-6) shows the error distribution of the neural network, most of the error occurs with underestimating the frequencies in the level of 0.1334 Hz, while the errors range between overestimating by 2 Hz for 0.85% of the input data, while underestimating 2.4 Hz for 0.75% of the data. 94.3% has an error ranging between -1 (over estimating) to 1.285 Hz (under estimating), and 73.75% of the data ranges between -0.44 to 0.71 Hz. Looking at Figure 3-7 we can say that the results shown validate our idea of simplicity of curve fitting through ANN, meaning that the training, test and validation data set are found to be similar. The regression coefficient for the training, validation, and training data set are almost 1. The errors found between those are very negligible.

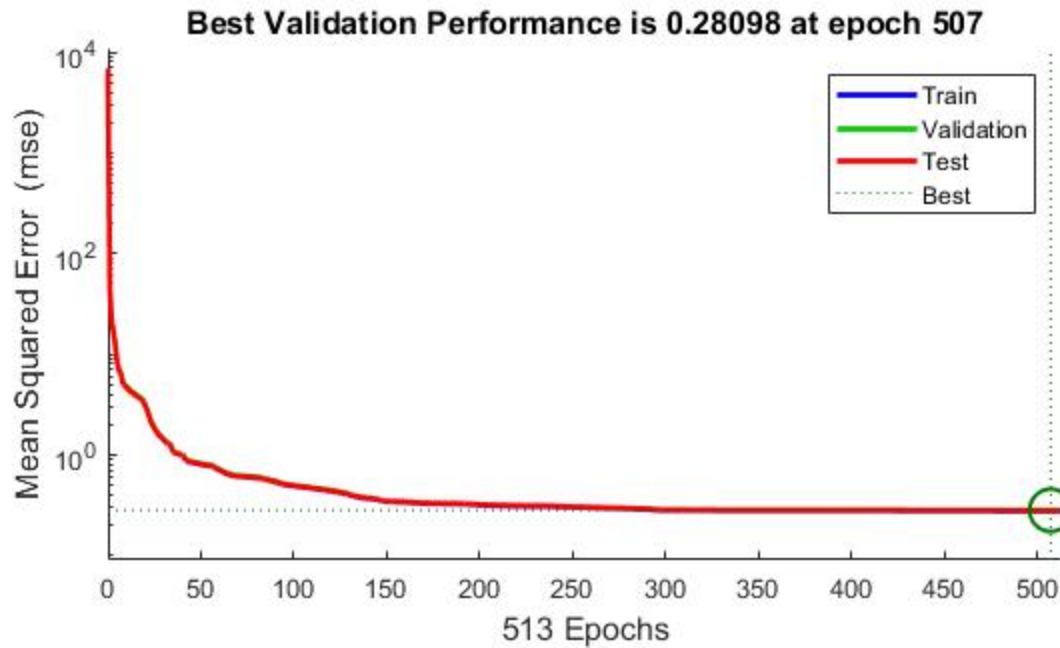


Figure 3-5 Schematic of the evolution of the mean squared errors (averaged over three runs) with increase in the number of epochs

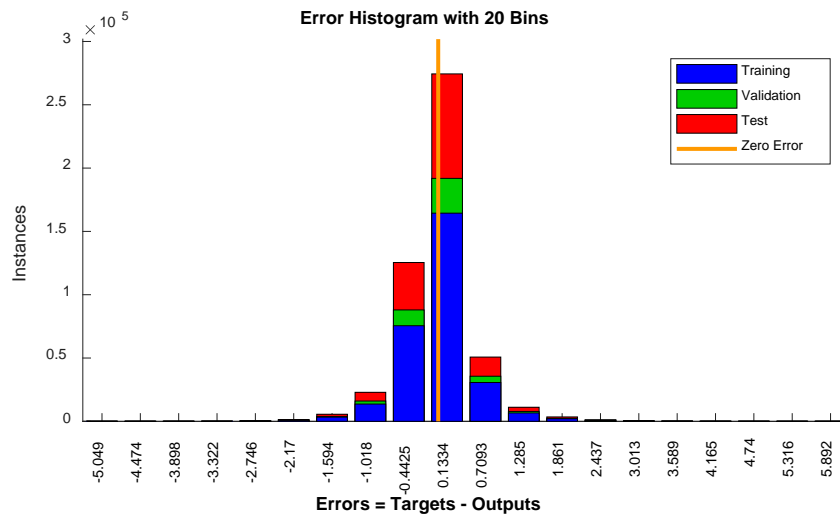


Figure 3-6 Histogram of errors

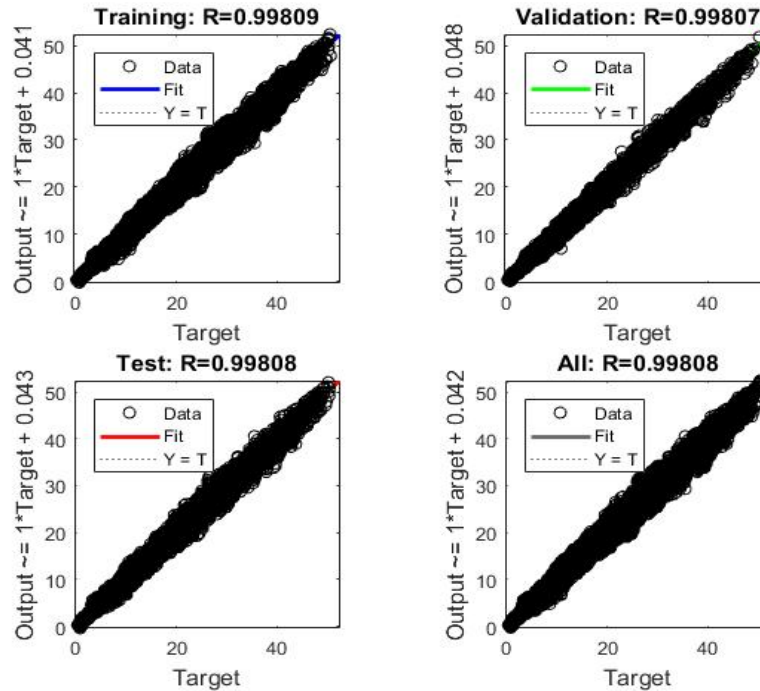


Figure 3-7 Curve fitting

To sum up, the following steps needs to be followed to determine the flexural rigidity D of RC T-beam bridges:

- Enter geometric parameters of the bridge as input to the developed neural network and obtain the non-dimensional frequency parameter λ_i
- From modal identification, determine the first modal frequency of the longitudinal first mode of the bridge and its corresponding damping ratio.
- Calculate the equivalent thickness using Eq.(3-5) for the T-beam bridges for the equivalent thickness of T-beam bridges.
- Use the λ_i and the identified modal frequency in Eq. (3-6) when working with SI units or use them in the following equation when working with US units to obtain flexural rigidity D :

$$D = \frac{3.6 \times \omega_1^2 \times \rho \times h_{eq}}{(1 - \xi^2) \times \lambda_1^2} \quad (3-7a)$$

Note that in Eq. (3-8) or Eq. (3-9a), the term ρ is the mass the density or unit weight of the concrete and generally taken as 145 *pcf*. Also, note that the inherent damping is generally very low in civil engineering structures and about or less than 5% for most of the concrete

structures. So the term $(1-\zeta_i^2)$ can be taken as 1 in Eq. (3-10b) . Thus, the equation of flexural rigidity can also be written as:

$$D = \frac{3.6 \times \omega_1^2 \times \rho \times h_{eq}}{\lambda_1^2} \quad (3-11b)$$

3.2.6 Step 6: Determine Elastic Modulus and Compressive Strength of Concrete

The flexural rigidity D of a plate-like structure is given as (Timoshenko and Woinowsky-Krieger 2009):

$$D = \frac{Eh^3}{12(1-\nu^2)} \quad (3-12)$$

where E and ν are the elastic modulus and Poisson's ratio of the plate's material, respectively. For a plate with unit width, this equation can also be written as:

$$D = \frac{EI_g}{(1-\nu^2)} \quad (3-13)$$

where I_g is the second moment of the area of the cross-section. Note that for RC structures, the cross-section consist of both concrete and steel materials and I_g should be calculated accordingly and E represents the elastic modulus of the composite section.

The composite cross-section can be transformed into an equivalent cross-section with only concrete material with the elastic modulus of E_c and the second moment of inertia of the transformed cross-section of I_t . Since $E_c I_t$ must be equal to $E I_g$, the elastic modulus of concrete can be determined from Eq. (3-14) as:

$$E_c = \frac{E I_g}{I_t} \quad (3-15)$$

and note that from equation (3-16) $E I_g$ for a unit width slab cross-section can be expressed as $E I_g = D(1-\nu^2)$, therefore, we obtain:

$$E_c = \frac{D(1-\nu^2)}{I_t} \quad (3-17)$$

Since D is determined in the previous step, this equation can be used to estimate E_c once I_t is determined. Note that I_t depends to the area of reinforcing steel used inside the slab and the modular ratio, $n=E_s/E_c$, of the cross-section, which are initially unknown. The transformed second moment of the area can be expressed as βI_g , where β is a coefficient that accounts for the different between the stiffness of the transformed versus gross section moment of inertia. A simple parametric study was conducted with a set of values for the modular ratio n and the area of reinforcing steel A_s to investigate the variation of the coefficient β . The ratio n was selected between 5 to 9 which correspond to an elastic modulus of 200 *GPa* for steel material and a range of elastic moduli values between 40 and 22 *GPa* for concrete. This range for concrete is assumed to correspond to concrete mixes with high to normal compressive strengths, respectively. The variation in the coefficient β is not significant for different cross-section properties. In particular, the coefficient β obtains values between a minimum of 1.03 and a maximum of about 1.20. Therefore, by selecting a value for β between these two values, I_t can be estimated by βI_g ; then, the elastic modulus of concrete can be determined by substituting I_t in Eq. (9). If a value of 1.11 is selected for the coefficient β , which represents the average across the parameter space, the maximum error in estimating the elastic modulus is to 9%. For this study, this error was assumed to be acceptable given the uncertainty surrounding the problem space and the coefficient β is recommended to be taken as 1.11.

Once the elastic modulus of concrete is determined, the ultimate compressive strength of concrete f_c can be estimated by available relationships between the elastic modulus and ultimate compressive strength. In this study, the following relationship was used to derive the ultimate compressive strength of concrete as (AASHTO 2014):

$$f_c = \left[\frac{E_c}{0.043 \rho^{1.5}} \right]^2 \text{ in } MPa \quad (3-18)$$

where E_c should be provided in *MPa*, and the compressive strength of concrete represents the strength at the current age of bridge. To evaluate the performance of the described methods in identifying the concrete compressive strength, the 28-day compressive strength of concrete f'_c , which is specified in the design documents, needs to be determined. The prediction model provided in ACI Committee 209 (ACI 209R-92 1998) was used to estimate the 28-day compressive strength of concrete as follows:

$$f'_c = \frac{4 + 0.85t}{t} f_c(t) \quad (3-19)$$

where t represents the age of bridge in days.

3.2.7 Step 7: Estimate Yield Strength and Area of Reinforcing Steel

The yield strength of unknown reinforcing steel used in a concrete bridge is estimated by considering the era of bridge construction. The AASHTO Manual for Bridge Evaluation provides guidance on identifying reinforcement characteristics when structural details are unknown (AASHTO Manual for Bridge Evaluation 2015). Table 1 provides a synthesis of this guidance through a list of the type of reinforcing steel and bridge construction's date with corresponding yield strength of reinforcing steel. The rib pattern of the reinforcing steel is also helpful in identifying the steel grade, if rebar happens to be exposed. Figure 3-8 shows the rib pattern of each type of reinforcing steel. Rib pattern with information provided in Table 3-1 help to identify the yield strength of reinforcing steel.

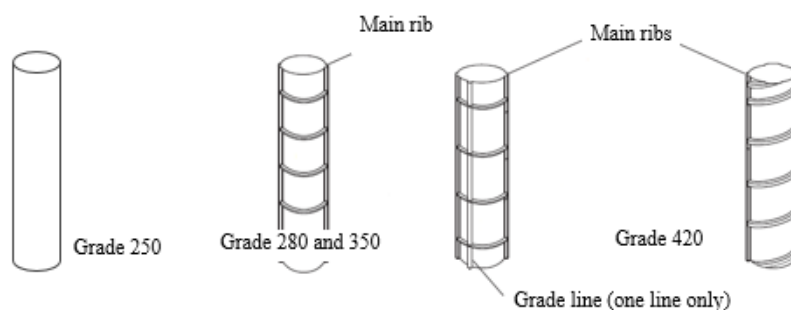


Figure 3-8 The rib pattern for each type of reinforcing steel

Table 3-1 Yield strengths of unknown reinforcing steel (adapted from [1])

Type of Reinforcing Steel	Yield Strength f_y (ksi)	Yield Strength f_y (MPa)
Unknown steel constructed prior to 1954	33	230
Structural grade	36	250
Billet or intermediate grade, Grade 40, or unknown steel constructed during or after 1954	40	280
Rail or hard grade, Grade 50	50	350
Grade 60	60	420

To estimate the area of reinforcing steel in a RC T-beam bridge without plans, an approach based on the measured strain data under a live load is used here. The amplitude of a strain measurement in the RC T-beam recorded during a quasi-static test depends on its cross-section, area of steel reinforcement, elastic modulus of concrete as well as the bending moment developed at the location of sensor under the applied load. Since the cross-section and the elastic modulus of concrete are determined as described in previous steps, the strain can be expressed as a function of two unknown parameters, namely, area of steel reinforcement and bending moment in the cross-section. One approach to obtain these unknown parameters is to minimize an objective function F which can be defined as the error between the experimental and analytical value for strain ε at a given location of bridge as:

$$\min_{A_s, M} F(A_s, M) = \frac{|\varepsilon^{Exp.} - \varepsilon^{Ana.}(A_s, M)|}{\varepsilon^{Exp.}} \quad (3-20)$$

where $\varepsilon^{Exp.}$ and $\varepsilon^{Ana.}$ are the experimental and analytical values of strain, respectively, and the analytical strain can be calculated as:

$$\varepsilon^{Ana.}(A_s, M) = \frac{M \bar{y}(A_s)}{EI_g} \quad (3-21)$$

where A_s and M are the area of steel reinforcement and the bending moment at the location of strain sensor, respectively, and \bar{y} represents the distance between the center of gravity of the stem cross-section and the bottom of the stem where strain sensor is installed.

The above defined objective function has multiple solutions when the bending moment is unknown. This can be seen in Figure 3-9(a) where the objective function is plotted against the various values of the bending moment M and the area of reinforcements A_s for a given experimental strain and measured cross-sectional properties. The figure shows that the objective function is more sensitive to the bending moment M . In order to have only one global minimum in the objective function, a second term should be added to the objective function for increasing the sensitivity of the function to the area of reinforcements. Thus, a term which is the error between EI_g obtained by the experimental and analytical approach, was added to Eq. (3-22) as follows:

$$\min_{A_s, M} F(A_s, M) = \frac{|\varepsilon^{Exp.} - \varepsilon^{Ana.}(A_s, M)|}{\varepsilon^{Exp.}} + \frac{|EI_g^{Exp.} - EI_g^{Ana.}(A_s)|}{EI_g^{Exp.}} \quad (3-23)$$

Experimental EI_g is given in Eq. (8) and the analytical EI_g is equal to:

$$EI_g^{Ana.}(A_s) = E_c I_t(A_s) \quad (3-24)$$

It can be seen that the second term is only a function of the area of reinforcements which only increases the sensitivity of the function to steel reinforcements for forming an objective function with a global minimum. A plot of the updated objective function (3-25) is shown in Figure 3-9(b), which demonstrates the ability of the proposed objective function to converge to a global minimum.

To identify the area of reinforcing steel at a given sensor location of the bridge, the maximum strain measured during a live load test is substituted in Eq. (3-26). Then, the area of reinforcements and the bending moment are determined by minimizing the objective function using a gradient based algorithm in *MATLAB* software.

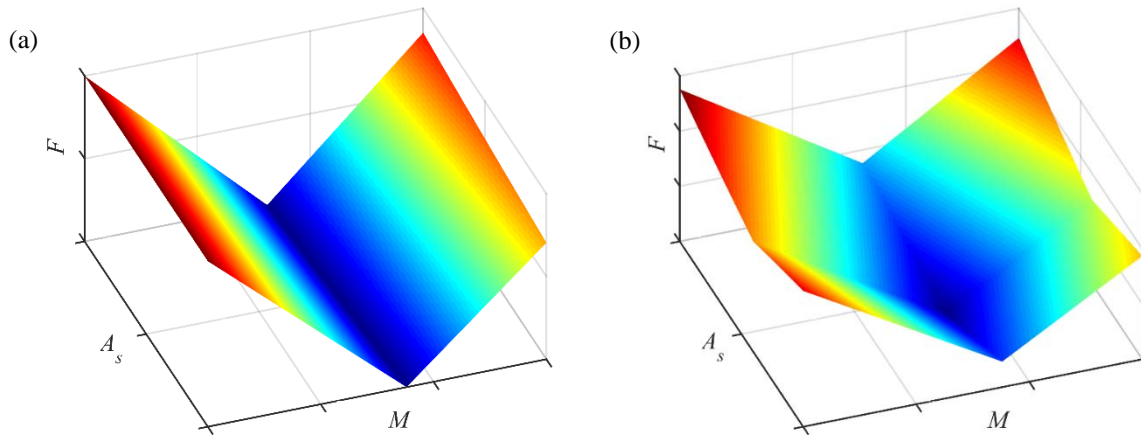


Figure 3-9 Plot of the objective functions defined in: (a) Eq. (11), and (b) Eq. (3-27) (Bagheri et al.2017)

To sum up, the following steps should be followed to determine the area of reinforcing steel in a RC T-beam bridge:

- Determine the elastic modulus of the concrete material using the following:

$$E_c = \frac{bD(1-\nu^2)}{\beta I_g} \quad (3-28)$$

where β is a coefficient for considering the effect of reinforcing steel in calculating the elastic modulus of the concrete material and that is 1.11. I_g represents the moment of inertia of the cross section limited by the spacing between the center-to-center hole and moment of inertia of the flanged section including one rib and the top slab of width S for T-beam bridges.

- The result above is then used for estimating the ultimate compressive strength of the bridge's concrete:

$$f_c = \left[\frac{E_c}{33\rho^{1.5}} \right]^2 \quad (3-29)$$

- Then, the 28-day compressive strength of the concrete is obtained by knowing the age of bridge t in years:

$$f_c^t = \frac{4+0.85t}{t} f_c(t) \quad (3-30)$$

- To identify the amount of longitudinal reinforcement area A_s used inside a stem cross-section of the T-beam bridge, the maximum strain of a strain signal measured during the live load test was used in forming the objective function.

$$\min_{A_s, M} F(A_s, M) = \frac{\left| \varepsilon^{Exp.} - \varepsilon^{Ana.}(A_s, M) \right|}{\varepsilon^{Exp.}} + \frac{\left| EI_g^{Exp.} - EI_g^{Ana.}(A_s) \right|}{EI_g^{Exp.}} \quad (3-31)$$

where I_g is the same as I_b for the stem of T-beam bridges since we have a homogeneous cross section and to avoid the ambiguity of the equation above, the equation can be stated as in the following:

$$\min_{A_s, M} F(A_s, M) = \frac{|\varepsilon^{Exp.} - \varepsilon^{Ana.}(A_s, M)|}{\varepsilon^{Exp.}} + \frac{|EI_b^{Exp.} - EI_b^{Ana.}(A_s)|}{EI_b^{Exp.}} \quad (3-32)$$

$I_b = \frac{bh^3}{12}$ and b and h refers to the unit width and height of the girder width and the equivalent height of the girder for T-beam bridges, respectively. In addition, $\varepsilon^{Ana.}(A_s, M)$ is computed as:

$$\varepsilon^{Ana.}(A_s, M) = \frac{M \bar{y}(A_s)}{EI_b} \quad (3-33)$$

$$\bar{y}(A_s) = \frac{\frac{bh^2}{2} + \left(\frac{E_s \beta I_b}{bD(1-\nu^2)} - 1 \right) \times A_s d'}{bh + \left(\frac{E_s \beta}{bD(1-\nu^2)} - 1 \right) \times A_s} \quad (3-34)$$

where d' is the concrete cover on reinforcing steel which can be assumed to be 2.5 in. $\varepsilon^{Exp.}$ is the maximum strain measured by the installed sensor at a selected location during the live load test. By substituting this experimental strain value and other parameters in the objective function, the reinforcement area A_s can be determined.

3.2.8 Step 8: Determine Capacity

Based on the determined values for material properties and reinforcing steel, the bending capacity is computed as from the following equation:

$$M_u = \phi A_s f_y \left(d_s - \frac{a}{2} \right) \text{ where } a = \frac{A_s f_y}{\beta_1 f_c' b_e} \quad (3-35)$$

where a is the size of the compression stress block and b_e is the effective width of the beam of the cross-section.

3.2.9 Step 9: Determine Load Effects

In general, there are two methods to determine load effects for bridge load rating. The first approach is to use an approximate method of analysis such as the equivalent strip widths, and the second approach is to employ a refined method of analysis such as finite element or finite difference methods (AASHTO 2014).

The approximate method analysis for T-beam bridges, the live load effects can be easily calculated as described below for interior and exterior beams:

Interior Beam:

- Determine distribution Factor for moment, g_m (LRFD Design Table 4.6.2.2b-1)
 - One Lane Loaded:

$$g_{m1} = 0.06 + \left(\frac{S}{14}\right)^{0.4} \left(\frac{S}{L}\right)^{0.3} \left(\frac{K_g}{12L_s^3}\right)^{0.1} \quad (3-36)$$

- Two or More Lanes Loaded

$$g_{m2} = 0.075 + \left(\frac{S}{9.5}\right)^{0.6} \left(\frac{S}{L}\right)^{0.2} \left(\frac{K_g}{12L_s^3}\right)^{0.1} \quad (3-37)$$

where K_g , longitudinal Stiffness Parameter, can be obtained as follows:

$$K_g = n(I + Ae_g^2) \quad (3-38)$$

The maximum between the two will govern and will be used in the calculation of live load effects.

Exterior Beam:

- Determine distribution factor for moment, (LRFD Design)
 - One Lane Loaded:

Use Lever rule (LRFD Design)

- Two or More Lanes Loaded

$$g = e \times g_{\text{int}} \quad (3-39)$$

$$e = 0.77 + \frac{d_e}{9.1} \quad (3-40)$$

- Check following equation as well:

Rigid Section: 4.6.2.2.d

$$R = \frac{N_L}{N_b} + \frac{X_{ext} \sum_1^{N_L} e}{\sum_1^{N_b} x^2} \quad (3-41)$$

- Determine Maximum Factored Moments

$$M_{DC} = \gamma_{DC} DC$$

$$M_{DW} = \gamma_{DW} DW$$

$$M_{LL+IM} = \gamma_{LL} (LL + IM)$$

$$\gamma_{DC} = 1.25$$

$$\gamma_{DW} = 1.50$$

$$\gamma_{LL} = 1.75$$

For these load combinations, loads are abbreviated as follows:

DC = dead load of structural components.

This includes temporary concrete barriers used in stage construction. Parapets, curbs, and railings using the standard details found in Section 3.2.4 of the Bridge Manual need not be included in this value. Standard details for these components include additional longitudinal reinforcement and stirrups that, when built integrally with the slab, are adequate for self-support.

DW = dead load of future wearing surface

IM = impact or dynamic load allowance

LL = vehicular live load.

For certain bridges, such as bridges with varying skews at supports and bridges with low ratings, refined analysis methods would be considered to be more appropriate (AASHTO 2016). In addition, a comparative study between the approximate method and finite element analysis of a large number of RC T-beam bridges found that the approximate method overestimates the bending moment by up to 40% for bridges with skew angles less than 30°, while this overestimation reaches to 50% for bridges with skew angle of 50° (Menassa et al. 2007). Therefore, a refined method of analysis for determining bending moments under dead and live loads provides more reliable results. To conduct a refined analysis using numerical simulations, geometric, material, and structural properties of a bridge should be defined in a numerical model. After identifying all these parameters described in previous sections, the model of bridge is simulated and analyzed under

dead loads and live loads defined in AASHTO Manual for Bridge Evaluation (AASHTO 2016) to obtain maximum bending moment for load rating factor computing.

3.2.10 Step 10: Compute Load Rating

A load rating factor (RF) is computed to estimate the safe load carrying capacity of a bridge. The RF provides an estimate of the relationship between the remaining live load carrying capacity of a bridge and the live load demand, with a value greater than 1.0 signifying remaining capacity is available and a value less than 1.0 indicating the specified loading exceeds available capacity. The RF used within the current AASHTO Manual for Bridge Evaluation is based on a load and resistance factor rating method and is given as follows (AASHTO 2016):

$$RF = \frac{C - \gamma_{DC}DC - \gamma_{DW}DW \pm \gamma_P P}{\gamma_{LL}(LL + IM)} \quad (3-42)$$

where C is the capacity of member, DC and DW are dead load effects due to structural components and wearing surface, respectively, P is applied permanent loads other than dead loads, LL and IM represent live load effect and its dynamic effect, respectively, and γ is a load factor that depends on the type of load and limit state. For bridges without plans, the parameter C is computed based on the methodology described above and the load effects are computed as described in Step 9.

3.3 Summary

In this section, a load rating methodology for RC T-beam bridges with as-built information was proposed. The methodology employs the results obtained from a live load testing and vibration testing to determine the capacity of a T-beam bridge without structural plans. Both tests require only a limited number of sensors and can easily be implemented in the field. The process to obtain the rating factor for such bridges were explained step-by-step in this section. Next section shows the implementation of the developed methodology into rating of two in-service bridges.

4 EXPERIMENTAL TESTING

4.1 Overview

This section provides a detailed description of experimental testing of two RC T-beam bridges and implementation of the load rating procedure proposed in earlier section to the rating of these bridges. The tested structures are called Flat Creek and Bratton's Creek bridges and are located in Richmond, Virginia. Here, first, the equipment used in the field testing is described. Then, geometric characteristics of the bridges and their instrumentation are provided. Finally, live load testing and vibration testing that were conducted on these bridges are explained.

4.2 Equipment

Instrumentation used for the live load test primarily consists of strain transducers connected to the same wireless data acquisition system described above. The device model is called the ST350 Strain transducers and manufactured by Bridge Diagnostics Inc. (BDI) Win-STS. The ST350 Strain Transducers have been designed for recording Live Load Strains only. This is because it is assumed that there will be little to no temperature change during any short time-span testing sequence. BDI Strain Transducers have been calibrated (within $\pm 2\%$) with a precision equipment traceable to NIST standards. The strain range is $\pm 2000\mu\epsilon$ and the sensitivity is approximately $500 \mu\epsilon/mV/V$. These transducers are also connected to the same based station that is described below. Data collected from the DAQ system was saved automatically by the BDI-STS software as an excel file.

Instrumentation used for the vibration test primarily comprised of a set of accelerometers connected to a wireless data acquisition system. An impact hammer was used for the forced vibration test and was also connected to the same data acquisition. The DAQ system used in this work was fabricated by BDI. The DAQ included the BDI Win-STS software that was installed on a standard laptop manufactured by Panasonic (Model CF350). The BDI package includes some accelerometers which were made of micro-machined capacitive sense element. The accelerometers were designed for dynamic structural testing in tough field conditions. These accurate, rugged, and fully-weatherproofed units can be installed very quickly and are in a range of $\pm 5g$ and a differential sensitivity of $1V/g$. These sensors were connected to a BDI STS-Wi-Fi node by 20 feet long field-grade instrumentation cables. Each BDI has a total 6 nodes with an individual capacity to hold 4 transducers providing a total capacity of 24 transducers capable of simultaneous data collection.

A Methodology for Condition Assessment of T-Beam Bridges without Structural Plans

However, due to the limited number of accelerometers that is 10, only a few of these nodes were used at a time. These were then connected wirelessly to a single base station which in turn was connected to the laptop using a Wi-Fi signal. For the forced vibration test, an impact hammer was used that was manufactured by PCB Piezotronics and had a force range of 0 – 5000 lbf. The hammer was of model 086D50 and included two different impact tips (a stiffer and softer tip). The hammer was connected to a PCB Piezotronics signal conditioner model 480E09 using BNC cables which in turn was connected to the BDI node using another BNC. Figure 4-1 shows the equipment used in the field testing.

Calibration files for each of the sensors connected to the DAQ system were factory computed and installed in the software. Calibration for the impact hammer was based on the impact hammer voltage to force sensitivity and was done manually. Data collected from the DAQ system was saved automatically by the BDI-STS software as an excel file.

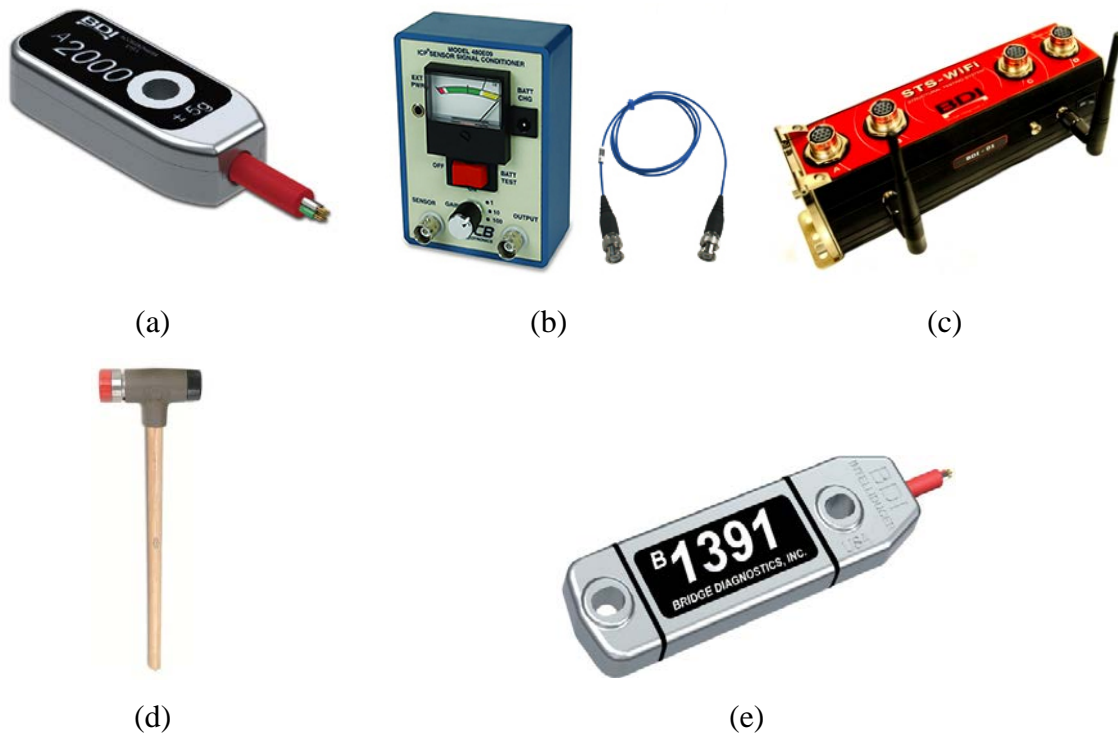


Figure 4-1 (a) BDI Accelerometer, (b) PCB Signal Conditioner, (c) BDI STS-Wi-Fi Node, (d) PCB Impact Hammer, (e) ST350 Strain Transducer

4.3 Bridge Descriptions and Instrumentation Plan

Two bridges, were selected for load testing. The first test was on a four-girder reinforced concrete T-beam bridge called Flat Creek and the second one was a three-span reinforced concrete T-beam bridge named Bratton's Creek.

4.3.1 Flat Creek Bridge

4.3.1.1 Geometric Characteristics

One of the selected bridge for the field testing is a concrete T-beam bridge, named as Flat Creek and built in 1957. It is a five-span simply-supported bridge located in Rockingham County, Virginia, USA. The recent inspection described the bridge to be in “fair” condition, with a deck/superstructure condition rating of 7. The bridge was selected from amongst the Virginia Department of Transportation (VDOT) population of reinforced concrete T-beam bridges with plans, with special consideration given to geometry similarity to the population of this major category of bridges without plans.



Figure 4-2 A side view of the Flat Creek bridge

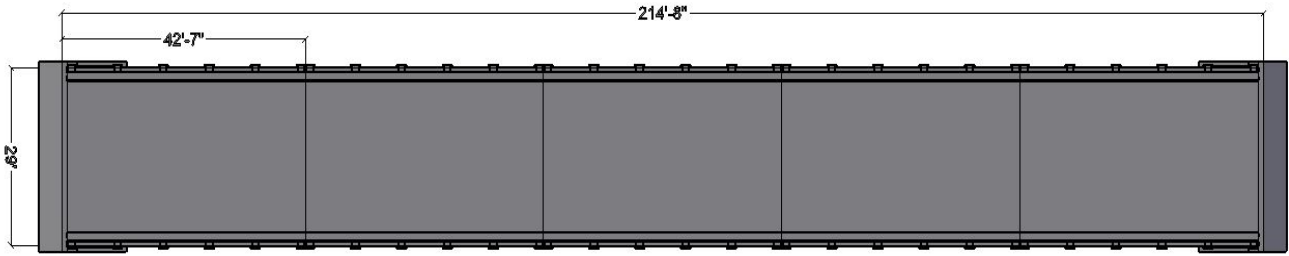


Figure 4-3 Plan view of Flat Creek bridge

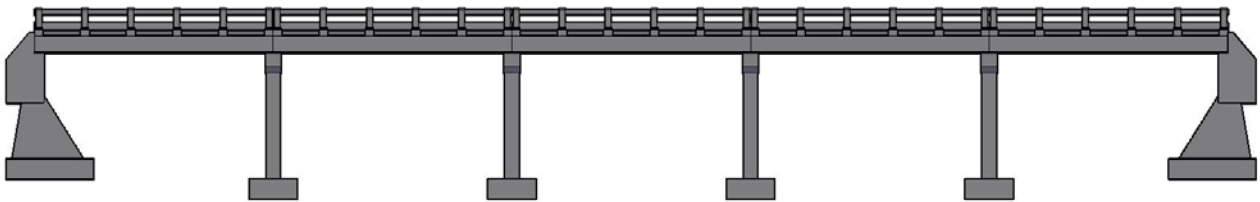


Figure 4-4 Elevation view of Flat Creek bridge

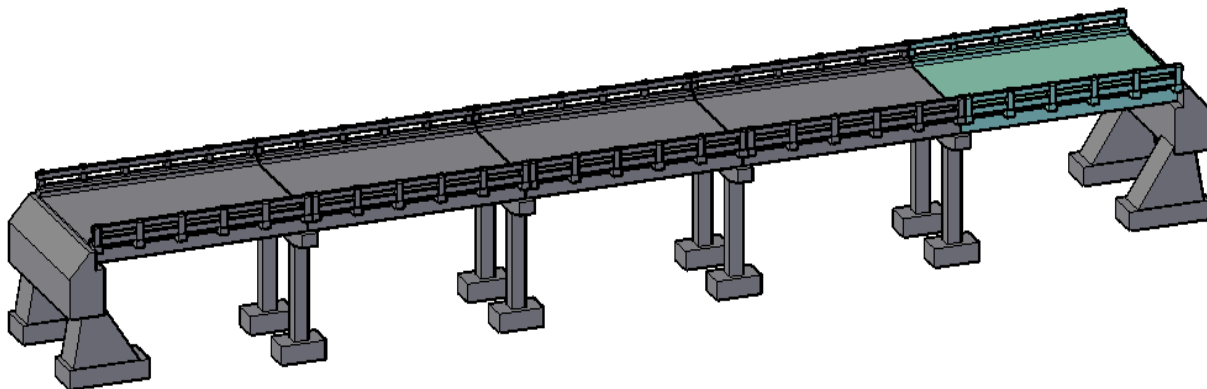


Figure 4-5 3D view of Flat Creek bridge

A Methodology for Condition Assessment of T-Beam Bridges without Structural Plans

In Flat Creek Bridge, the superstructure is comprised of two 42.5-ft long, simply-supported cast-in-place reinforced concrete T-beam that has bridge has a total length of 214.67 ft and a total width of 29 ft, and consists of four longitudinal T-beams. Each T-beam has vertical rectangular stem with a width of 16 ft and a thickness of 32 inches, and a wide top flange of 7.5 ft. The wide top flange is the transversely reinforced deck slab and the riding surface for the traffic. The bridge shown is skewed at an angle of 0 degrees to the main road (See Figure 4.1).

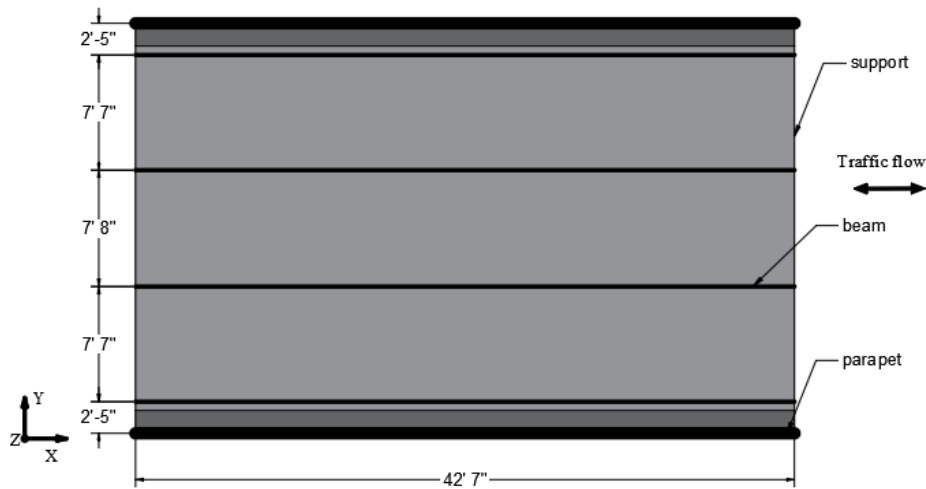


Figure 4-6 Dimensions of the tested Spans (Plan View)

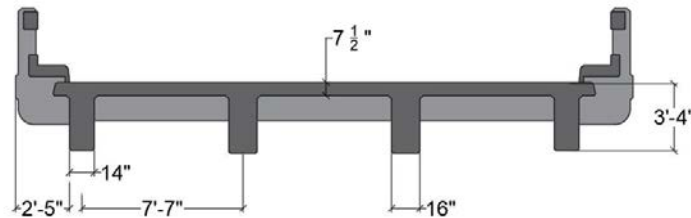


Figure 4-7 Dimensions of the bridge (elevation view)

4.3.1.2 Instrumentation for Live Load Testing

For live load testing, one span of the bridge was instrumented with strain transducers on the underside of the girders of the bridge according to the instrumentation plan in Figure 4-8. Strain sensors were installed at mid-point of span in longitudinal direction. All instrumentation and acquisition comprised of Bridge Diagnostics, Inc. equipment, where individual sensors physically connected to four-channel nodes, which in turn interfaced wirelessly with a base station/data acquisition unit.

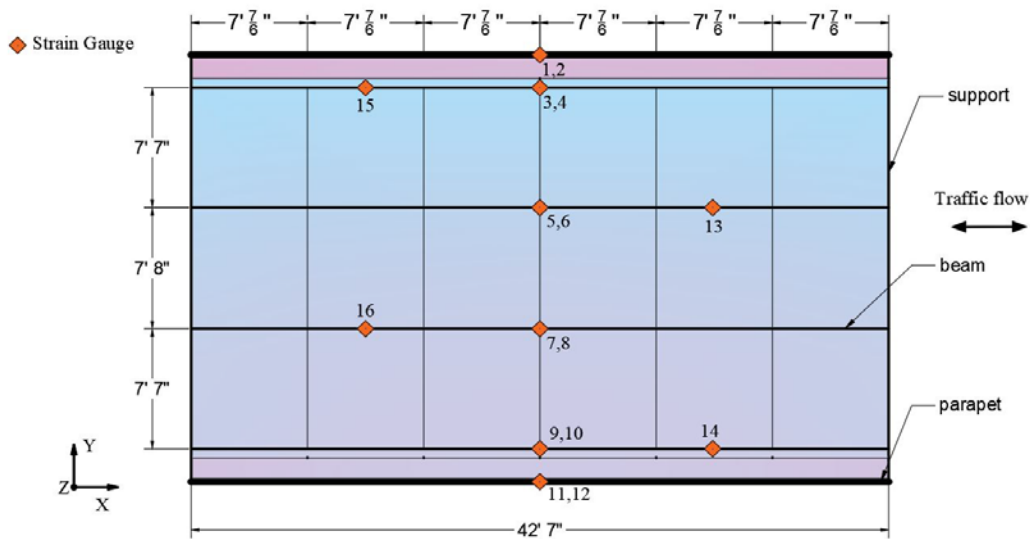


Figure 4-8 Instrumentation layout and strain sensors location

4.3.1.3 Instrumentation for Vibration Testing

The dynamic bridge assessment procedure involves the attachment of nine accelerometers underneath of the span of the bridge at 19 measurement points in two set-ups as shown in Figure 4-9. Note that two common sensors were used as reference in each set-up. The uniaxial accelerometers with a measuring range of $\pm 5g$ were used.

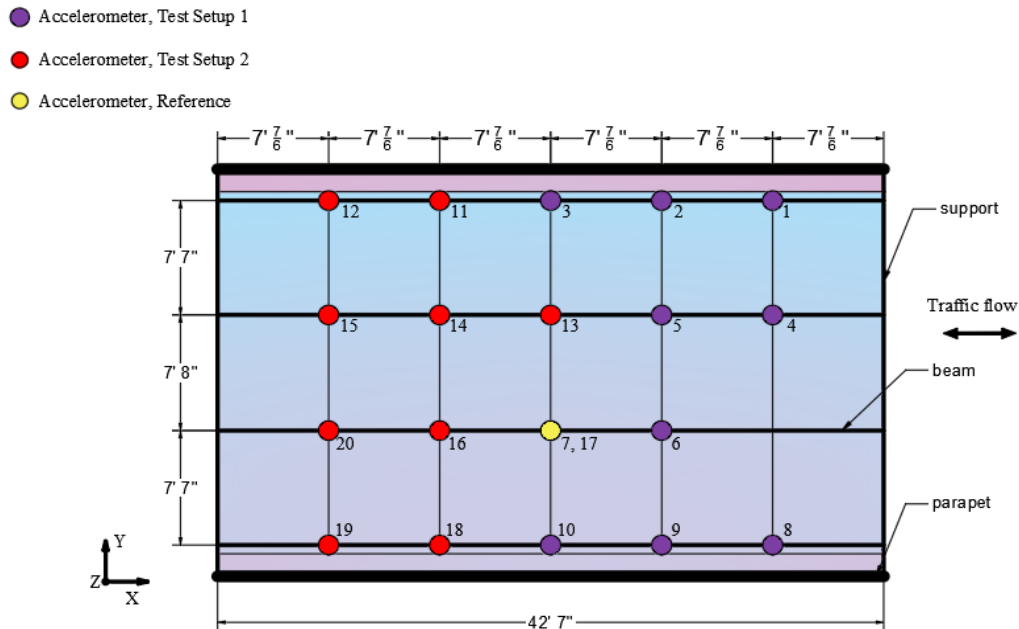


Figure 4-9 – Instrumentation Configuration for Flat Creek Bridge: Vibration Testing

4.3.2 *Bratton Creek Bridge*

4.3.2.1 Geometric Characteristics

The selected bridge for the field testing is a concrete T-beam bridge, named as Bratton's Creek and built in 1952. It is a three-span simply-supported bridge located in Rockbridge County, Virginia, USA. Each span of the bridge has a total length of 32 ft with a total length of 98'-2", and a total width of 23'-8", and consists of four longitudinal T-beams. Each T-beam has vertical rectangular stem with a width of 16" and a thickness of 2 ft, and a wide top flange of 8 ft. The wide top flange is the transversely reinforced deck slab and the riding surface for the traffic. The bridge shown is skewed at an angle of 0 degrees to the main road. The recent inspection described the bridge to be in "poor" condition, with a deck/superstructure condition rating of 5. The bridge was selected from amongst the Virginia Department of Transportation (VDOT) population of reinforced concrete T-beam bridges with plans, with special consideration given to geometry similarity to the population of this major category of bridges without plans. The load rating using LRFR method conducted in 2011, for design load HL-93, listed the inventory load rating at 0.77 and the operating rating at 1.02 (Figure 14d).



Figure 4-10 Side View of Bratton's Creek Bridge

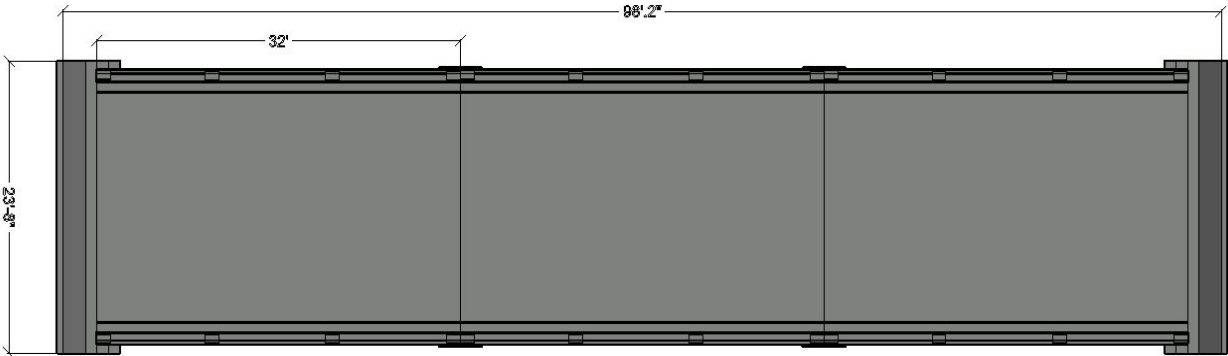


Figure 4-11 Plan View of Bratton's Creek

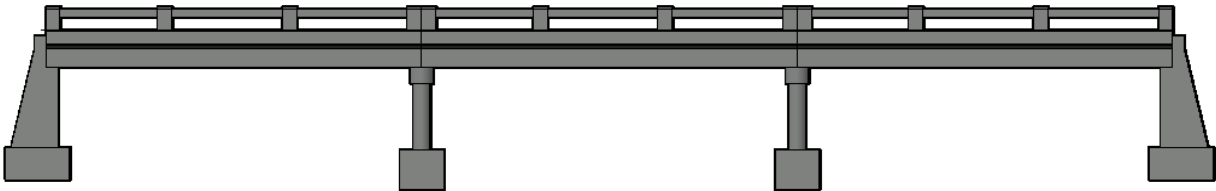


Figure 4-12 Elevation View of Bratton

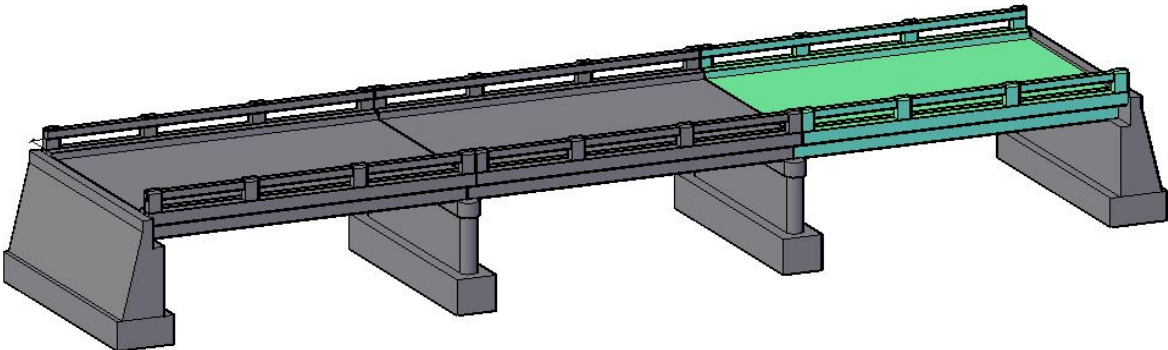


Figure 4-13 3D View of Bratton's Creek (Showing the tested span in green)

A Methodology for Condition Assessment of T-Beam Bridges without Structural Plans

In Bratton's Creek Bridge, the superstructure is comprised of three 32-ft long, simply-supported cast-in-place reinforced concrete T-beam that has bridge has a total length of 92'-2" and a total width of 23'-8", and consists of four longitudinal T-beams. Each T-beam has vertical rectangular stem with a width of 16 ft. and a thickness of 24 inches, and a wide top flange of 9'-5". The wide top flange is the transversely reinforced deck slab and the riding surface for the traffic. The bridge shown is skewed at an angle of 0 degrees to the main road (Figure 4-14).

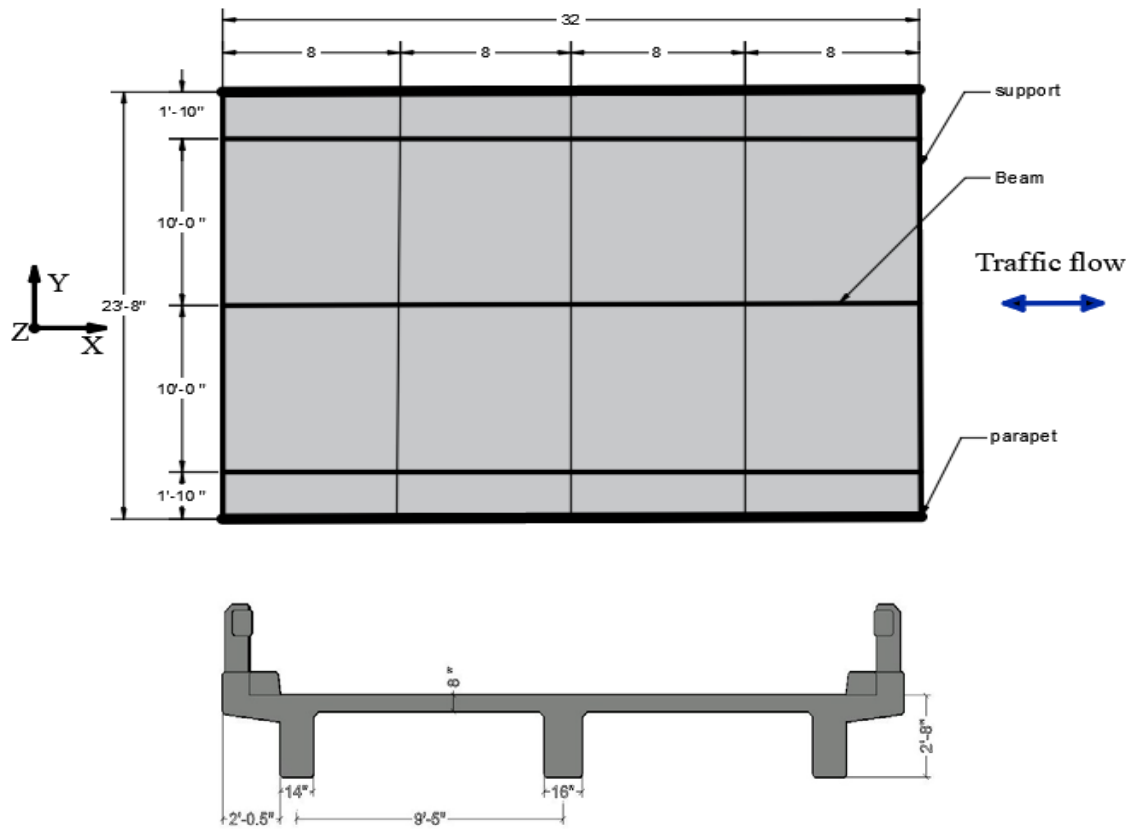


Figure 4-14 Dimensions of the Bridge

4.3.2.2 Instrumentation for Live Load Testing

For live load testing, one span of the bridge was instrumented with strain transducers on the underside of the girders according to the instrumentation plan in Figure 4-15. Strain sensors were installed at mid-point of span in transversal direction.

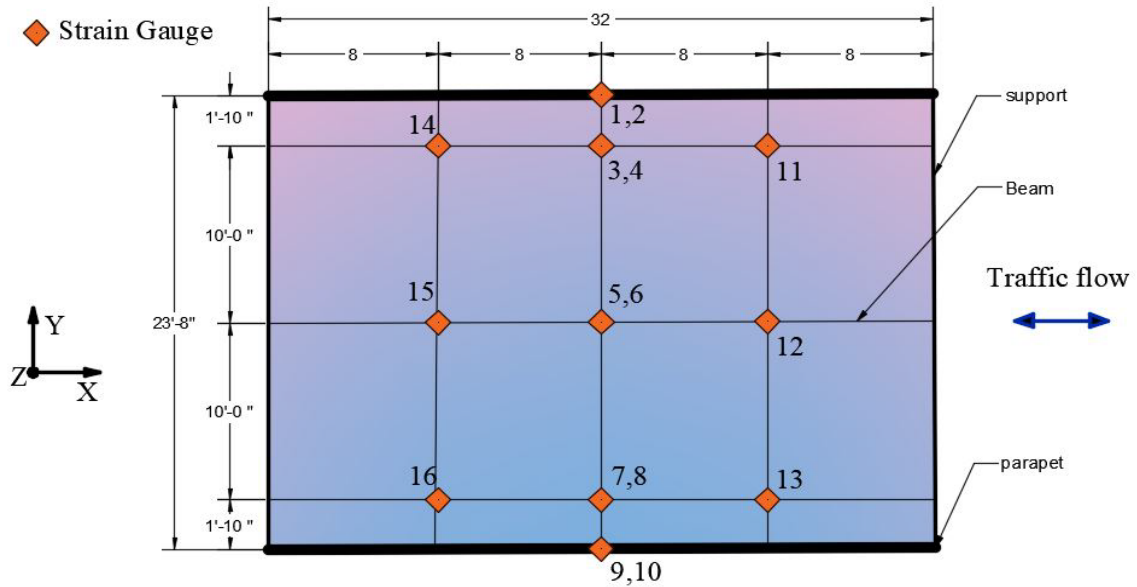


Figure 4-15 Live Load Testing: Strain Sensors Location

4.3.2.3 Instrumentation for Vibration Testing

For the vibration testing, one of the five spans in the bridge was instrumented with accelerometers on the underside of one the girder of the bridge according to the instrumentation plan in Figure 4-16. Only a few accelerometers are enough for identifying modal properties of the bridge from measuring acceleration responses in vertical direction. Accelerometers should be installed at mid-span to maximize the sensitivity to the amplitude of vibration response of the bridge.

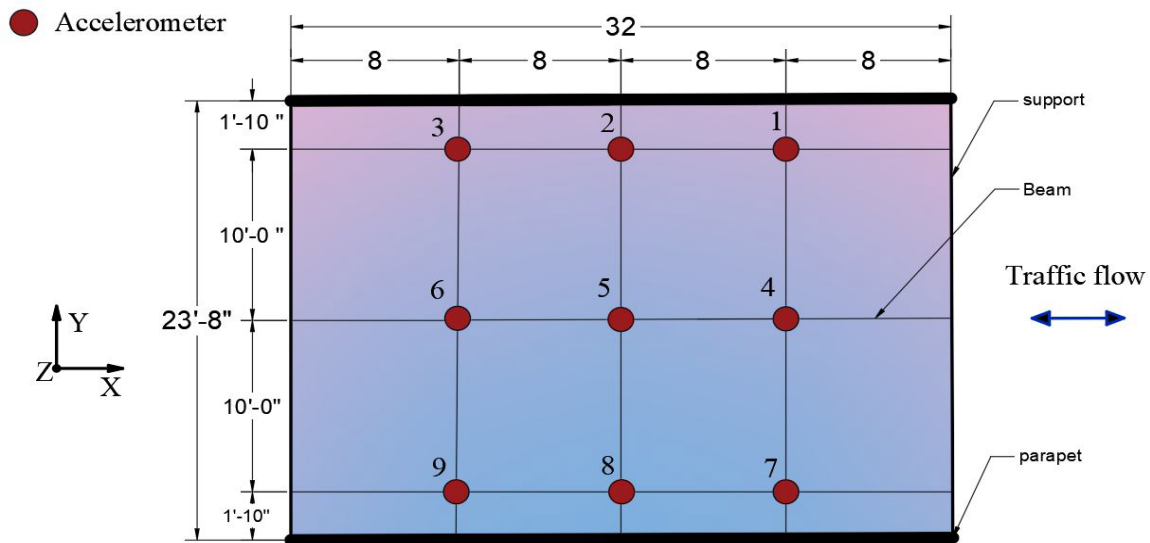


Figure 4-16 Instrumentation Configuration for Bratton's Creek Bridge: Vibration Testing

4.4 Bridge Testing

4.4.1 Live Load Testing

Live load testing consisted of a load configuration of the bridge under quasi-static condition. The load vehicles were VDOT dump trucks fully loaded with stone. The live load testing experiments consisted of vehicles crossing the bridge at bridge's lanes at crawl speed ~5 mph (See Figure 4-17). Crossing was repeated three times to ensure repeatability and reliability of the results. The vehicle used for the live load testing were two axle dump trucks provided by VDOT with gross weight of 15.35 tons. In the live load testing, a 1 min of strain signal was recorded with a sampling frequency of 100 Hz.



Figure 4-17 Live Load Testing

4.4.2 Vibration Testing

Both ambient vibration testing and impact hammer testing were conducted on the selected bridges. Note that the proposed methodology requires the identification of the natural frequencies of the bridge and conducting either vibration testing or impact hammer testing would be sufficient for that purpose. However, here, both test methods were implemented to provide a comparison and enable for a recommendation for future testing. First, the response of the bridges under ambient excitations was measured. Ambient vibrations were generated by the passing traffic, wind and walking people and recorded for a total of 15 minutes. During the ambient vibration test, normal traffic flow was permitted. Then, the impact testing was conducted by exciting the bridge with a large sledge impulse hammer that has a force capacity of 22.2 kN. The bridge was excited at two selected points (point C2 and C4 for Flat Creek bridge and point C2 and C3 for Bratton's Creek Bridge (See Appendix-Figure X and Figure Y)) for five times at each point and the data was collected for 15 seconds. All data is collected with a sampling frequency of 500 Hz.

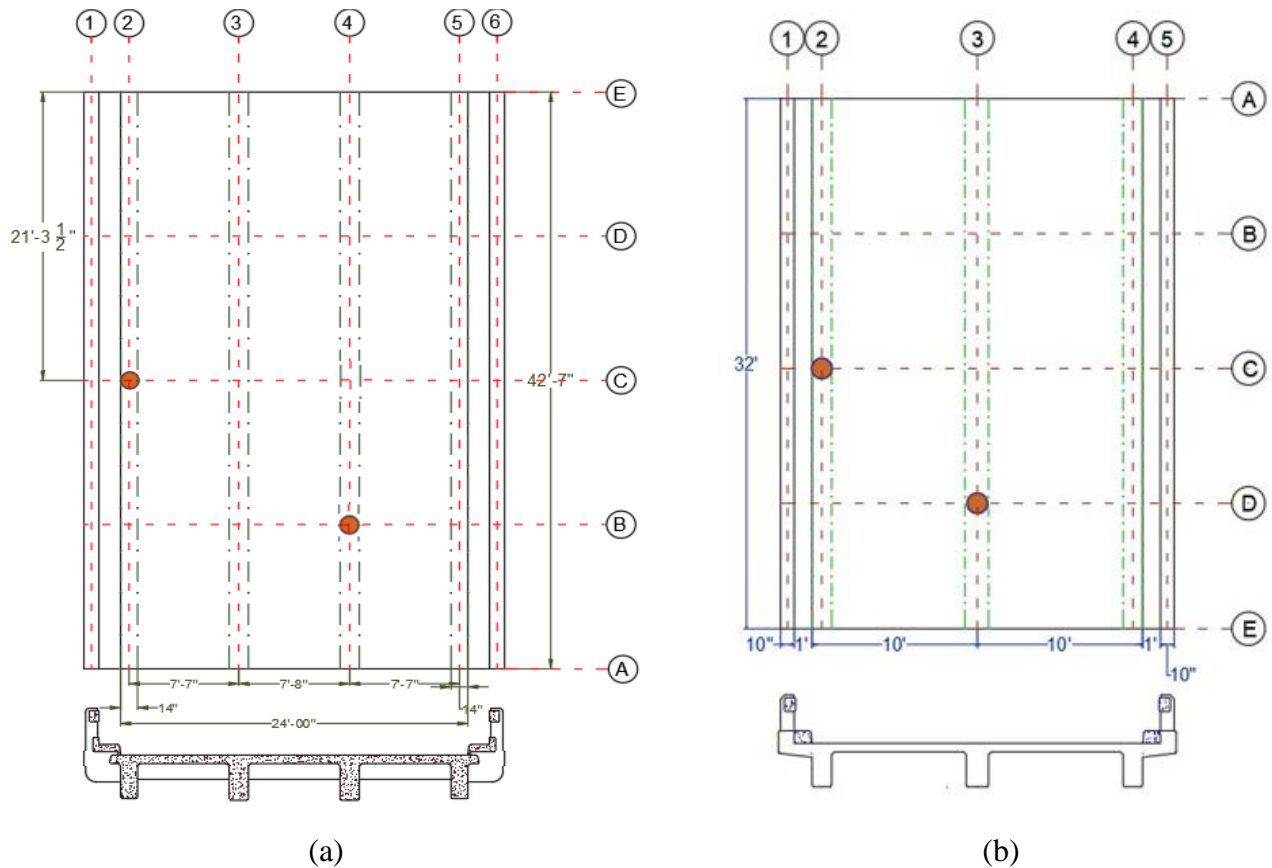


Figure 4-18 Impact Excitation Location: (a) Flat Creek, (b) Bratton's Creek

4.5 Summary

In this section, two bridge structures selected for field testing were described. Both bridges were simply supported RC T-beam bridges. Strain sensors and accelerometers were installed on the bridges. Data from the sensors were collected using a DAQ system manufactured by Bridge Diagnostics Inc. (BDI) connected to sensors by cables. The live load testing conducted on the bridges to gather the strain response and the vibration testing conducted to obtain the natural frequencies of the bridges were described. Both ambient excitation and an impact hammer testing were considered for the vibration testing. The data collected from these tests are processed through signal processing techniques discussed in the next section and used to obtain the rating factors of the bridges following the methodology described in the earlier section

5 EXPERIMENTAL RESULTS

5.1 Overview

This section presents the results obtained from field testing of two T-beam bridges and apply the load rating method proposed in this work to the tested bridges. The collected vibration data was processed through Enhanced Frequency Domain Decomposition (EFDD) method to determine the modal properties of the bridges. The geometric properties of the bridge as well as the estimated natural frequencies were used as input for the artificial neural network (ANN) described in the previous section and the non-dimensional frequencies parameter (λ) associated to the i -th vibration mode was obtained. Using the determined modal properties and λ , the flexural rigidity of the tested bridges was determined. The flexural rigidity was further used to obtain the material properties of the bridges such as the Young's Modulus of the composite section and compressive strength of the concrete. Next, the cross-sectional area of the internal reinforcing steel was estimated through a quasi-static load test coupled with an optimization approach. The yield strength of unknown reinforcing steel used in a concrete bridge was estimated by considering the era of bridge construction. These structural and material properties were then used to determine load effects and ultimately the bridge's capacity. Finally, with the capacity calculated, the load rating was derived. The results for the estimated parameters and derived load rating factors are discussed herein.

5.2 Modal Identification Method

For parameter estimation using the ambient data, the ARTeMIS software was used. The Enhanced Frequency Domain Decomposition (EFDD) method (Brincker et al. 2001), which usually provides improved estimates of modal parameters, and which transforms the SDOF power density function back into the time domain is used. In this method, the natural frequencies are obtained by calculating number of zero-crossings as a function of time and the damping ratio is estimated from the logarithmic envelope of the corresponding SDOF correlation function using the logarithmic decrement method.

The estimation of the damping ratio is performed by identification of the positive and negative extremes of the correlation function. Taking the logarithm of this decaying curve will for viscous damped linear systems result in a straight line on which the damping ratio can be estimated by linear regression. However, due to broad-banded noise and / or non-linearity, the beginning and

end of the curve might not be straight. Such non-straight parts should not be included in the regression.

The Modal Assurance Criterion Analysis (MAC) analysis (Ewins 2000) is used to determine the similarity of two mode shape and to verify that the identified modes are separate modes. When considering several true modes shapes, an $M \times M$ MAC is formed with each component calculated as:

$$MAC_{ik} = \frac{\left[\sum_{n=1}^N A_{ni} B_{nk} \right]^2}{\left[\sum_{n=1}^N (A_{ni})^2 \right] \left[\sum_{n=1}^N (B_{nk})^2 \right]} \quad (5-1)$$

where A and B represents the $N \times M$ matrices that have columns corresponding to the mode shapes. MAC values range from one for mode shapes that are exactly the same to zero for mode shapes that are orthogonal.

- If the mode shapes are identical (i.e., all points move the same) the MAC will have a value of one or 100%
- If the mode shapes are very different, the MAC value will be close to zero.

If a mode shape was compared to itself, the Modal Assurance Criterion value should be one.

5.3 Load Rating of Flat Creek Bridge through VSM

5.3.1 Time Domain Data

Figure 5-1 and Figure 5-2 show the accelerations data collected during the ambient excitation tests through all sensors from the test setup 1 and test setup 2 for Flat Creek bridge. The acceleration data recorded from impact hammer excitations for both test setups 1 and 2 with excitation at forcing location C2 and C4 is shown in Figure 4-18 (a). Visual analysis of the time domain can provide insight into the quality of the recorded signals. No anomalies were observed.

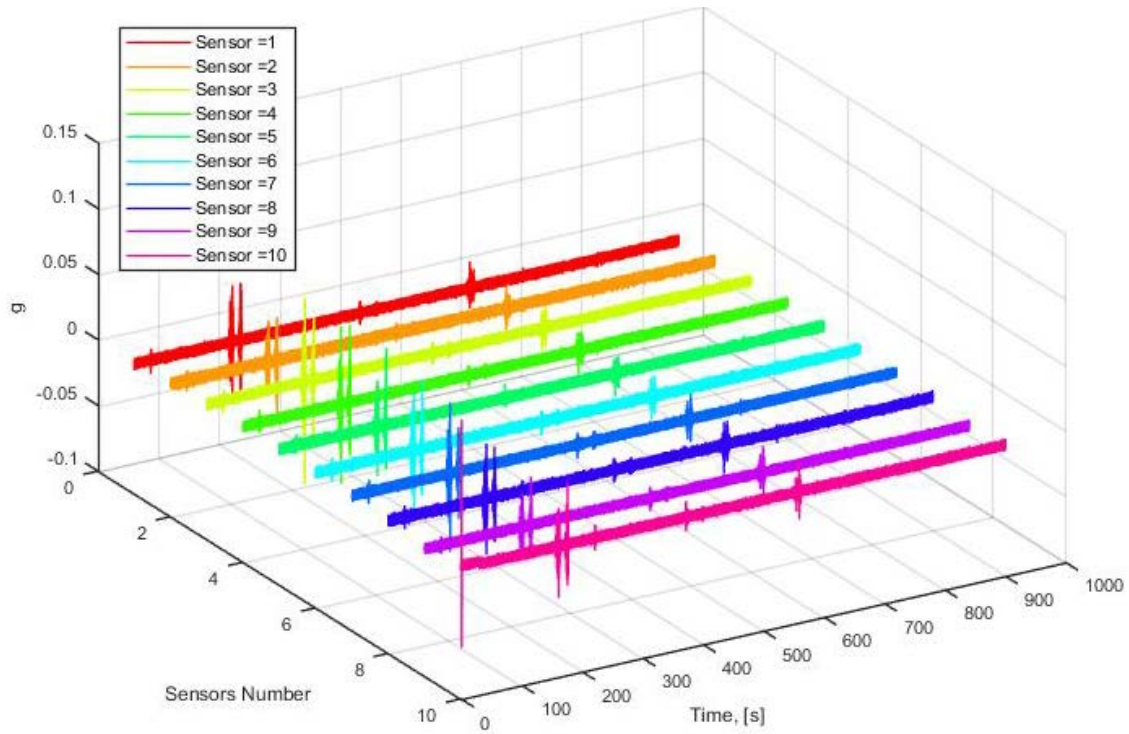


Figure 5-1 Time histories of acceleration data from all sensors of test setup 1 during ambient vibration testing of Flat Creek bridge

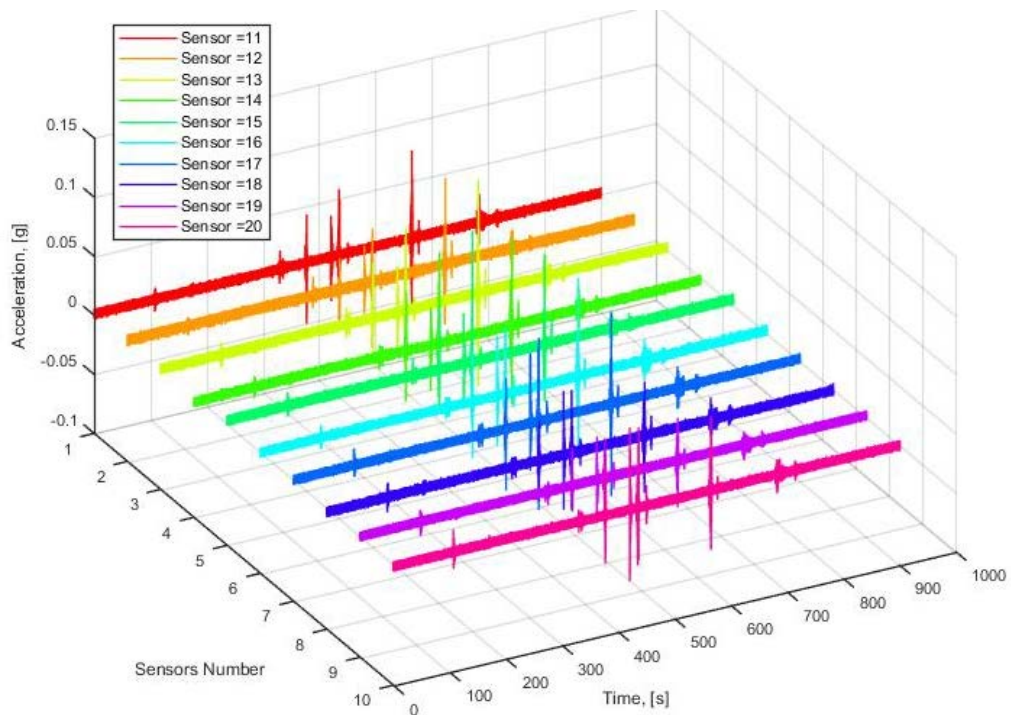


Figure 5-2 Time histories of acceleration data from all sensors of test setup 2 during ambient vibration testing of Flat Creek bridge

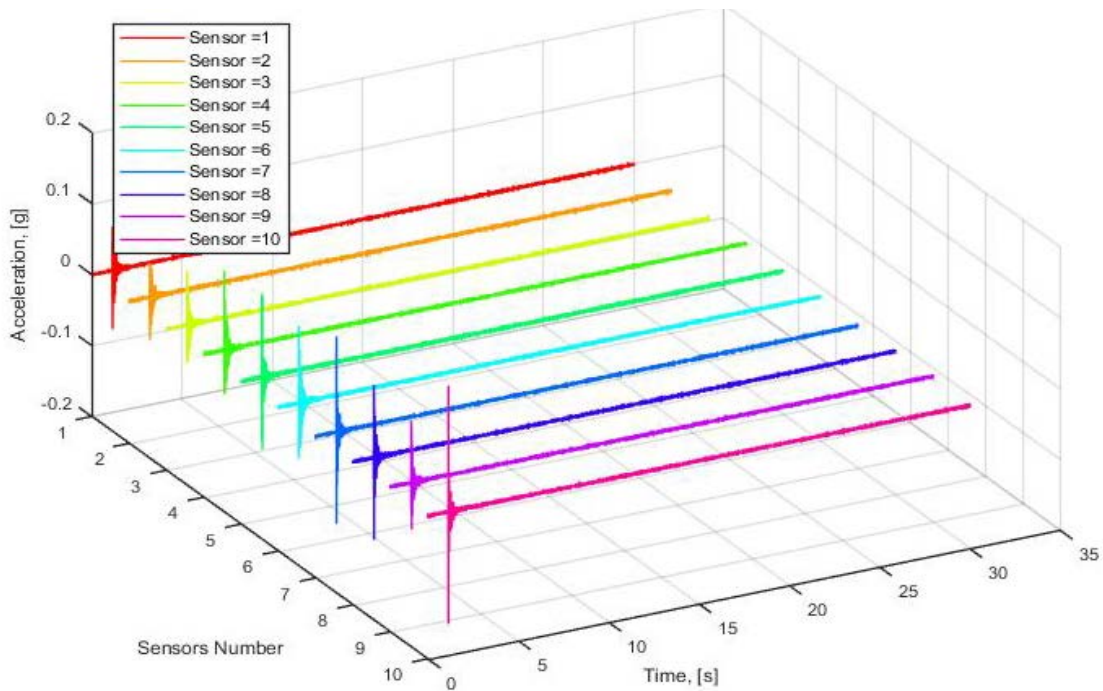


Figure 5-3 Time histories of acceleration data from all sensors of test setup 1 during impact hammer testing of Flat Creek bridge

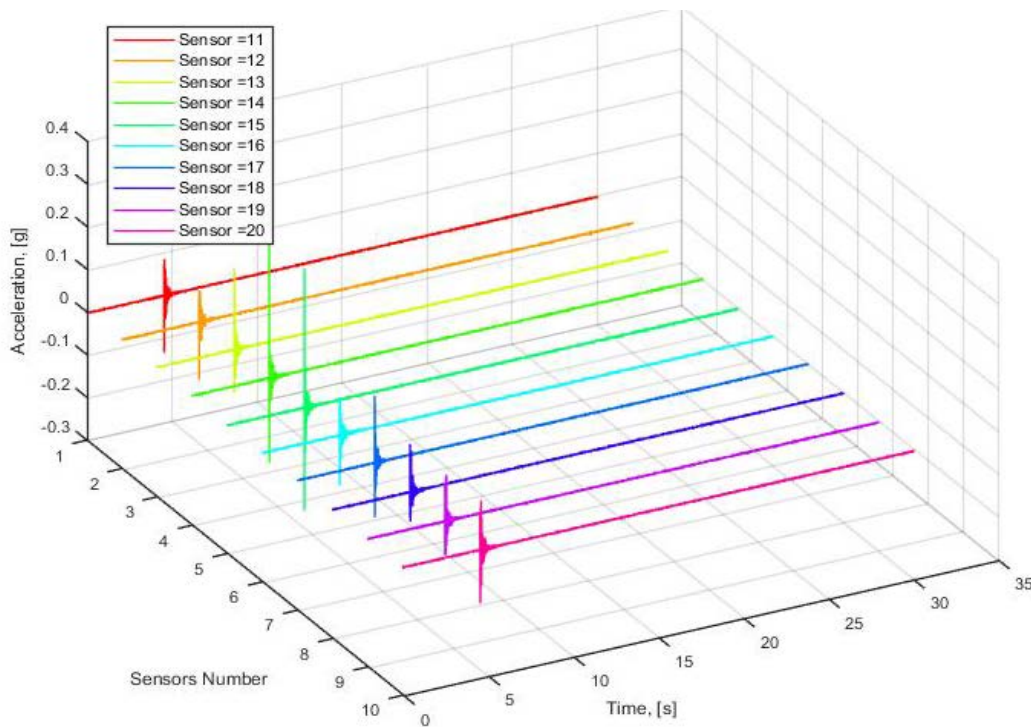


Figure 5-4 Time histories of acceleration data from all sensors of test setup 2 during impact hammer testing of Flat Creek bridge

5.3.2 Frequency and Damping Ratio Extraction

All recorded acceleration signals were processed using the enhanced frequency domain decomposition method in *ARTEMIS* software to identify the modal frequencies and damping ratios. The measured data was digitally filtered using a five-order band pass with cut-off frequencies of 0.1 Hz and 80 Hz in the software. Using EFDD method, the first three natural frequencies and damping ratios were obtained and provided in Table 5-1.

As a direct result of the modal analysis, the dynamic properties, such as the natural frequencies, damping ratio and mode shapes are obtained. However, the proposed dynamic method requires only the first three flexural natural frequencies to do the model updating. Table 5-1 shows the Natural frequencies and damping ratios obtained from ambient vibrations and Impact Hammer excitations using EFDD, respectively. Figure 5-7, summarize the modal properties of Modes 1-3. The dots show the external measured locations. In the process of modal identification in this paper, all mode shapes were normalized to unity. For the first mode, the natural frequency is 10.73 Hz with a damping ratio of 6.06 %. The mode is shown in two different views. The mode shape in Figure 5-7 is depicted by the red dashed lines and the blue solid lines which represent the left and right sides, respectively. It is obvious from Mode 1, that in Figure 5-5 that the two mode shapes on the two sides are symmetric and coincide with each other. In this mode the deformation of the bridge reaches its maximum at the center and minimum at the ends. This is the typical bending mode of a simply supported beam. The second mode has a natural frequency of 13.73 Hz with a damping ratio of 0%. Looking at the Figure 5-5b we can see that this mode is a torsional mode seen that the two opposite side have mode shapes with a form of an arc and with opposite directions. The third mode of a frequency of 18.541 and a damping ratio of 2.36% is a bending mode with the two ends that arc upward but having their maximum at the quarter position of the opposite edges.

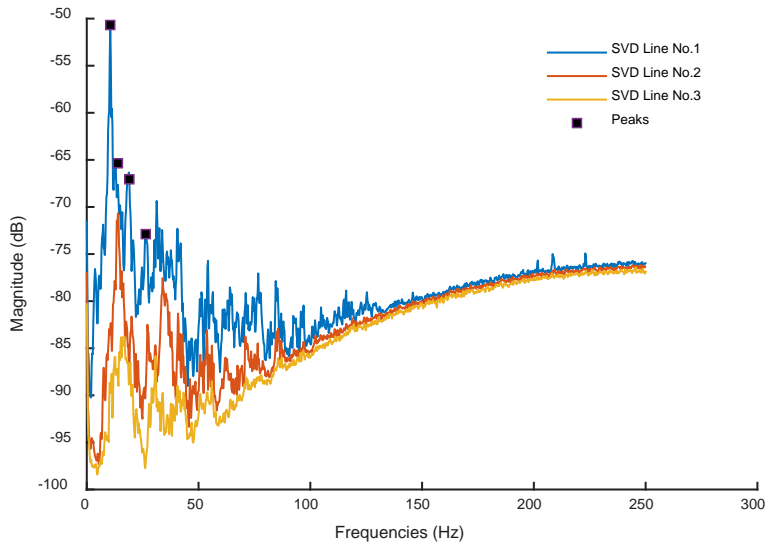


Figure 5-5 Singular values for EFDD method (Ambient Data)

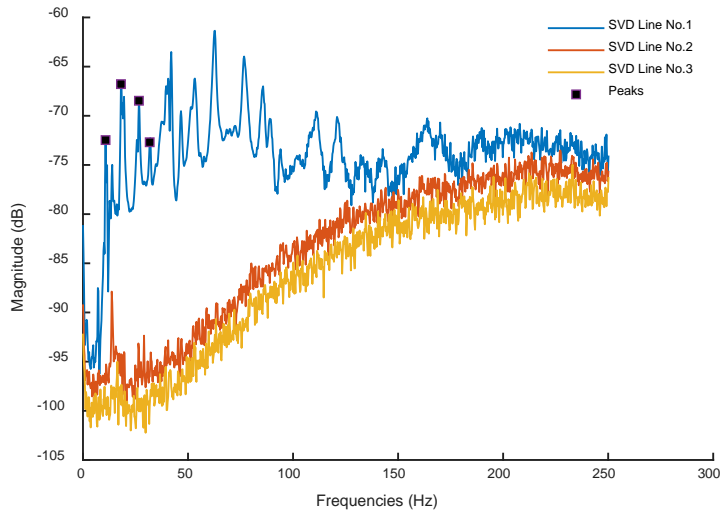
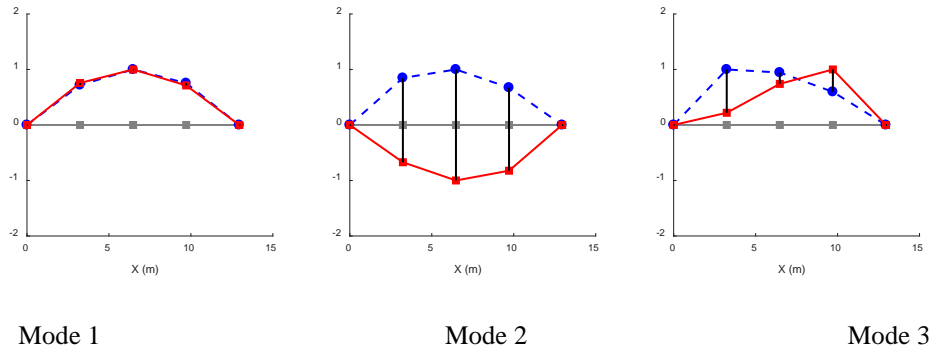
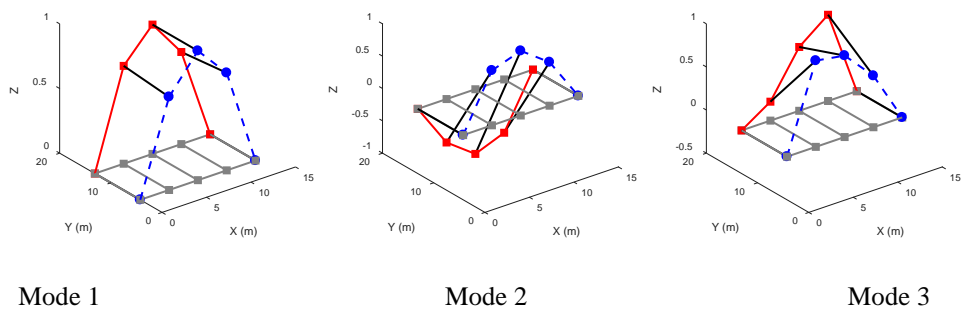


Figure 5-6 Singular values for FDD method (Impact Hammer data)

A Methodology for Condition Assessment of T-Beam Bridges without Structural Plans



Mode shapes of Modes 1-3, 2D representation



Mode shapes of Modes 1-3, 3D representation

Figure 5-7 Mode shapes of Modes 1-3, 3D representation

Table 5-1 Modal Parameters

Modes	Frequency (Hz)	Damping (%)
Mode 1	10.74	6.06
Mode 2	13.77	0
Mode 3	18.54	2.36

The modal assurance criterion (MAC) was used to quantify the variance of the extracted mode shapes. Only the vertical displacements of the mode shapes were considered as only the vertical components were of interest for comparison.

In Figure 5-8, the first mode shape at 10.743 Hz is identical to itself, hence a value of 1. Along the diagonal, every mode is identical to itself, 1 to 1 (10.743 Hz), 2 to 2 (13.773 Hz), 3 to 3 (18.541 Hz). Off of the diagonal, the MAC values are very low. Ideally, each mode should be uniquely

observed and have a different shape than the other modes. This is the case for this mode set. The highest off diagonal mode pair is mode 2 with a MAC value of 11.6 %. All the other off-diagonal mode pairs are below 3%. The results are summarized in Table 5-2.

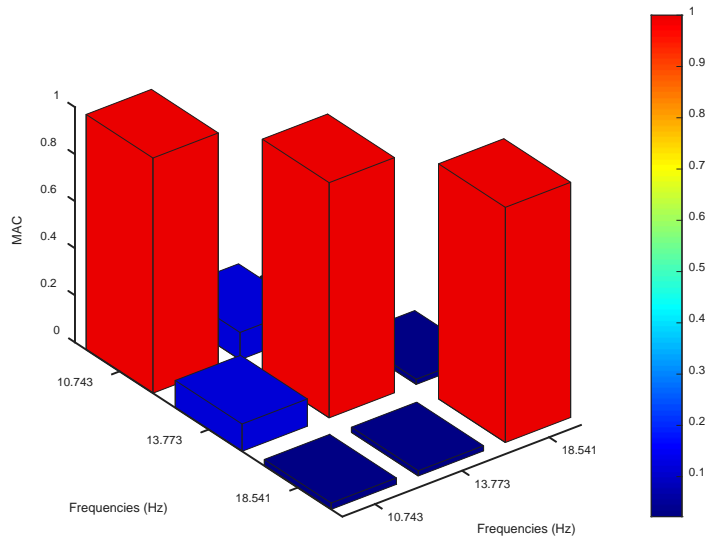


Figure 5-8 Modal Assurance Criterion

Table 5-2 MAC Values

	MAC		
Frequencies	10.743	13.773	18.541
10.743	1	0.116	0.027
13.773	0.116	1	0.022
18.541	0.027	0.022	1

5.3.3 Flexural Rigidity Estimation

For identifying the flexural rigidity of the bridge, the trained ANN was used to obtain the value of the non-dimensional frequency parameters based on the bridge characteristic. For the Flat Creek Bridge, the bridge’s effective span a , width b , skew angle θ , stem width w , stem height h_s , cantilever e , spacing between girders s and slab thickness h are equal to 42.5 ft, 29 ft., 0°, 16 in, 32 in, 29 in., 91 in, and 7.5 in, respectively, (and parapet of height of 32 in. and top width of 4 in)

which are the input of the network. The value of λ_i for the first mode which is the output of the neural network for these parameters was determined to be 0.0375.

With the derived value of λ_1 , the first angular modal frequency of 67.48 rad/s ($2\pi \times 10.74$ rad/s) identified from ambient vibration data, and the damping ratio of 6.01% for the first mode, the flexural rigidity D was determined:

$$h_{eq} = \left(\frac{12I}{S} \right)^{1/3} \quad (5-2)$$

$$D = \frac{3.6 \times \omega_1^2 \times \rho \times h_{eq}}{(1 - \xi^2) \times \lambda_1^2} \quad (5-3)$$

$$D = \frac{3.6 \times (2\pi \times 10.74)^2 \times 145 \times 2.048}{(1 - 0.0601^2) \times 0.0375^2} = 3.4687 \times 10^9 \text{ lb.ft} = 4.1624 \times 10^{10} \text{ lb.in}$$

With $\lambda_1 = 0.0375$

5.3.4 Elastic Modulus and Compressive Strength of Concrete

To compute the bending capacity, the material properties of concrete and reinforcing steel are first determined.

The elastic modulus of the concrete material is determined as:

$$E_c = \frac{\beta D (1 - \nu^2)}{\beta I_g} \quad (5-4)$$

where β is a coefficient for considering the effect of reinforcing steel in calculating the elastic modulus of the concrete material.

$$E_c = \frac{16 \times 4.1624 \times 10^{10} \times (1 - 0.2^2)}{1.11 \times 1.1250 \times 10^5} = 5266 \text{ ksi}$$

This result is then used for estimating the ultimate compressive strength of the bridge's concrete:

$$f_c = \left[\frac{E_c}{33\rho^{1.5}} \right]^2 \quad (5-5)$$

$$f_c = \left[\frac{5266 \times 1000}{33 \times 145^{1.5}} \right]^2 = 8.04 \text{ ksi}$$

Then, the 28-day compressive strength of the concrete is obtained by knowing the age of bridge which is 40 years:

$$f_c' = \frac{4 + 0.85t}{t} f_c(t)$$

$$f_c' = \frac{4 + 0.85 \times 60 \times 365}{60 \times 365} \times 8.04$$

$$f_c' = 6.83 \text{ksi}$$

5.3.5 Live Load Test results

The maximum strain responses corresponding to each girder for different paths are plotted in Figure 5-9.

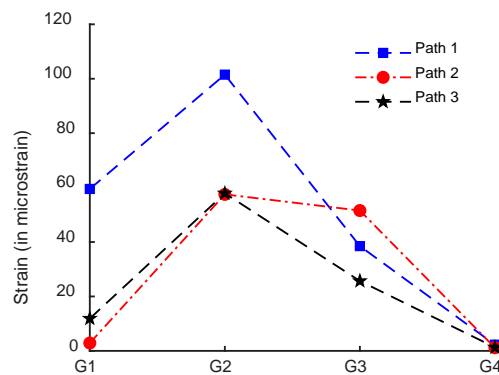


Figure 5-9 Maximum Strain at each Girder

5.3.6 Yield Strength and Area of Steel Estimation

Yield strengths of unknown reinforcing steel used in a concrete bridge is estimated by considering the date of bridge construction and the type and shape of reinforcing steel. Based on the age of the bridge which is 40 years, the yield strengths of reinforcing steel is also estimated to be 40 *ksi* from the Table 1.1. An elastic modulus of $E_s=29000 \text{ ksi}$ is used for reinforcing steel material.

To identify the amount of longitudinal reinforcement area A_s used inside the beam's cross-section, the maximum strain of a strain signal measured during the live load test was used in forming the objective function. Then, two unknown parameters in the objective function were determined by minimizing the function namely reinforcement area A_s and bending moment M due to live lode:

$$\min_{A_s, M} F(A_s, M) = \frac{|\varepsilon^{Exp.} - \varepsilon^{Ana.}(A_s, M)|}{\varepsilon^{Exp.}} + \frac{|EI_b^{Exp.} - EI_b^{Ana.}(A_s)|}{EI_b^{Exp.}} \quad (5-6)$$

$$I_b = \frac{bh^3}{12}$$

$$I_b = \frac{16 \times 32.5^3}{12} = 45770 in^4$$

$$\varepsilon^{Ana.}(A_s, M) = \frac{M \bar{y}(A_s)}{EI_b}$$

$$\bar{y}(A_s) = \frac{\frac{bh^2}{2} + \left(\frac{E_s \beta I_b}{bD(1-\nu^2)} - 1 \right) \times A_s d'}{bh + \left(\frac{E_s \beta}{bD(1-\nu^2)} - 1 \right) \times A_s}$$

$$\bar{y}(A_s) = \frac{\frac{16 \times 32.5^2}{2} + \left(\frac{29000 \times \beta I_b}{b \times 4.16244 \times 10^{10} \times (1-0.2^2)} - 1 \right) \times A_s \times 2.5}{16 \times 32.5 + \left(\frac{29000 \times \beta I_b}{b \times 4.16244 \times 10^{10} (1-0.2^2)} - 1 \right) \times A_s}$$

$$EI_b = bD(1-\nu^2)$$

$$EI_b = 16 \times 4.16 \times 10^{10} \times (1-0.2^2) = 6.39 \times 10^{11} lb.in^2$$

$$EI_b^{Ana.}(A_s) = \frac{b \times D(1-\nu^2)}{\beta} \times I_t(A_s)$$

$$I_t(A_s) = \frac{16 \times 32.5^3}{12} + 16 \times 32.5 \times \left(\bar{y}(A_s) - \frac{32.5}{2} \right)^2 + \left(\frac{29000 \times 1.11}{16 \times 4.16 \times 10^{10} (1-0.2^2)} - 1 \right) \times A_s \left(\bar{y}(A_s) - 2.5 \right)^2$$

$$I_t(A_s) = \frac{bh^3}{12} + bh \left(\bar{y}(A_s) - \frac{h}{2} \right)^2 + \left(\frac{E_s \beta I_b}{bD(1-\nu^2)} - 1 \right) \times A_s \left(\bar{y}(A_s) - d' \right)^2$$

where d' is the concrete cover on reinforcing steel which is equal to 2.5 in. In the live load test, the maximum strain for sensor 1 is equal to $\varepsilon^{Exp.} = 105 \mu\varepsilon$. By substituting this experimental strain value and other parameters in the objective function, the reinforcement area A_s and the bending moment M were determined to be 11.8 in² and 775.25 ft.-kip, respectively. This determined reinforcement

area is for a cross-section with the width of 16 in, and it is equal to 11.8 in^2 a unit width which will be used for calculating bending capacity.

Table 5-3 lists the value of the measured strain with the obtained reinforcement area and the bending moment at the location of sensor due to the live load. Sensor 3 in test 1 and sensor 1 in test 2 were not included in the table because of their low value for strain. It can be seen that the identified reinforcing steel from the data of different sensors at two tests is identical, and it is also close to the actual value of reinforcing steel of 9 in^2 . The identified reinforcing steel is less than the reinforcing steel mentioned in the plan of the bridge, and this may be related to the presence of corrosion in rebars.

Table 5-3 Estimated reinforcement area and bending moment

Sensor	Load Test 1 (Path 1)		Load Test 2 (Path 2)	
	2	1	2	3
Strain ($\mu\epsilon$)	105	58.6	59.3	52.3
$A_s \text{ (in}^2\text{)}$	11.8	11.8	11.8	11.8
M (ft-kip)	775.25	433.83	425.7	386.06

Note that the same one should be done for exterior beam by just changing the b by 14" in the expression above. The result is summarized in Table 5-4.

Table 5-4 Estimated reinforcement area and bending moment

Sensor	Load Test 1 (Path 1)		Load Test 2 (Path 2)	
	2	1	2	3
Strain ($\mu\epsilon$)	105	58.6	59.3	52.3
$A_s \text{ (in}^2\text{)}$	9.27	9.27	9.27	9.27
M (ft-kip)	679.26	378.42	383.01	337.79

5.3.7 Bending Capacity Estimation

5.3.7.1 Interior Beam

Based on the determined values for material properties and reinforcing steel, the bending capacity is computed:

$$f_c' = 6830 \text{ psi}$$

$$\beta_1 = 0.85 - 0.05 \frac{f_c' - 4000}{1000} = 0.71$$

$$a = \frac{A_s f_y}{\beta_1 f_c' b_e} = \frac{11.8 \times 40000}{0.71 \times 6830 \times 91} = 1.07$$

$$a = 1.07 \text{ p } 7.5 \text{ in (neutral axis located in the slab region)}$$

$$M_u = \phi A_s f_y \left(d_s - \frac{a}{2} \right)$$

$$M_u = 0.9 \times 11.8 \times 40000 \times \left(37.5 - \frac{1.07}{2} \right) = 1308.56 \text{ kip.ft}$$

5.3.7.2 Exterior Beam

Based on the determined values for material properties and reinforcing steel, the bending capacity is computed:

$$f_c' = 6830 \text{ psi}$$

$$\beta_1 = 0.85 - 0.05 \frac{f_c' - 4000}{1000} = 0.71$$

$$a = \frac{A_s f_y}{\beta_1 f_c' b_e} = \frac{9.27 \times 40000}{0.71 \times 6830 \times 91} = 0.84$$

Assume that the compression block is in the deck. Calculate the capacity as if it is a rectangular section (with the compression block in the flange). The neutral axis location, calculated in accordance with LRFD 5.7.3.1.1 for a rectangular section, is:

$$a = 0.84 p \ 7.5in \text{ (neutral axis located in the slab region)}$$

Calculate the factored moment capacity of the composite section in accordance with LRFD [5.7.3.2]:

$$M_u = \phi A_s f_y \left(d_s - \frac{a}{2} \right)$$

$$M_u = 0.9 \times 9.27 \times 40000 \times \left(37.5 - \frac{0.84}{2} \right) = 1031.2 \text{ kip.ft}$$

5.3.8 Load Effects Computation

This section presents a discussion of determination of service live load effects on bridge superstructures. Distribution factors are applied to the live load effects only; they are not applicable to the permanent load effects. The superstructure under consideration is one of the types listed in LRFD Table 4.6.2.2.1-1 and the superstructure is within the range of applicability listed in applicable LRFD tables.

5.3.8.1 Interior Beams

Distribution factors

Distribution factors are calculated in accordance with LRFD [Table 4.6.2.2.2b-1]. For an interior beam, the distribution factors are shown below. The values of the governing distribution factors for bending moment in interior as well as exterior girders are taken as the largest of all the values.

- Longitudinal Stiffness Parameter, K_g

According to LRFD Design Eq. 4.6.2.2.1-1, the longitudinal stiffness parameter K_g shall be taken as: $K_g = n(I + Ae_g^2)$

$$n = 1, I = 43690.67in^4, A = 512in^2, e_g = 19.75, K_g = 243402$$

A Methodology for Condition Assessment of T-Beam Bridges without Structural Plans

- Distribution Factor for moment, g_m (LRFD Design Table 4.6.2.2.2b – 1)

One Lane Loaded:

$$g_{m1} = 0.06 + \left(\frac{S}{14}\right)^{0.4} \left(\frac{S}{L}\right)^{0.3} \left(\frac{K_g}{12L_t^3}\right)^{0.1} = 0.53$$

Two or More Lanes Loaded

$$g_{m2} = 0.075 + \left(\frac{S}{9.5}\right)^{0.6} \left(\frac{S}{L}\right)^{0.2} \left(\frac{K_g}{12L_t^3}\right)^{0.1} = 0.71$$

$$\therefore \text{Use } g_m = 0.71$$

Load effects

According to LRFD Design 4.6.2.2.1 Permanent loads on the deck are distributed uniformly among the beams (i.e. Components and Attachments, DC are computed and distributed among the beams).

- Structural Concrete:

Consisting of deck + stem + haunches (conservative, 2, 1/2 -in. chamfers were not deducted)

$$W_{sc} = [16 \times 32 + 7.5 \times 90.96] \times \frac{0.150}{144} = 1.24 \text{ kip/ft}$$

$$\text{Railing and curb} = 0.100 \text{ kip/ft.}$$

$$\text{Total per beam, DC} = 1.34 \text{ kcf}$$

$$M_{DC} = \frac{1}{8} \times 1.34 \times 42.5^2 = 302.5 \text{ kip-ft}$$

No wearing surface, DW=0.00

- Compute Maximum Live Load Effects

Maximum Design Live Load (HL-93) Moment at Midspan:

$$\text{Design Lane Load Moment} = 54.1 \text{ kip-ft.}$$

$$\text{Design Truck Moment} = 208.0 \text{ kip-ft.}$$

$$\text{Tandem Axles Moment} = 275 \text{ kip-ft.}$$

$$IM = 33\%$$

- Design Live Load HL-93:

According to the table E6A-1 Live Load Moments on Longitudinal Stringers or Girders (Simple Span) (AASHTO Manual for Bridge Evaluation 2015)

$$M_{LL+IM} = 796 \text{ k-ft (after interpolation)}$$

Distributed Live Load Moments

Design Live Load HL-93:

$$M_{LL+IM} = 796 \times 0.707 = 563.00$$

Table 5-5 Design Bending Moment of each load for Interior Beam

DC	DW	HL-93
M_{DC}	M_{DW}	M_{LL+IM}
302.50	0.00	563.00

5.3.8.2 Exterior Beams

Distribution factors

One lane loaded: Lever rule

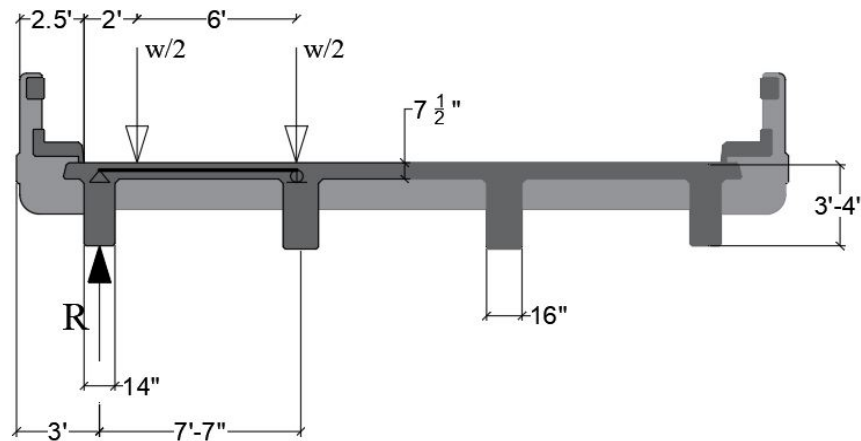


Figure 5-Schematics showing loaded lanes on bridge cross section for special analysis: Position of HL-93 truck for one design lane loaded case

$$R = \frac{\frac{w}{2} \times 6.125 + \frac{w}{2} \times 0.125}{7.125} = 0.41 \quad (5-7)$$

$$R = 0.41w \times 1.2 = 0.49 \text{ multiple presence of trucks}$$

Two lane loaded:

$$g = e \times g_{\text{int}}$$

$$e = 0.77 + \frac{d_e}{9.1} = 0.77 + \frac{5.5}{9.1} = 0.82$$

$$g = 0.82 \times 0.71 = 0.58$$

Rigid Section: 4.6.2.2.d

$$R = \frac{N_L}{N_b} + \frac{X_{\text{ext}} \sum_1^{N_L} e}{\sum_1^{N_b} x^2} \quad (5-8)$$

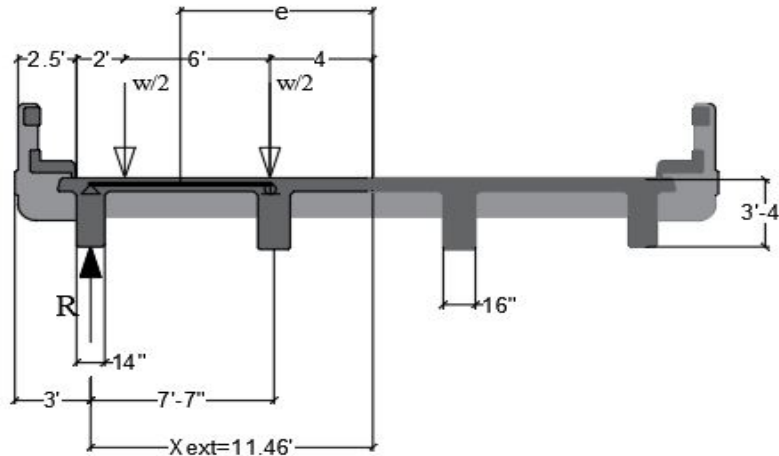


Figure 5-10 Schematics showing loaded lanes on bridge cross section for special analysis:
Position of HL-93 trucks for two design lanes loaded case

One truck:

$$e = 11.46 + 3 - 2.5 - 2 - 3 = 6.96$$

$$R = \frac{1}{4} + \frac{11.455 \times 6.955}{2 \times (3.83^2 + 11.455^2)} = 0.52 \quad \text{governs}$$

Multiple truck presence:

$$R = 0.52 \times 1.2 = 0.63 \text{ governs}$$

Load effects

According to LRFD Design 4.6.2.2.1 Permanents loads on the deck are distributed uniformly among the beams (i.e. Components and Attachments, DC are computed and distributed among the beams).

A Methodology for Condition Assessment of T-Beam Bridges without Structural Plans

- Components and Attachments, DC

Structural Concrete:

Consisting of deck + stem + haunches (conservative, 2, 1/2 -in. chamfers were not deducted)

$$= (14 \times 32 + 7.5 \times 81.75) \times \frac{0.15 \text{ k.cf}}{144} = 1.11 \text{ kip/ft}$$

$$\text{Railing and curb} = 0.10 \text{ kip/ft}$$

Total per beam, DC = 1.21 kcf

$$M_{DC} = \frac{1}{8} \times 1.21 \times 42.50^2 = 273.20 \text{ kip.ft}$$

No Wearing surface, DW=0.00

- Compute Maximum Live Load Effects

Maximum Design Live Load (HL-93) Moment at Midspan

According to AASHTO Manual for Bridge Evaluation 2015, from Table Appendix E6A- Live Load Moments on Longitudinal Stringers or Girders (Simple Span) is:

$$M_{LL+IM} = 796.77 \text{ kip.ft}$$

- Distributed Live Load Moments

Design Live Load HL-93:

$$M_{LL+IM} = 796.77 \times 0.63 = 500.40$$

Table 5-6 Design Bending Moment of each load

DC	DW	HL-93
M _{DC}	M _{DW}	M _{LL+IM}
273.20	0.00	500.40

5.3.9 Load Rating Computation

5.3.9.1 Interior Beam

By considering the obtained value for the capacity and load effects listed in Table 4.4, the load rating factor is calculated as:

$$RF = \frac{M_u - \gamma_{DC}M_{DC} - \gamma_{DW}M_{DW}}{\gamma_{LL}M_{LL+IM}} \quad (5-9)$$

The rating factor for the inventory evaluation level:

$$RF = \frac{1308.56 - 1.25 \times 302.5 - 1.5 \times 0.00}{1.75 \times 563.00} = 0.94$$

$$RF = 0.94$$

The rating factor for the operating evaluation level:

$$RF = \frac{1308.56 - 1.25 \times 302.5 - 1.5 \times 0.00}{1.35 \times 563.00} = 1.22$$

$$RF = 1.22$$

5.3.9.2 Exterior Beam

By considering the obtained value for the capacity and load effects listed in Table 4.5, the load rating factor is calculated as:

$$RF = \frac{M_u - \gamma_{DC}M_{DC} - \gamma_{DW}M_{DW}}{\gamma_{LL}M_{LL+IM}}$$

The rating factor for the inventory evaluation level:

$$RF = \frac{1031.20 - 1.25 \times 273.20 - 1.5 \times 0.00}{1.75 \times 500.40} = 0.79$$

$$RF = 0.79$$

The rating factor for the operating evaluation level:

$$RF = \frac{1031.20 - 1.25 \times 273.20 - 1.5 \times 0.00}{1.35 \times 500.40} = 1.02$$

$$RF = 1.02$$

5.4 Load Rating of Bratton's Creek Bridge through VSM

5.4.1 Time Domain Data

Figure 5-11 shows the ambient accelerations data collected through all sensors from the field testing of Bratton's Creek bridge. The acceleration data of all sensors recorded from impact hammer excitations is shown in Figure 5-12. The acceleration data recorded from impact hammer excitations for this test with excitation at forcing location C2 and C3 is shown in Figure 4-18 (b). No anomalies were observed from the measured time-domain data.

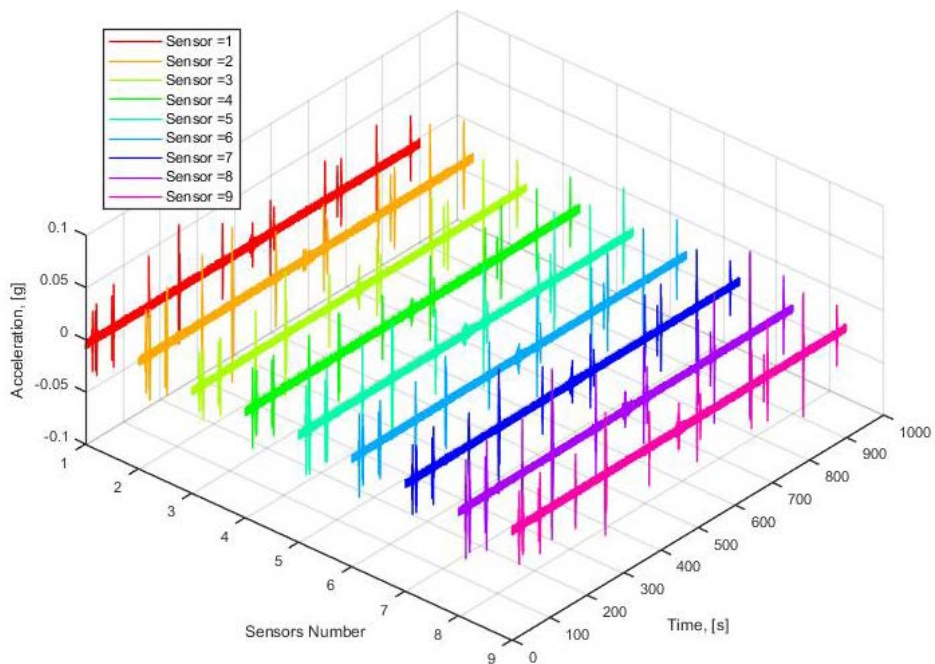


Figure 5-11 Time histories of acceleration data from all sensors during ambient vibration testing of Bratton's Creek bridge

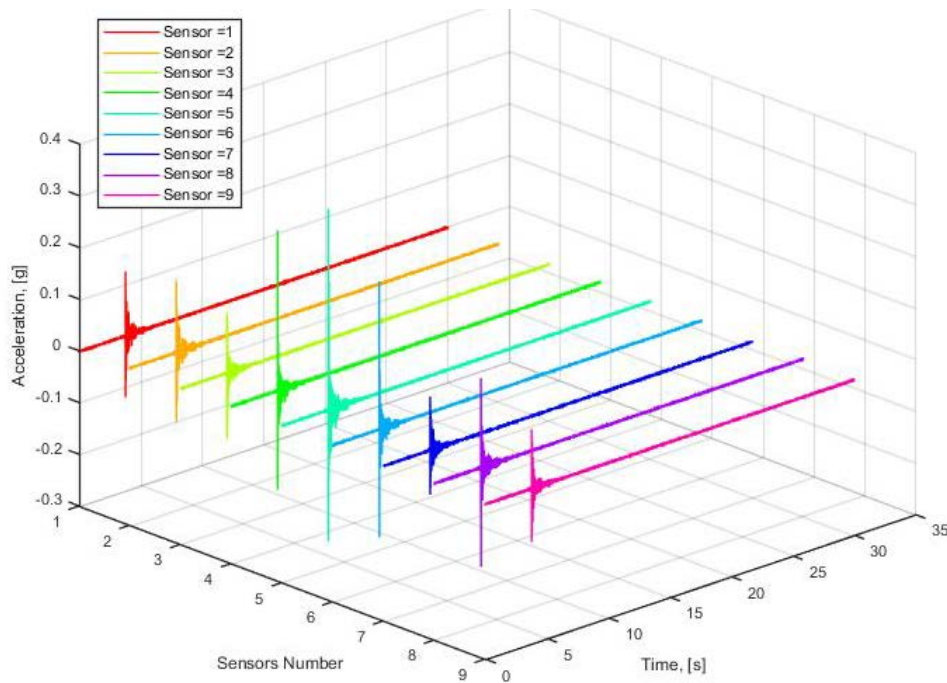


Figure 5-12 Time histories of acceleration data from all sensors during impact hammer testing of Bratton’s Creek bridge

5.4.2 Frequency and Damping Ratio Extraction

All recorded acceleration signals were processed using the enhanced frequency domain decomposition method in *ARTEMIS* software to identify the modal frequencies and damping ratios. The measured data was digitally filtered using a five-order band pass with cut-off frequencies of 0.1 Hz and 80 Hz in the software. Using EFDD method, the first three natural frequencies and damping ratios were obtained and provided in Table 5-7.

As a direct result of the modal analysis, the dynamic properties, such as the natural frequencies, damping ratio and mode shapes are obtained. However, the proposed dynamic method requires only the first three flexural natural frequencies to do the model updating. Table 5-7 shows the Natural frequencies and damping ratios obtained from ambient vibrations and Impact Hammer excitations using EFDD, respectively. Figure 5-13, summarize the modal properties of Modes 1-3. Referring to Figure 5-15, the dots show the external measured locations. In the process of modal identification in this paper, all mode shapes were normalized to unity. For the first mode, the natural frequency is 14.24 Hz with a damping ratio of 1.97 %. The mode is shown in two different views. The mode shape in Figure 5-15 is depicted by the red dashed lines and the blue solid lines

which represent the left and right sides, respectively. It is obvious from Mode 1, that in Figure 5-13 that the two mode shapes on the two sides are symmetric and coincide with each other. In this mode the deformation of the bridge reaches its maximum at the center and minimum at the ends. This is the typical bending mode of a simply supported beam. The second mode has a natural frequency of 17.53 Hz with a damping ratio of 0.76%. Looking at the Figure 5-13b we can see that this mode is a torsional mode seen that the two opposite side have mode shapes with a form of an arc and with opposite directions. The third mode of a frequency of 25.06 Hz and a damping ratio of 0.54% is a bending mode with the two ends that arc upward but having their maximum at the quarter position of the opposite edges.

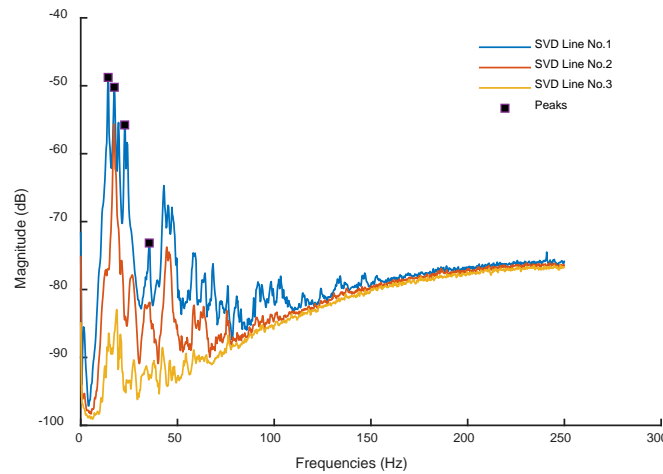


Figure 5-13 Singular values for EFDD method (Ambient Data)

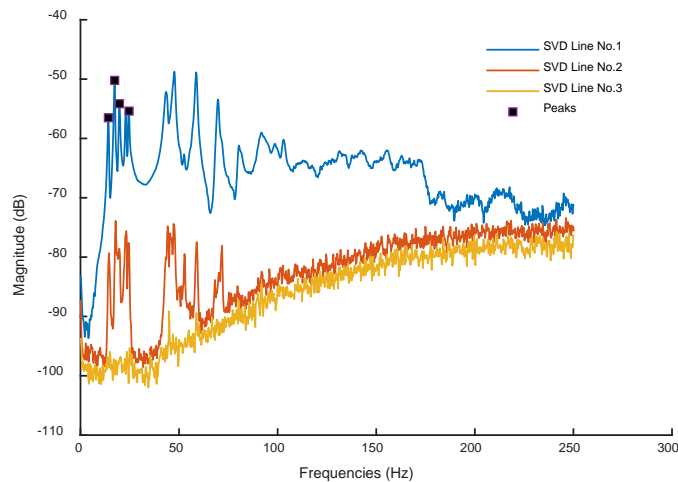
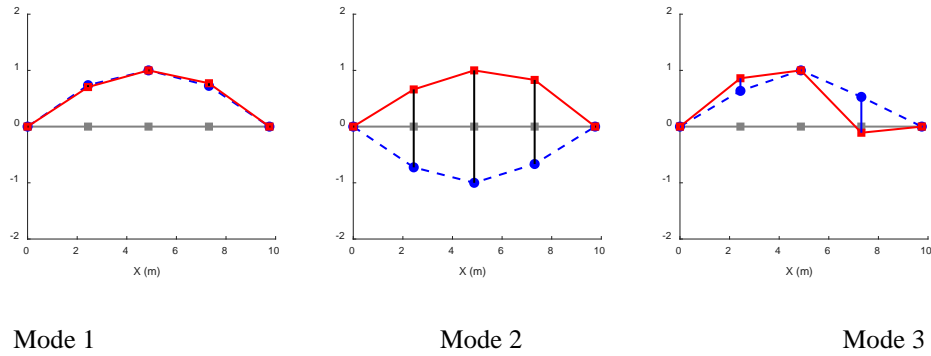
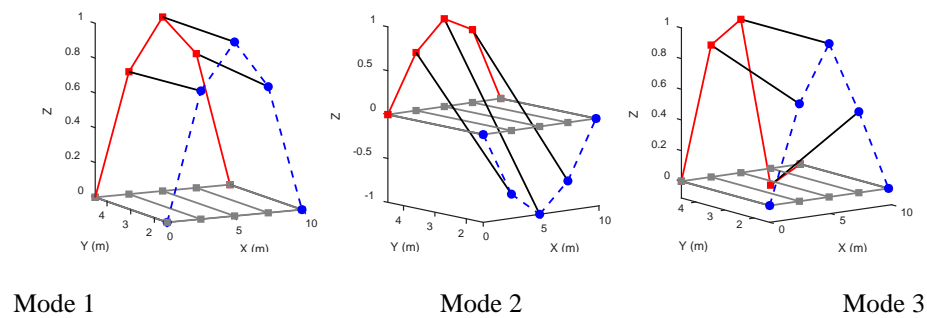


Figure 5-14 Singular values for EFDD method (Impact Hammer Data)



Mode shapes of Modes 1-3, 2D representation



Mode shapes of Modes 1-3, 3D representation

Figure 5-15 Mode shapes of Modes 1-3, 3D representation

Table 5-7 Modal Parameters

Modes	Frequency (Hz)	Damping (%)
Mode 1	14.24	1.97
Mode 2	17.53	0.76
Mode 3	25.06	0.54

In Figure 5-16, the first mode shape at 14.24 Hz is identical to itself, hence a value of 1. Along the diagonal, every mode is identical to itself, 1 to 1 (14.24 Hz), 2 to 2 (13.773 Hz), 3 to 3 (18.541 Hz). Off of the diagonal, the MAC values are very low. Ideally, each mode should be uniquely observed and have a different shape than the other modes. This is the case for this mode set. The highest off diagonal mode pair is mode 2 with a MAC value of 2.9 %. All the other off-diagonal mode pairs are below 3%.

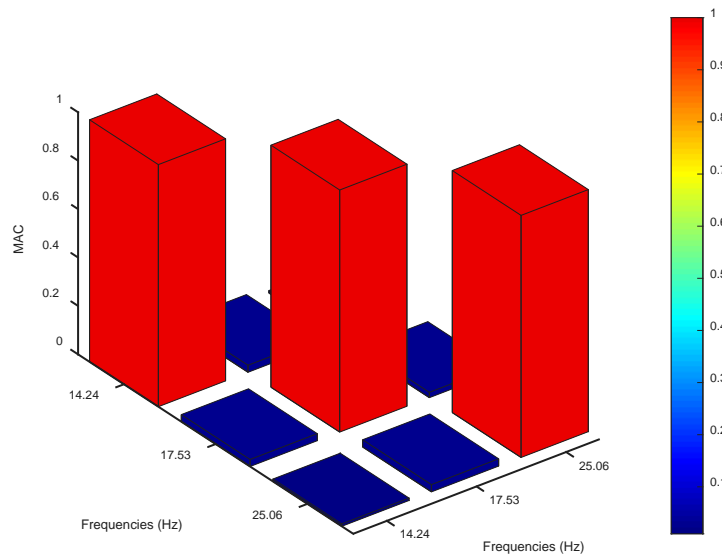


Figure 5-16 Modal Assurance Criterion

Table 5-8 MAC Values

	MAC		
Frequencies	14.24	17.53	25.06
14.24	1	0.029	0.01
17.53	0.029	1	0.022
25.06	0.01	0.03	1

5.4.3 Flexural Rigidity Estimation

For identifying the flexural rigidity of the bridge, the trained ANN was used to obtain the value of the non-dimensional frequency parameters based on the bridge characteristic. For the Bratton’s Creek Bridge, the bridge’s effective span a , width b , skew angle θ , stem width w , stem height h_s , cantilever e , spacing between girders s and slab thickness h (and parapet of height of 26 in. and top width of 4 in) are equal to 32 ft, 23.67 ft, 0°, 16 in, 24.5 in, 24 in., 91 in, and 7.5 in, respectively, which are the input of the network.. The value of λ_i for the first modes which is the output of the neural network for these parameters was determined to be 0.071.

With the derived value of λ_1 , the first angular modal frequency of 89.47 rad/s ($2\pi \times 14.24 \text{ rad/s}$) identified from ambient vibration data, and the damping ratio of 1.97% for the first mode, the flexural rigidity D was determined:

$$h_{eq} = \left(\frac{12I}{S} \right)^{1/3} \quad (5-10)$$

$$D = \frac{3.6 \times \omega_1^2 \times \rho \times h_{eq}}{(1 - \xi^2) \times \lambda_1^2} \quad (5-11)$$

$$D = \frac{3.6 \times (2\pi \times 14.24)^2 \times 145 \times 1.45}{(1 - 0.0197^2) \times 0.071^2} = 1.212 \times 10^9 \text{ lb.ft} = 1.443 \times 10^{10} \text{ lb.in}$$

With $\lambda_1 = 0.071$

5.4.4 Elastic Modulus and Compressive Strength of Concrete

To compute the bending capacity, the material properties of concrete and reinforcing steel are first determined.

The elastic modulus of the concrete material is determined as:

$$E_c = \frac{\beta D (1 - \nu^2)}{\beta I_g} \quad (5-12)$$

where β is a coefficient for considering the effect of reinforcing steel in calculating the elastic modulus of the concrete material.

$$E_c = \frac{16 \times 1.443 \times 10^{10} \times (1 - 0.2^2)}{1.11 \times 4.405 \times 10^4} = 4571 \text{ ksi}$$

This result is then used for estimating the ultimate compressive strength of the bridge's concrete:

$$f_c = \left[\frac{E_c}{33 \rho^{1.5}} \right]^2 \quad (5-13)$$

$$f_c = \left[\frac{4571 \times 1000}{33 \times 145^{1.5}} \right]^2 = 6.29 \text{ ksi}$$

Then, the 28-day compressive strength of the concrete is obtained by knowing the age of bridge which is 40 years:

$$f_c' = \frac{4 + 0.85t}{t} f_c(t)$$

$$f_c' = \frac{4 + 0.85 \times 65 \times 365}{65 \times 365} \times 6.29$$

$$f_c' = 5.35 \text{ksi}$$

$$f_c' = 6.83 \text{ksi}$$

5.4.5 Live Load Test results

The maximum strain responses corresponding to each girder for different paths are plotted in Figure 5-17.

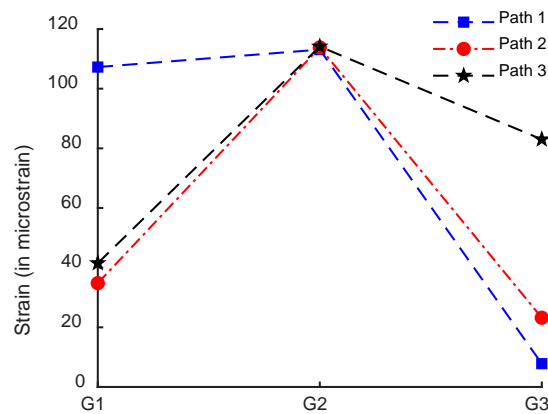


Figure 5-17 Maximum Strain at each Girder

5.4.6 Yield Strength and Area of Steel Estimation

Yield strengths of unknown reinforcing steel used in a concrete bridge is estimated by considering the date of bridge construction and the type and shape of reinforcing steel. Based on the age of the bridge which is 40 years, the yield strengths of reinforcing steel is also estimated to be 40 *ksi* from the Table 1.1. An elastic modulus of $E_s=29000 \text{ksi}$ is used for reinforcing steel material.

To identify the amount of longitudinal reinforcement area A_s used inside the beam's cross-section, the maximum strain of a strain signal measured during the live load test was used in forming the

objective function. Then, two unknown parameters in the objective function were determined by minimizing the function namely reinforcement area A_s and bending moment M due to live lode:

$$\min_{A_s, M} F(A_s, M) = \frac{|\varepsilon^{Exp.} - \varepsilon^{Ana.}(A_s, M)|}{\varepsilon^{Exp.}} + \frac{|EI_b^{Exp.} - EI_b^{Ana.}(A_s)|}{EI_b^{Exp.}} \quad (5-14)$$

$$I_b = \frac{bh^3}{12}$$

$$I_b = \frac{16 \times 24^3}{12} = 18432 \text{ in}^4$$

$$\varepsilon^{Ana.}(A_s, M) = \frac{M \bar{y}(A_s)}{EI_b}$$

$$\bar{y}(A_s) = \frac{\frac{bh^2}{2} + \left(\frac{E_s \beta I_b}{bD(1-\nu^2)} - 1 \right) \times A_s d'}{bh + \left(\frac{E_s \beta}{bD(1-\nu^2)} - 1 \right) \times A_s}$$

$$\bar{y}(A_s) = \frac{\frac{16 \times 32.5^2}{2} + \left(\frac{29000 \times \beta I_b}{b \times 1.443 \times 10^{10} \times (1-0.2^2)} - 1 \right) \times A_s \times 2.5}{16 \times 32.5 + \left(\frac{29000 \times \beta I_b}{b \times 1.443 \times 10^{10} (1-0.2^2)} - 1 \right) \times A_s}$$

$$EI_b = bD(1-\nu^2)$$

$$EI_b = 16 \times 1.443 \times 10^{10} \times (1-0.2^2) = 2.216 \times 10^{11} \text{ lb.in}^2$$

$$EI_b^{Ana.}(A_s) = \frac{b \times D(1-\nu^2)}{\beta} \times I_t(A_s)$$

$$I_t(A_s) = \frac{16 \times 32.5^3}{12} + 16 \times 32.5 \times \left(\bar{y}(A_s) - \frac{32.5}{2} \right)^2 + \left(\frac{29000 \times 1.11}{16 \times 4.16 \times 10^{10} (1-0.2^2)} - 1 \right) \times A_s \left(\bar{y}(A_s) - 2.5 \right)^2$$

$$I_t(A_s) = \frac{bh^3}{12} + bh \left(\bar{y}(A_s) - \frac{h}{2} \right)^2 + \left(\frac{E_s \beta I_b}{bD(1-\nu^2)} - 1 \right) \times A_s \left(\bar{y}(A_s) - d' \right)^2$$

A Methodology for Condition Assessment of T-Beam Bridges without Structural Plans

Where d' is the concrete cover on reinforcing steel which is equal to 2.5 in. In the live load test, the maximum strain for sensor 1 is equal to $\varepsilon^{Exp}=105 \mu\varepsilon$. By substituting this experimental strain value and other parameters in the objective function, the reinforcement area A_s and the bending moment M were determined to be 11.8 in^2 and 775.25 ft.-kip, respectively. This determined reinforcement area is for a cross-section with the width of 16 in, and it is equal to 11.8 in^2 a unit width which will be used for calculating bending capacity.

Table 5-9 lists the value of the measured strain with the obtained reinforcement area and the bending moment at the location of sensor due to the live load. Sensor 3 in test 1 and sensor 1 in test 2 were not included in the table because of their low value for strain. It can be seen that the identified reinforcing steel from the data of different sensors at two tests is identical, and it is also close to the actual value of reinforcing steel of 3.87 in^2 . The identified reinforcing steel is less than the reinforcing steel mentioned in the plan of the bridge, and this may be related to the presence of corrosion in rebars.

Table 5-9 Estimated reinforcement area and bending moment

	Load Test 1 (Path 1)		Load Test 2 (Path 2)	
Sensor	2	1	2	3
Strain ($\mu\varepsilon$)	117	111	116	83
A_s (in^2)	7.40	7.40	7.40	7.40
M (ft-kip)	431	406	425	304

Note that the same one should be done for exterior beam by just changing the b by 14" in the expression above. The result is summarized in Table 5-10.

Table 5-10 Estimated reinforcement area and bending moment

	Load Test 1 (Path 1)		Load Test 2 (Path 2)	
Sensor	2	1	2	3
Strain ($\mu\varepsilon$)	117	111	116	83
A_s (in^2)	5.70	5.70	5.70	5.70
M (ft-kip)	315.77	310.75	323.75	253.54

5.4.7 Bending Capacity Estimation

5.4.7.1 Interior Beam

Based on the determined values for material properties and reinforcing steel, the bending capacity is computed:

$$f'_c = 5351 \text{ psi}$$

$$\beta_1 = 0.85 - 0.05 \frac{f'_c - 4000}{1000} = 0.78$$

$$a = \frac{A_s f_y}{\beta_1 f'_c b_e} = \frac{7.43 \times 40000}{0.71 \times 6830 \times 91} = 0.63$$

Assume that the compression block is in the deck. Calculate the capacity as if it is a rectangular section (with the compression block in the flange). The neutral axis location, calculated in accordance with LRFD 5.7.3.1.1 for a rectangular section, is:

$$a = 0.63 \text{ p } 8 \text{ in (neutral axis located in the slab region)}$$

Calculate the factored moment capacity of the composite section in accordance with LRFD [5.7.3.2], [5.7.3.2.2]:

$$M_u = \phi A_s f_y \left(d_s - \frac{a}{2} \right)$$

$$M_u = 0.9 \times 7.43 \times 40000 \times \left(32 - \frac{0.63}{2} \right) = 706.26 \text{ kip.ft}$$

5.4.7.2 Exterior Beam

Based on the determined values for material properties and reinforcing steel, the bending capacity is computed:

$$f'_c = 5351 \text{ psi}$$

$$\beta_1 = 0.85 - 0.05 \frac{f'_c - 4000}{1000} = 0.78$$

Assume that the compression block is in the deck. Calculate the capacity as if it is a rectangular section (with the compression block in the flange). The neutral axis location, calculated in accordance with LRFD 5.7.3.1.1 for a rectangular section, is:

$$a = \frac{A_s f_y}{\beta_1 f_c' b_e} = \frac{5.70 \times 40000}{0.71 \times 6830 \times 91} = 0.48$$

$$a = 0.48 \text{ p } 8in \text{ (neutral axis located in the slab region)}$$

Calculate the factored moment capacity of the composite section in accordance with LRFD [5.7.3.2], [5.7.3.2.2]:

$$M_u = \phi A_s f_y \left(d_s - \frac{a}{2} \right)$$

$$M_u = 0.9 \times 5.70 \times 40000 \times \left(32 - \frac{0.63}{2} \right) = 543.78 \text{ kip.ft}$$

5.4.8 Load Effects Computation

5.4.8.1 Interior Beams

Distribution factors

This section presents a discussion of determination of service live load effects on bridge superstructures. Distribution factors are computed in accordance with LRFD [Table 4.6.2.2b-1]. For an interior beam, the distribution factors are shown below. The values of the governing distribution factors for both bending moment and shear in interior as well as exterior girders are taken as the largest of all the values.

- Longitudinal Stiffness Parameter, K_g

LRFD Design Eq. 4.6.2.2.1-1 indicates that $K_g = n(I + Ae_g^2)$ where

$$n = 1, I = 18432in^4, A = 384in^2, e_g = 16, K_g = 116736$$

A Methodology for Condition Assessment of T-Beam Bridges without Structural Plans

- Distribution Factor for moment, g_m (*LFRD Design Table 4.6.2.2.2b – 1*)

One Lane Loaded:

$$g_{m1} = 0.06 + \left(\frac{S}{14}\right)^{0.4} \left(\frac{S}{L}\right)^{0.3} \left(\frac{K_g}{12Lt_s^3}\right)^{0.1} = 0.62 \text{ lane/girder}$$

Two or More Lanes Loaded

$$g_{m2} = 0.075 + \left(\frac{S}{9.5}\right)^{0.6} \left(\frac{S}{L}\right)^{0.2} \left(\frac{K_g}{12Lt_s^3}\right)^{0.1} = 0.81 \text{ lane/girder}$$

Lever rule:

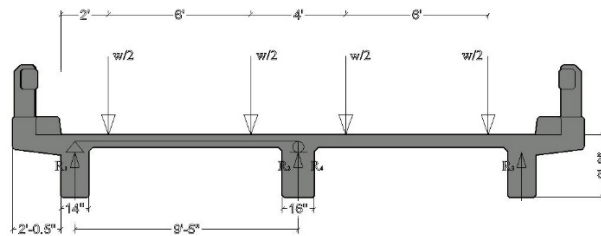


*Figure 5-18 Schematics showing loaded lanes on bridge cross section for special analysis:
Position of HL-93 trucks for two design lanes loaded case*

$$R_1 = \frac{\frac{w}{2} \times 8 + \frac{w}{2} \times 2}{9.42} = 0.531$$

$$R_1 = 0.469 \times 1.2 = 0.531$$

Two Lanes:

$$R_3 = \frac{\frac{w}{2} \times 2 + \frac{w}{2} \times 8}{9.42} = 0.531$$

$$R_4 = 0.469$$

$$R_{\text{int}} = R_2 + R_4 = 2 \times 0.469 \times 1 = 0.938$$

$$DF_{\text{int,1lane}} = \min(0.634, 0.536) = 0.536$$

$$DF_{\text{int,morelanes}} = \min(0.831, 0.938) = 0.831$$

$$\therefore \text{Use } g_m = 0.831$$

Load Effects

According to LRFD Design 4.6.2.2.1 Permanent loads on the deck are distributed uniformly among the beams (i.e. Components and Attachments, DC are computed and distributed among the beams).

- Structural Concrete:

Consisting of deck + stem + haunches (conservative, 2, ½ -in. chamfers were not deducted)

$$W_{sc} = [16 \times 24.5 + 7.5 \times 113.01] \times \frac{0.150}{144} = 1.29 \text{ kip / ft}$$

$$\text{Railing and curb} = 0.100 \text{ kip/ft}$$

$$\text{Total per beam, DC} = 1.39 \text{ kcf}$$

$$M_{DC} = \frac{1}{8} \times 1.39 \times 31^2 = 167.10 \text{ kip - ft}$$

$$\text{No wearing surface, DW} = 0.00$$

A Methodology for Condition Assessment of T-Beam Bridges without Structural Plans

- Compute Maximum Live Load Effects

Maximum Design Live Load (HL-93) Moment at Midspan are:

$$\text{Design Lane Load Moment} = 54.1 \text{ kip-ft}$$

$$\text{Design Truck Moment} = 208.0 \text{ kip-ft}$$

$$\text{Tandem Axles Moment} = 275 \text{ kip-ft}$$

$$IM = 33\%$$

- Design Live Load HL-93:

According to the table E6A-1 Live Load Moments on Longitudinal Stringers or Girders (Simple Span) (AASHTO Manual for Bridge Evaluation 2015)

$$M_{LL+IM} = 543 \text{ k-ft after interpolating from table E6A-1}$$

Distributed Live Load Moments

Design Live Load HL-93:

$$M_{LL+IM} = 543 \times 0.83 = 451.23$$

Table 5-11 Design Bending Moment of each load for interior beam

DC	DW	HL-93
M_{DC}	M_{DW}	M_{LL+IM}
167.10	0.00	451.23

5.4.8.2 Exterior Beams

Distribution Factor

One lane loaded:

$$R = 0.531 \times 1.2 = 0.637$$

Two lane loaded:

$$g = e \times g_{\text{int}}$$

$$e = 0.77 + \frac{d_e}{9.1} = 0.77 + \frac{5.585}{9.1} = 0.83$$

$$g = 0.83 \times 0.831 = 0.693$$

Lever rule:

$$D_{\text{morelane}} = 0.531 \times 1 = 0.531$$

$$DF_{\text{morelanes}} = \min(0.693, 0.531) = 0.531$$

Rigid Section: 4.6.2.2.d

$$R = \frac{N_L}{N_b} + \frac{X_{\text{ext}} \sum_1^{N_L} e}{\sum_1^{N_b} x^2}$$

One truck:

$$R = \frac{1}{3} + \frac{9.42 \times 5}{2 \times (9.42^2)} = 0.60 \text{ governs}$$

Multiple truck presence:

$$R = 0.52 \times 1.2 = 0.637 \text{ governs}$$

Load Effects

According to LRFD Design 4.6.2.2.1 Permanent loads on the deck are distributed uniformly among the beams (i.e. Components and Attachments, DC are computed and distributed among the beams).

- Components and Attachments, *DC*

Structural Concrete:

Consisting of deck + stem + haunches (conservative, 2, 1/2 -in. chamfers were not deducted)

$$= (88.02 \times 7.5 + 24.5 \times 14) \times \frac{0.15 \text{ k.c.f}}{144} = 1.04 \text{ kip/ft}$$

Railing and curb = 0.10 kip/ft

Total per beam, DC = 1.14 kcf

$$M_{DC} = \frac{1}{8} \times 1.21 \times 42.50^2 = 136.90 \text{ kip.ft}$$

No Wearing surface, DW=0.00

- Compute Maximum Live Load Effects

Maximum Design Live Load (HL-93) Moment at Midspan.

From Table Appendix E6A- Live Load Moments on Longitudinal Stringers or Girders (Simple Span) (AASHTO Manual for Bridge Evaluation 2015)

$$M_{LL+IM} = 521.70 \text{ kip.ft}$$

- Distributed Live Load Moments

Design Live Load HL-93:

$$M_{LL+IM} = 521.70 \times 0.637 = 332.30$$

Table 5-12 Design Bending Moment of each load

DC	DW	HL-93
M_{DC}	M_{DW}	M_{LL+IM}
136.9	0.00	332.3

5.4.9 Load Rating Computation

5.4.9.1 Interior Beam

By considering the obtained value for the capacity and load effects listed in Table 4.4, the load rating factor is calculated as:

$$RF = \frac{M_u - \gamma_{DC}M_{DC} - \gamma_{DW}M_{DW}}{\gamma_{LL}M_{LL+IM}} \quad (5-15)$$

The rating factor for the inventory evaluation level:

$$RF = \frac{706.26 - 1.25 \times 167.10 - 1.5 \times 0.00}{1.75 \times 451.23} = 0.63$$

$$RF = 0.94$$

The rating factor for the operating evaluation level:

$$RF = \frac{706.26 - 1.25 \times 167.10 - 1.5 \times 0.00}{1.35 \times 451.23} = 0.82$$

$$RF = 0.82$$

5.4.9.2 Exterior Beam

By considering the obtained value for the capacity and load effects listed in Table 4.5, the load rating factor is calculated as:

$$RF = \frac{M_u - \gamma_{DC}M_{DC} - \gamma_{DW}M_{DW}}{\gamma_{LL}M_{LL+IM}}$$

The rating factor for the inventory evaluation level:

$$RF = \frac{543.78 - 1.25 \times 136.9 - 1.5 \times 0.00}{1.75 \times 332.3} = 0.64$$

$$RF = 0.64$$

The rating factor for the operating evaluation level:

$$RF = \frac{543.78 - 1.25 \times 136.9 - 1.5 \times 0.00}{1.35 \times 332.3} = 0.64$$

$$RF = 0.83$$

5.5 Summary

This section described the application of the load rating method proposed in this work for two T-beam bridges. The results obtained from a live load testing and vibration testing were processed to relate these measurements to unknown structural and material properties. These structural and material properties were then used to determine load effects and ultimately the bridge's capacity. Finally, with the capacity calculated, the load rating factors were derived. A summary of results for the estimated parameters and derived load rating factors are provided in Table 5-13 for each of the bridges evaluated.

Table 5-13 Estimated Parameters and Load Ratings based on VSM-LR Approach

	VSM-LR	
	Flat Creek	Bratton's Creek
$f_1 (Hz)$	10.74	14.24
$f_2 (Hz)$	13.77	17.53
$\xi_1 (\%)(damping)$	6.06	1.97
$\xi_2 (\%)(damping)$	0.00	0.76
$E_c (ksi)$	5266	4571
$A_s (in^2)$	11.80	7.40
$f_y (ksi)$	40	33
$f_c' (ksi)$	6.83	5.35
$M_n (kip - ft)$	1308.56	581.96
RF (inventory)	0.94(0.79)	0.48(0.48)
RF(Operating)	1.22(1.02)	0.63(0.62)

A comparison of the final load ratings derived from the traditional AASHTO LRFR approach will serve as the basis for performance comparison. Table 5-13 **Error! Reference source not found.** presents a summary of the various load rating methods explored in this study. The comparison uses the Inventory load rating factor for comparison, but similar outcomes exist for the operating load rating factor. The estimates of the rating factors relative to those derived using the baseline AASHTO LRFR method are reasonable. In this case reasonable is defined as rational estimates on the same order of magnitude. In the case of Flat Creek bridge, these estimates are above the AASHTO LRFR estimate by 12.4%. However in Bratton’s Creek, the VSM-LR approach underestimates the value by 12.6%. The proposed method is not expected to predict load ratings that will exactly match traditional load rating tools (e.g. load rating through AASHTO LRFR methods or through AASHTO diagnostic testing method) due to the assumptions and approximations (e.g., area of steel, transformed moment of inertia, concrete strength, etc.) used to arrive at capacity; however, it is expected that the method will be able to yield conservative approximations of load rating and the rational behavior- or physics-based estimates that cannot be achieved with subjective rating practices.

Table 5-14 Inventory Load Rating Results from Different Analyses

	Flat Creek	Brattons Creek
AASHTO LRFR (RF_c)	0.85	0.71
VDOT Database	0.84	0.77
VSM-LR	0.97	0.63

6 CONCLUSION AND RECOMMENDATIONS

Load rating of bridges is vital to ensure public safety. It is a strategy for temporal condition assessment of the built environment. The load rating of a given bridge depends heavily on knowledge about the structural details of the structure. For a reinforced concrete structure, these details can include geometric information about the internal structure, material properties, as well as location and quantity of reinforcing steel. These parameters are ultimately needed to determine the nominal capacity of the bridge. However, additional factors can also contribute to the uncertainty surrounding the estimation of a load rating including features such as condition state, design approximations, and unanticipated contributions (e.g. parapets, bracing, etc.).

In this study, a method was developed to formulate a sound approach of load rating of T-beam bridges when plans are missing or insufficient structural details are available to derive a load rating. The method described in this work is a nondestructive method called the Vibration-based Simplified Method. It mainly relies on vibration measurements for estimating the load carrying capacity of RC T-beam bridges without structural plans. To use the Vibration-based Simplified Method for T-Beam bridges, the vibration data of the four bridges was collected first. These data were processed through Enhanced Frequency Domain Decomposition (EFDD) method to determine the modal properties (ω , ξ) of the bridges. The geometric properties of the bridge were used as input for the developed artificial neural network (ANN) and the non-dimensional frequencies parameter (λ) associated to the i -th vibration mode was obtained. Using the determined modal properties and λ , the flexural rigidity (D) was determined. The obtained flexural rigidity was further used to obtain the material properties of the bridges such as the Young Modulus (E) of the composite section and thus compressive strength (f_c') of the concrete materials of the bridge. Next, the cross-sectional area of the internal reinforcing steel was estimated through a quasi-static load test coupled with an optimization approach. The yield strength of unknown reinforcing steel used in a concrete bridge was estimated by considering the era of bridge construction. The AASHTO Manual for Bridge Evaluation provides guidance on identifying reinforcement characteristics when structural details are unknown. These structural and material properties were then used to determine load effects and ultimately the bridge's capacity. Finally, with the capacity calculated, the load rating was derived.

The comparison of the final load ratings derived from the traditional AASHTO LRFR approach serve as the basis for performance comparison. The estimates of the rating factors relative to those derived using the baseline AASHTO LRFR method are reasonable.

As described in this work, the VSM-LR mainly focused on developing rational engineering solutions to determine the load ratings of bridges with limited or missing as-built information. The outcomes of the study highlighted a general approach that are suitable for estimating load ratings in the absence of sufficient details.

For any structural system, the general expectation would be that a refined analysis approach would likely yield an improvement in load ratings relative to the design approximation-driven analytical approach, due to a more representative description of load sharing characteristics. For the developed approach, this characteristic is inherent to the analyses, but also includes the estimation of uncertain parameters within the solution. When evaluating the results, it is evident that the proposed methodology is able to provide reasonable estimates of the rating factors relative to those derived based on AASHTO LRFR method. In this case reasonable is defined as rational estimates on the same order of magnitude; in some cases, these estimates are similar to the AASHTO LRFR estimate. However, it should be noted that the VSM-LR method has been developed as an approach that emphasizes limited testing and modeling, thus provides a mechanism for easier application.

REFERENCES

- AASHTO (2015). "LRFD Bridge Design Specifications, 7th Ed., American Association of State Highway and Transportation Officials, Washington, DC,.
- AASHTO Manual for Bridge Evaluation (2015). "Manual for Bridge Evaluation, 2nd Ed. with 2016 Interim Revisions. American Association of State Highway and Transportation Officials, Washington, DC,.
- Abdul-Wahab, H. M., and Khalil, M. H. (2000). "Rigidity and strength of orthotropic reinforced concrete waffle slabs," *Journal of structural engineering*, 126(2), 219-227.
- ACI 209R-92 (1998). "Prediction of creep, shrinkage, and temperature effects in concrete structures. Farmington Hills, Michigan, USA: American Concrete Institute."
- ARTEMIS Modal Pro (2016). "Operational Modal Analysis, (OMA)", ARTEMIS Extractor pro – academic licence. User's manual. In: ApS SVS, editor. Aalborg, Denmark, "Structural Vibration Solutions A/S, NOVI Science Park.
- Azizinamini, A., Boothby, T. E., Shekar, Y., and Barnhill, G. (1994a). "Old concrete slab bridges. I: experimental investigation." *Journal of Structural Engineering, ASCE*, 120(11), 3284-3304.
- Azizinamini, A., Boothby, T. E., Shekar, Y., and Barnhill, G. (1994b). "Old concrete slab bridges. II: analysis." *Journal of Structural Engineering, ASCE*, 120(11), 3305-3319.
- Azizinamini, A., Boothby, T.E., Shekar, Y. and Barnhill, G., 1994. Old concrete slab bridges. I: Experimental investigation. *Journal of Structural Engineering*, 120(11), pp.3284-3304.
- Azizinamini, Atorod, Ahmed Elremaily, and Fred Choobineh. "Advanced Methodology for Rating Concrete Slab Bridges." *Advanced Technology in Structural Engineering*. 2000. 1-8.
- Bagheri, A., M. Alipour, S. Usmani, O. E. Ozbulut & D. K. Harris (2017) "Structural Stiffness Identification of Skewed Slab Bridges with Limited Information for Load Rating Purpose.", . In *Dynamics of Civil Structures*, Springer, Cham,, 2, 243-249.
- Boothby, T. and Atamturktur, S., 2007. A guide for the finite element analysis of historic load bearing masonry structures. In *Proceedings of the 10 th North American Masonry Conference*, St. Louis, Missouri.
- Boothby, T. E., Domalik, D. E., and Dalal, V. A. (1998). "Service load response of masonry arch bridges." *J. Struct. Engrg., ASCE*, 124(1), 17–23.
- Boothby, T.E., 2001. Load rating of masonry arch bridges. *Journal of Bridge Engineering*, 6(2), pp.79-86.
- Brincker, R., Zhang, L., and Andersen, P. (2001). "Modal identification of output-only systems using frequency domain decomposition." *Smart Mater Struct.*, 10(3):441-5(3), 441-445.

Brincker, Rune, C. Ventura, and Palle Andersen. "Damping estimation by frequency domain decomposition." 19th International Modal Analysis Conference. 2001.

Caglayan, B.O., Ozakgul, K. and Tezer, O., 2012. Assessment of a concrete arch bridge using static and dynamic load tests. *Structural Engineering and Mechanics*, 41(1), pp.83-94.

Cai, C. S., Shahawy, M., and El-Saad, A. ~1999. "Comparison of bridge load rating based on analytical and field testing methods." Proc., *Nondestructive Evaluation of Bridges and Highways II*, Vol. 3587, SPIE, Bellingham, Wash., 127–136.

Cai, C.S. and Shahawy, M., 2004. Predicted and measured performance of prestressed concrete bridges. *Journal of Bridge Engineering*, 9(1), pp.4-13.

Catbas, F. N., Shah, M., Burkett, J., and Basharat, A. (2004). "Challenges in structural health monitoring." Proc., 4th Int. Workshop on Structural Control, A. Smyth and R. Betti, eds., Columbia University, New York, 195–202.

Catbas, F.N., Zaurin, R., Gul, M. and Gokce, H.B., 2011. Sensor networks, computer imaging, and unit influence lines for structural health monitoring: Case study for bridge load rating. *Journal of Bridge Engineering*, 17(4), pp.662-670.

Chajes, M.J., Mertz, D.R. and Commander, B., 1997. Experimental load rating of a posted bridge. *Journal of Bridge Engineering*, 2(1), pp.1-10.

Chajes, M.J., Mertz, D.R. and Commander, B., 1997. Experimental load rating of a posted bridge. *Journal of Bridge Engineering*, 2(1), pp.1-10.

Chen, Y., and Feng, M. Q. (2006). "Modeling of traffic excitation for system identification of bridge structures." *Comput. Aided Civ. Infrastruct. Eng.*, 21(1), 57–66.

D.W. Marquardt. An Algorithm for the Least-Squares Estimation of Nonlinear Parameters. *SIAM Journal of Applied Mathematics*, 11(2):431–441, Jun. 1963.

Davids, William G., Timothy J. Poulin, and Keenan Goslin. "Finite-element analysis and load rating of flat slab concrete bridges." *Journal of Bridge Engineering* 18.10 (2012): 946-956.

Ewins, D., J. 2000. *Modal Testing: Theory, Practice and Application*, Research Studies Press Ltd., USA.

Fanning, P.J., Boothby, T.E. and Roberts, B.J., 2001. Longitudinal and transverse effects in masonry arch assessment. *Construction and Building Materials*, 15(1), pp.51-60.

Ferreira, A. (2008). "MATLAB codes for finite element analysis: solids and structures,." Springer Science & Business Media, 157.

Fraser, M., and Elgamal, A. (2006). "Video and motion structural monitoring framework." 4th China-Japan-US Symposium on Structural Control and Monitoring (CD-ROM).

Fraser, M., Elgamal, A., He, X., and Conte, J. P. (2010). "Sensor network for structural health monitoring of a highway bridge." *J. Comput. Civ. Eng.*, 24(1), 11–24.

Huang, J. and Shenton, H.W., 2010. Load Rating of Concrete Bridge Without Plans. In *Structures Congress 2010* (pp. 298-309).

Islam, A.A., Jaroo, A.S. and Li, F., 2014. Bridge load rating using dynamic response. *Journal of Performance of Constructed Facilities*, 29(4), p.04014120.

Jáuregui, D. V., Licon-Lozano, A., and Kulkarni, K. (2010). "Higher level evaluation of a reinforced concrete slab bridge." *J. Bridge Eng.*, 15(2), 172–182.

K. Levenberg. A Method for the Solution of Certain Non-linear Problems in Least Squares. *Quarterly of Applied Mathematics*, 2(2):164–168, Jul. 1944.

Leissa, A. W. (1969). "Vibration of plates. National Aeronautics and Space Administration,," *NASA SP-160*, .

Mabsout, M., Tarhini, K., Jabakhanji, R., and Awwad, E. (2004). "Wheel load distribution in simply supported concrete slab bridges." *J. Bridge Eng.*, 9(2), 147–155.

Menassa, C., Mabsout, M., Tarhini, K., and Frederick, G. (2007). "Influence of skew angle on reinforced concrete slab bridges,," *J Bridge Eng.*, 12(2), 205-214.

Samali, B., Crews, K., Li, J., Bakoss, S. and Champion, C., 2003, March. Assessing the load carrying capacity of timber bridges using dynamic methods. In *Proceedings*.

Samali, B., Li, J., Crews, K.I. and Al-Dawod, M., 2007. Load rating of impaired bridges using a dynamic method. *Electronic Journal of Structural Engineering*.

Saraf, V. K. (1998). "Evaluation of existing RC slab bridges." *J. Perform. Constr. Facil.*, 12(1), 20–24.

Schulz, J. L. (1993). "In search of better load ratings." *Civ. Engrg., ASCE*, 63(9), 62-65.

Siswobusono, P., Chen, S.E., Jones, S., Callahan, D., Grimes, T. and Delatte, N., 2004. Serviceability-Based dynamic load rating of a LT20 bridge. *Experimental Techniques*, 28(6), pp.33-36.

Thomson, N.H., Smith, B.L., Almqvist, N., Schmitt, L., Kashlev, M., Kool, E.T. and Hansma, P.K., 1999. Oriented, active *Escherichia coli* RNA polymerase: an atomic force microscope study. *Biophysical journal*, 76(2), pp.1024-1033.

Timoshenko, S., and Woinowsky-Krieger, S. (2009). *Theory of plates and shells*, McGraw-Hill, New York, NY, USA,.

Turer, A. and Shahrooz, B.M., 2011. Load rating of concrete-deck-on-steel-stringer bridges using field-calibrated 2D-grid models. *Engineering Structures*, 33(4), pp.1267-1276.

Turer, A., 2000. Condition evaluation and load rating of steel stringer highway bridges using field calibrated 2D-grid and 3D-FE models (Doctoral dissertation, University of Cincinnati).

Wahbeh, A. M., Caffrey, J. P., and Masri, S. F. (2003). "A vision-based approach for the direct measurement of displacements in vibrating systems." *Smart Mater. Struct.*, 12(5), 785–794.

Wang, X., Kangas, S., Padur, D., Liu, L., Swanson, J.A., Helmicki, A.J. and Hunt, V.J., 2005. Overview of a modal-based condition assessment procedure. *Journal of Bridge Engineering*, 10(4), pp.460-467.

Weaver, W., and Johnston, P. (1987). *Structural dynamics by finite elements*, Prentice-Hall, Inc., Englewood Cliffs, NJ, USA,.